SYSTEMS TECHNOLOGY, INC.
2672 BAYSHORE FRONTAGE ROAD • MOUNTAIN VIEW, CALIFORNIA 94043 • PHONE (415) 961-4674

Technical Report No. 1172-1R

AN ANALYSIS OF AIRLINE LANDING FLARE DATA BASED ON FLIGHT AND TRAINING SIMULATOR MEASUREMENTS

Robert K. Heffley
Ted M. Schulman
Robert J. Randle, Jr.
Warren F. Clement

July 1981
Revised May 1982

Contract No. NAS2-10817

National Aeronautics and Space Administration
Ames Research Center
Moffett Field, California 94035

ABSTRACT

Landings by experienced airline pilots transitioning to the DC-10, performed in flight and on a simulator, were analyzed and compared using a pilot-in-the-loop model of the landing maneuver. By solving for the effective feedback gains and pilot compensation which described landing technique, it was possible to discern fundamental differences in pilot behavior between the actual aircraft and the simulator. These differences were then used to infer simulator fidelity in terms of specific deficiencies and to quantify the effectiveness of training on the simulator as compared to training in flight. While training on the simulator, pilots exhibited larger effective lag in commanding the flare. The inability to compensate adequately for this lag was associated with hard or inconsistent landings. To some degree this deficiency was carried into flight, thus resulting in a slightly different and inferior landing technique than exhibited by pilots trained exclusively on the actual aircraft.

FOREWORD

The research reported here was performed under NASA Contract NAS2-10817. The NASA contract technical monitor was Robert J. Randle, Jr., of the Man-Vehicle Systems Research Division of Ames Research Center; and the project engineer was Robert K. Heffley of Systems Technology, Inc. The work on this project was accomplished during the period from November 1980 to April 1981.

TABLE OF CONTENTS

ILLUSTRATIONS

ILLUSTRATIONS (Continued)

ILLUSTRATIONS (Concluded)

TABLES

AN ANALYSIS OF AIRLINE LANDING FLARE DATA

BASED ON FLIGHT AND TRAINING SIMULATOR MEASUREMENTS*

Robert K. Heffley, Ted M. Schulman, Robert J. Randle, Jr.**
and Warren F. Clement

Systems Technology, Inc.

SUMMARY

An analysis of pilot behavior, taken both from an airline training simulator and an actual DC-10, is presented for the landing maneuver. An emphasis is placed on developing a mathematical model in order to identify useful metrics, quantify piloting technique, and define training effectiveness and simulator fidelity. On the basis of DC-10 flight measurements recorded for 32 pilots--13 flight-trained and the remainder simulator-trained--a revised model of the landing flare is hypothesized which accounts for reduction of sink rate and preference for touchdown point along the runway. The flare maneuver and touchdown point adjustment can be described by a pitch-attitude-command pilot guidance law consisting of lead-compensated height feedback. The pilot gain and compensation, which are identified directly from the flight and simulator data, show that the flare is being executed differently in each of the two media. In flight most of the subject pilots exhibit a near-optimum effective lead-lag combination which is essential for well controlled sink rate reduction over a wide-range of response bandwidths. In the simulator, however, the compensation appears to be compromised by excessive lag which leads to substantially inferior landing performance. This inferior simulator technique appears to have an unfortunate carry-over into at least the first few actual landings performed by those pilots trained solely on the simulator. The inappropriate piloting technique observed in the simulator implies a simulator fidelity and validity problem, and several specific possibilities are discussed. The pilot model of the maneuver provides insight into which aircraft types might be simulated without incurring the apparent fidelity limitation encountered in this case.

---

*Performed under NASA Contract NAS2-10817.

**NASA, Ames Research Center.

INTRODUCTION

Study Objectives

The main objective of the study presented in this report was to analyze a recently acquired set of airline landing data for the purpose of supporting the Man-Vehicle Systems Research Facility (MVSRF) now under development at the Ames Research Center of the National Aeronautics and Space Administration (NASA) (Refs. 1 through 3). This new facility will focus upon human-engineering research topics not currently possible with existing NASA flight simulators, such as the complex interactions between pilots, crew members, and their aircraft and the issue of pilot error (Refs. 4 and 5).

More specifically, the purpose of this study was to focus on the landing maneuver as it is performed both in flight and in an airline training simulator in order to:

1. Measure absolute differences between pilot-vehicle behavior,
2. Develop a landing maneuver performance metric,
3. Define how to use such a metric in both simulator and flight.

Objectives of the Data Analysis

The data base used in this analysis was collected during a NASA field evaluation of the sole use of simulator training in transitioning airline pilots to a new aircraft type (Ref. 6). The unique aspect of the data acquired is that they involve both actual flight and simulator measurements for a reasonably large number of pilots. Furthermore specific attention was devoted to making the flight and simulator data directly comparable in terms of pilots, aircraft, and environmental conditions.

The procedure used in analyzing the available data was based on manual control theory (Ref. 7) which treats human psychomotor and cognitive behavior as rational, well-tailored actions dependent upon the task, vehicle dynamics, and environment. These actions can be essentially closed loop and compensatory in nature or progressively more open loop and precognitive depending upon the pilot's level of skill or workload demands. The technical approach is described in more detail below.

The issue of simulator fidelity has been stated in terms of manual control theory in Ref. 8 and is highly relevant to the analysis, not only in terms of the data base itself but also for the objectives related to the MVSRF. In fact, perceptual fidelity is addressed in terms of "essential cueing" as dis-

cussed in Ref. 9. As will be seen, there is evidence that the training simulator involved in this study is somehow deficient in inducing the pilot behavior observed in flight. This kind of deficiency should be duly noted in the design and actual use of the MVSRF or, for that matter, in any simulator where flight task and aircraft conditions are similar to those studied here.

Flight training is another topic considered in this report since that was a prime objective of the program which produced the data base. If training is viewed as the development of essential loop structure which describes psychomotor and cognitive behavior of the task-pilot-vehicle system (Refs. 8 and 10), then the analysis results presented should serve to quantify some aspects of the transition training imparted to the pilots. Furthermore, as a result of quantifying pilot-vehicle loop structure, a means of viewing the transfer of training from simulator to flight should ensue. This means may be a useful training tool in itself.

Background of the Data Acquisition Effort

The use of flight simulators as substitutes for aircraft in airline pilot training has increased dramatically during the current era of the jet transport. A series of changes and exemptions to the Federal Air Regulations (FARs) to allow the increased use of simulators in training has culminated in the current regulation for advanced simulation (FAR 121, Appendix H), which defines the requirements for total simulation training and checking. This regulation defines three phases of simulator upgrade, each allowing progressively more critical types of training to be accomplished in the simulator, so that in the final phase, all pilot training and checking may be done in the simulator.

The simulator upgrade requirements include hardware improvements to increase the fidelity of the motion and visual systems and software improvements to provide more realistic representation of aerodynamics and ground handling. Also required, although less well defined, are changes in the simulator training programs or in the ways simulators are used, including requirements for line-oriented flight training (simulation of complete missions and mission segments) and increased training requirements for simulator instructors and check airmen. These latter requirements reflect recognition of the goal of implementing the regulation: There must be complete confidence in the ability of instructors and check airmen to predict a pilot's performance in the airplane from his performance in the simulator.

In spite of the previously demonstrated value of the simulator in training, complete confidence in simulator training, in the absence of an airplane check, may require that increased attention be given to the validity and reliability of pilot proficiency assessment during training and checking. Proficiency assessment will have to be made more objective and standardized to increase its validity and reliability. Any significant contribution that can be made in this area should increase confidence in simulator training and checking.

In anticipation of the advanced simulation regulation, the United Airlines Training Center and the Man-Vehicle Systems Research Division of NASA's Ames Research Center, encouraged by the Air Transport Association's Simulator Training Task Force, conducted the study of total simulator training first reported in Ref. 6. The study was limited to transition training (pilots moving to a new aircraft) of captains and first officers. Under the regulation for advanced simulation, transition training is permitted only after simulator upgrade according to Phase II of the regulation, although the study was conducted on simulators that would qualify only for Phase I. Therefore the test of the simulators for training was more severe than would be allowed under the regulation. However, to insure safety in the study and on the line after the study, an airplane check and (if needed) airplane training were provided after the exclusively simulator training.

The purpose of the study (of Ref. 6) was to evaluate a transition training program that replaced the airplane with a state-of-the-art flight simulator. The evaluation procedure involved analysis of various objective measures and subjective ratings of pilot performance as a step toward objectifying and standardizing assessment techniques. The method of evaluation was to compare the performance in a standard check ride (FAR 121, Appendix F) of pilots trained exclusively in the simulator with the performance of pilots trained partially in the airplane in accordance with FAR 121, Appendix E. Performance measures used in the evaluation and reported in Ref. 6 were: (a) check-pilot pass-fail ratings; (b) check-pilot ratings of specific check-ride segments; (c) a NASA-employed observer's rating of specific maneuvers; (d) trainee ratings of their own performance and of the training they received; and (f) automatically measured system variables. The statistical analysis of these data was designed to (a) compare the performance of the simulator-trained with that of the airplane-trained pilots; (b) identify any anomalies peculiar to the performance of the simulator-trained pilots; and (c) explore the possibility of developing a predictive equation of pilot performance that in the future might be used to support training and checking.

The analysis study reported herein is, in effect, an extension to the original study for the purpose of considering additional metrics and ways of examining the data.

Technical Approach

As stated earlier, the technical approach applied to this analysis effort is based on a manual control theory of human psychomotor and cognitive behavior. The specific area studied is the landing maneuver in the vertical plane; lateral-directional aspects are not considered. Furthermore the focus is on the "outer loop" aspects of the landing, i.e., control of flight path and position. The "inner loop" regulation of pitch attitude is recognized but is already reasonably well understood and can be partitioned from the outer loops. In effect pitch attitude is routinely viewed as the "control" rather than elevator or control column deflection, per se. This greatly simplifies

the vehicle dynamics and helps to focus on only those airframe parameters which are directly involved in the landing. Nevertheless carrying along a complete detailed description of the pilot and aircraft is not precluded if that were necessary.

The specific steps in the technical approach are reflected in the report organization and include:

- A preliminary examination of the experimental results and data obtained
- Development of a mathematical model of the landing maneuver and theoretically derived metrics
- Analysis of the flight and simulator data in mathematical model terms and discussion of findings.

The first of these steps involved a cursory inspection of the landing data in order to gain an appreciation of the information available and how the data could be improved or augmented by smoothing or estimation procedures. In addition the flight data were carefully reviewed in order to revise old modeling notions or to formulate new ones.

Next the development and statement of a mathematical model was considered after a review and discussion of earlier modeling attempts. As will be seen, the flight data provided new insights into the nature of the landing maneuver, but the net result was a reduction in complexity--not an increase. A presentation and discussion of model features leads naturally into consideration of performance metrics. The aim was to point out or clarify relationships among the many metrics cited rather than to promote a favored metric.

The presentation of analysis results is made primarily in terms of the closed-loop response parameters identified from landing phase plane portraits of sink rate plotted against altitude. The numerical results provide, in terms of the metrics established, a basic definition of the nominal piloting technique, the effects of flight versus simulator training, and the effective simulator fidelity in these circumstances.

The key ideas behind the approach taken here were (a) to recognize the net, overall behavior of the closed-loop pilot-vehicle system, (b) to factor out the known essential physical behavior of the aircraft, and (c) to infer from what is left the likely actions of the human pilot. The guides for this process consist of all available descriptive material concerning the task, aircraft, environment, and pilot.

SYMBOLS

$\mathcal{AR}$	Wing aspect ratio
a	Real component of frequency for the flare maneuver ($\triangleq \zeta_{FL}\omega_{FL}$); also constant in complementary filter formulation
b	Damped frequency of the flare maneuver
$C_{L_{max}}$	Maximum lift coefficient
C_{L_α}	Non-dimensional lift curve slope
e	Naperian base, 2.7182...
F	Thrust
g	Gravitational acceleration ($\approx$ 32.2 ft/sec^2 or 19 kt/sec)
H	Absolute height
h	Perturbed height (usually equal to absolute)
$\dot{H}$	Absolute vertical velocity
$\dot{h}$	Perturbed vertical velocity
$\hat{\dot{h}}$	Estimated vertical velocity
$\ddot{H}$	Absolute vertical acceleration
$\ddot{h}$	Perturbed vertical acceleration
I_y	Pitching moment of inertia
k_h	Pilot's effective height gain
$k_{\dot{h}}$	Pilot's effective vertical velocity gain
k_γ	Pilot's effective flight path angle gain, Uk_h
$(L/D)_{max}$	Maximum lift-to-drag ratio
ℓ_f	Fuselage length
ℓn	Natural logarithm
IM	Speed margin above stall

m	Aircraft mass
R_o	Perceptual preview distance
S	Wing area
s	Laplace operator
T_I	Effective lag time constant
T_L	Effective lead time constant
T_{L_h}	Effective height lead time constant of pilot
T_{θ_1}	Airspeed response time constant
T_{θ_2}	Flight path response time constant
t	Time
U	Velocity vector along x-axis
u	Perturbed x-axis velocity (airspeed)
V_T	Airspeed ($\approx U$)
W	(1) Velocity vector along z-axis; (2) gross weight
$\ddot{Y}_h$	Pilot's effective acceleration transfer function
α	Angle of attack
γ	Flight path angle ($\approx \dot{h}/U$)
Δ	Prefix denoting incremental quantity
$\Delta\tau$	Incremental lag associated with discrete pitch attitude commands
δ_c	Column displacement
ε	General state variable
ζ_{FL}	Effective damping ratio of landing maneuver
Θ	Absolute pitch attitude
θ	Perturbed pitch attitude
θ_{GS}	Glide slope angle

π	3.14159...
ρ	Air density ($\approx$ 0.002377 slug/ft^3)
ϕ_{m_h}	Height phase margin
ω_{FL}	Effective undamped natural frequency of landing maneuver
ω_{c_θ}	Pitch attitude crossover frequency
ω_{c_h}	Height crossover frequency
ω_p	Phugoid frequency

Subscripts

c	Command
FL	Flare
max	Maximum
o	Initial condition
TD	Touchdown condition

ABBREVIATIONS

a.c.	Aerodynamic center
cg	Center of gravity
FAA	Federal Aviation Administration
FAR	Federal Aviation Regulation
MVSRF	Man-Vehicle Systems Research Facility
STI	Systems Technology, Inc.

EXPERIMENTAL RESULTS

Description of Experimental Design and Data Obtained

Facilities. The study from whence the data base was obtained was accomplished at United Airlines Flight Training Center in Denver, Colorado. To enhance the generality of the results, two types of airplanes were included in that study: the Boeing 727 and the McDonnell-Douglas DC-10; but only the DC-10 results are considered in this analysis. (Reference 6 includes results for both aircraft types.)

The aircraft involved in the collection of data were unmodified McDonnell-Douglas DC-10-10 wide-body jet transports. Gross weight at landing ranged from 270,000 to 340,000 lb. (A nominal value of 300,000 lb was assumed for analysis purposes.) Normal landing procedures are described in both the manufacturer's and airline's flight manuals (Refs. 11 and 12), the latter is more explicit in terms of nominal attitude excursions and height of flare initiation.

Flight training and check rides were conducted primarily at Denver's Stapleton International Airport. The normal approach was made on the instrument landing system (ILS) for Runway 34R; however, visual meteorological conditions prevailed. Due to aircraft availability, most if not all of the flights were made at night.

The United Airlines DC-10 simulator (No. 605) was used for pilots transitioning to the DC-10. The simulator was a Redifon DC-10 system with a moving base and outside visual scene. Relatively large amplitude vertical motion was provided by a "Synergistic" type of motion platform characterized by a pendulum support structure. A Redifon NOVOVIEW visual system was used to display a 36 deg by 48 deg field-of-view computer-generated image of a nighttime runway environment. No details were available on motion or visual simulator response characteristics or mathematical model software and digital computer implementation. Therefore judgment is reserved on specific sources of any of the simulator fidelity effects which are measured in the data. The aerodynamic model was, however, upgraded to comply with Phase I of FAR 121, Appendix H. This included modification of the ground effects model. This simulator thus received approval by the Federal Aviation Administration (FAA) for simulator training of the landing maneuver. Except for the special provision that the study trainees receive all of their simulator training on an approved upgraded simulator, all of the training center facilities used in normal training were used in the study.

Trainees. Captains and first officers arriving at the training center for transition training to the DC-10 were selected on a random basis to be part of the study or to receive normal transition training and checking according to FARs 61 and 121 (including Appendices E and F). Those trainees selected for the study were randomly assigned to either the exclusive-simulator-training (experimental) group or to the normal training (control) group. Occasionally simulator availability modified the random assignment of trainees to the

study. This modification to the study procedure was necessary to minimize disruption of the regular flow of trainees of all types through the training center. Also, for a variety of reasons including simulator and airplane availability, some pilots originally assigned to the study had to be dropped later, in which case they became normal transition trainees. These will be discussed in more detail later in the report. A total of 87 pilot trainees, transitioning to the DC-10, completed the study, 34 captains and 53 first officers. Data are analyzed in this report for 32 of these trainees.

Procedure. Trainees of both the experimental and control groups received normal ground school and simulator training in the appropriate landing-approved simulator without being informed of their group status. After passing their normal simulator check, the control-group trainees progressed, as routinely done, receive Appendix E (FAR 121) training in the airplane. Appendix-E-type training will be referred to as landing training since landing is considered to be the most critical part thereof. Trainees in the experimental group received their landing training in the landing-approved simulator. The simulator landing training course was developed by personnel of the training center and was designed to duplicate as closely as possible the standard landing training received by the control group in the aircraft.

Trainees next proceeded to the NASA check ride. For many in the experimental group, the NASA check ride was their first experience at the controls of the DC-10. The NASA check ride was designed to simulate the normal check ride that would result in certification of the trainee to fly the new airplane type in revenue flights. A United Airlines check pilot served in his normal capacity in checking the first officer trainees and in simulating the role of an FAA check ride inspector on the basis of availability. The check ride consisted of the maneuvers specified in FAR 121, Appendix F, plus one additional normal landing in the following sequence: (a) taxi; (b) normal takeoff; (c) VFR approach without instrument guidance; (d) normal full-stop landing; (e) normal takeoff; (f) hooded approach, one engine inoperative; (g) missed approach; (h) VFR approach, one engine inoperative, instrument guidance available; (i) engine-out landing, touch-and-go; (j) VFR approach without instrument guidance; and (k) normal landing. The second normal VFR landing was added to provide additional data.

Upon completion of the final maneuver, the check pilot had the option of requiring or offering additional practice in the airplane before completion of the flight. This option was almost invariably exercised regardless of the trainee's performance on the check-ride maneuvers. In order to maintain his responsibility as safety pilot, the check pilot did not interrupt his monitoring of the flight to record his ratings of the trainees' performance until after the additional practice; however, it was understood that his ratings were to be based only on the check-ride maneuvers.

To guard against bias in their ratings, the check pilots were not told prior to their ratings whether the trainee had received the landing training in the airplane or the simulator; that is, they were not told to which group the trainee belonged.

Throughout the check flight the NASA observer sat in the jump seat directly behind the captain's seat. The observer was one of two retired United Airlines captains who worked under contract with Ames Research Center. The observer's responsibility was basically to supervise data collection. In addition to scoring his own rating sheets, he installed and actuated the automatic data recording system on the airplane, and issued and collected the rating sheets of the check pilots and trainees. The observer's ratings consisted of instrument recordings and evaluative judgments made during the various maneuvers. A two-axis accelerometer was mounted on the cabin floor over the airplane's center of gravity. Vertical and lateral accelerations were recorded on an FM tape recorder starting during the approach at an altitude of 200 ft. Simultaneously, altitude was recorded from the airplane's radio altimeter. During Phase II, similar automatic recordings were also taken in the simulator.

Following the check ride, the trainee completed a questionnaire about his flying history and made ratings of both his performance in the check ride and of how well he thought his training prepared him for the check ride.

After the check ride, all of the collected data remained in the custody of the NASA observer until it was mailed to Ames Research Center, where it was analyzed. The data packages had no identifying trainee names; trainees were identified by numbers only.

The study was completed for the trainee when the NASA check ride was completed (about 35 minutes). Additional training was then given to all trainees. First officers were then certified, and captains proceeded to the FAA check ride.

The kinds of data obtained for the landing maneuver were somewhat different between the aircraft and the simulator. Flight data were necessarily sparse because of instrumentation limitations and restrictions. For the simulator a reasonably wide range of data were accessible. Data analysis and comparisons were therefore constrained mainly by the flight data.

A portable NASA instrumentation package was placed aboard the various DC-10 aircraft used for training. This package recorded:

- Vertical acceleration
- Lateral acceleration
- Radio altitude (production installation)
- Time

Analog samples were recorded starting at about 300 ft and continuing well into the landing rollout. FM recordings were then transferred to a NASA PDP-12

computer for the initial analyses reported in Ref. 6, giving smoothed data every 50 ms.

The simulator data included most of the aircraft states and controls. They were:

- Body axis translational accelerations
- Body axis translational velocities
- Vertical velocity
- Radio altitude
- Pitch attitude
- Lateral and vertical glide slope deviations
- Wheel, yoke, and rudder positions
- Slant range to touchdown zone
- Touchdown flag
- Time

Samples were recorded every 200 ms also starting at about 300 ft and continuing well into the landing rollout.

It should be noted that there is a lack of symmetry in the data available for the two groups. Data were obtained for both the simulator training and check-ride phases for the simulator-trained pilots, but only for the check ride in the case of the flight-trained pilots. Data recorded by the NASA-observer during the check rides consisted of:

- Gross weights
- Computed reference airspeed
- Flap settings
- Glide slope and speed deviations at specific altitudes
- Touchdown distance from touchdown zone
- Occasional landing specific comments about wind and turbulence conditions

It should also be noted that the second landing of each of the series of three check-ride landings was with a simulated engine failure.

Data Preparation

Nature of Data. The longitudinal aircraft states and controls desirable for studying the landing maneuver are:

- Pitch attitude
- Pitch rate
- Altitude
- Vertical velocity
- Control column position
- Range from threshold

All of these variables are typically available from aircraft simulations but are more difficult to obtain from flight, especially when there is no experiment-dedicated aircraft and recording package. In the present case all of the above variables, except pitch rate, were recorded from the simulator, and only altitude and vertical and lateral acceleration were recorded from flight. Hence the flight measurements were the limiting factor in data analysis. Steps were taken to enhance the data by estimation and smoothing techniques. Estimation of vertical velocity and pitch attitude for the flight data met with mixed success as will be described.

Approach. There are a number of different ways that flight data can be examined, each having its strengths and weaknesses depending upon what variables are to be considered. The study of piloting techniques in landing imposes further constraints. Since the flare takes only about one quarter of a cycle of the predominant closed-loop flight path response mode, describing function identification techniques are untenable. Terminal performance measures, such as touchdown sink rate and distance from the touchdown zone, measure the outcome of a particular maneuver. Summary statistics can show trends in groups of landings or groups of pilots, but they do not tell why a particular maneuver succeeded or failed or if the technique is a good one (i.e., will continue to result in good landings in spite of different wind conditions, turbulence levels, or deviations from reference airspeed). Also needed are ways of looking at the data which show "how the pilot got there" as well as the final result itself. Two such ways of displaying this information are (a) the time history and (b) the phase plane portraits or state variable crossplots. Time histories, which are commonly used, are simply graphs of the

variables of interest versus time. State variable crossplots describe two variables of interest against each other, with time becoming an implicit parameter on the curves. (These curves are referred to as "trajectories," as following the curve in the direction of increasing time shows the path through the state space.) Phase planes can have advantages over time histories when comparing repeated performance of a maneuver since they present the information in a more concise form. For example Ref. 13 suggests one way of modeling the landing. It hypothesizes a proportional control law for pitch attitude which depends on height above the ground, extending from flare height to touchdown. Looking for this behavior directly in time histories is difficult; because flare height, pitch attitude, and sink rate vary significantly from landing to landing, screening any inter-relationship between states. On the other hand, a number of crossplots of pitch attitude versus height would reveal the above-mentioned hypothesis directly or perhaps suggest other relationships.

Phase plane portraits are special cases of state variable crossplots. These are crossplots of a variable and its derivative, such as altitude versus vertical velocity. As one variable is the derivative of the other, important features of the dynamic response are visible. For example, a landing maneuver in which no ballooning takes place will produce a trajectory entirely in the right lower quadrant as this corresponds to a positive altitude and negative vertical velocity.

The first step in the data reduction was to use the existing flight data to estimate those additional states desired. A constraint in the choice of methods was that the task was to study landing techniques, not techniques in state variable estimation. Without doubt it would be possible, using more sophisticated filtering and estimation techniques, to reconstruct desired states using the altitude and acceleration data. This was not performed, however, due to constraints of time and computer resources. Simpler methods were used with good results, at least in estimating vertical velocity. Pitch attitude estimates were not adequate; but, as will be seen in the following sections, the lack of good pitch attitude information did not detract from the analysis. The following is a discussion of the estimation techniques used and how they were validated.

The estimation of sink rate is easier than the estimation of pitch attitude as there is no need to consider the aircraft's dynamics. Complementary filtering was used to take advantage of all of the data available. The altitude data is appropriate for low-frequency estimation of sink rate, while vertical acceleration is appropriate for high frequencies. Complementary filtering allows the data to be combined in a way that takes advantage of these relative strengths. The continuous form of the filter is:

$$\hat{\dot{h}} = \underbrace{\frac{a\,s}{s+a}\,h}_{\text{"washed out" altitude}} + \underbrace{\frac{1}{s+a}\,\ddot{h}}_{\text{"lagged" acceleration}} \qquad (1)$$

where

s is the Laplace operator

h is the measured altitude

$\ddot{h}$ is the measured vertical acceleration

$\hat{\dot{h}}$ is the estimated sink rate

and a is the characteristic frequency of the filter

In the continuous case, with no noise, the identities $sh = \dot{h}$ and $\ddot{h} = s\dot{h}$ can be substituted into Eq. 1, giving the identity $\hat{\dot{h}} = \dot{h}$. For a more complete discussion of complementary filtering, see Ref. 14.

The complementary filter was implemented in finite difference equation form as:

$$\hat{\dot{h}}_n = e^{-at}\,\hat{\dot{h}}_{n-1} + a\,h_n - a\,h_{n-1} + \left(1 - e^{-at}\right)\ddot{h}_n \qquad (2)$$

The characteristic frequency, a, of the filter was determined empirically to accommodate the sample period as well as the noise content of the measured altitude and vertical acceleration. Figure 1 shows four different values for a: 5, 2, 1, and 0.6 rad/sec. The value of 1 rad/sec was chosen for use. Larger values produced too noisy an estimate, and smaller values began to introduce a noticeable lag and further attenuated the noise level only slightly.

One improvement to the estimation algorithm was made. For the plots shown in Fig. 1, the portion of the filter that operates on altitude was initialized with a zero sink rate. This causes the estimate initially to have a large variance. This problem was eliminated by using the average of the derivative of the altitude over the first ten points as the initial value. Computation was also halted at the previously computed touchdown point. The result of these changes is shown in Fig. 2. This method was validated using the simulator data. Estimates were made of the sink rate and the results compared favorably with the recorded values.

All of the plots in this report are labeled with the word "PILOT," followed by a letter and two numbers. The letter indicates whether the data is from flight (F) or simulation (S). The first number (in the four hundreds for this report) is the pilot identification number. Interpretation of the second number depends upon whether the data are from flight or simulation. If the data are from flight, the number indicates the check ride landing number (1, 2,

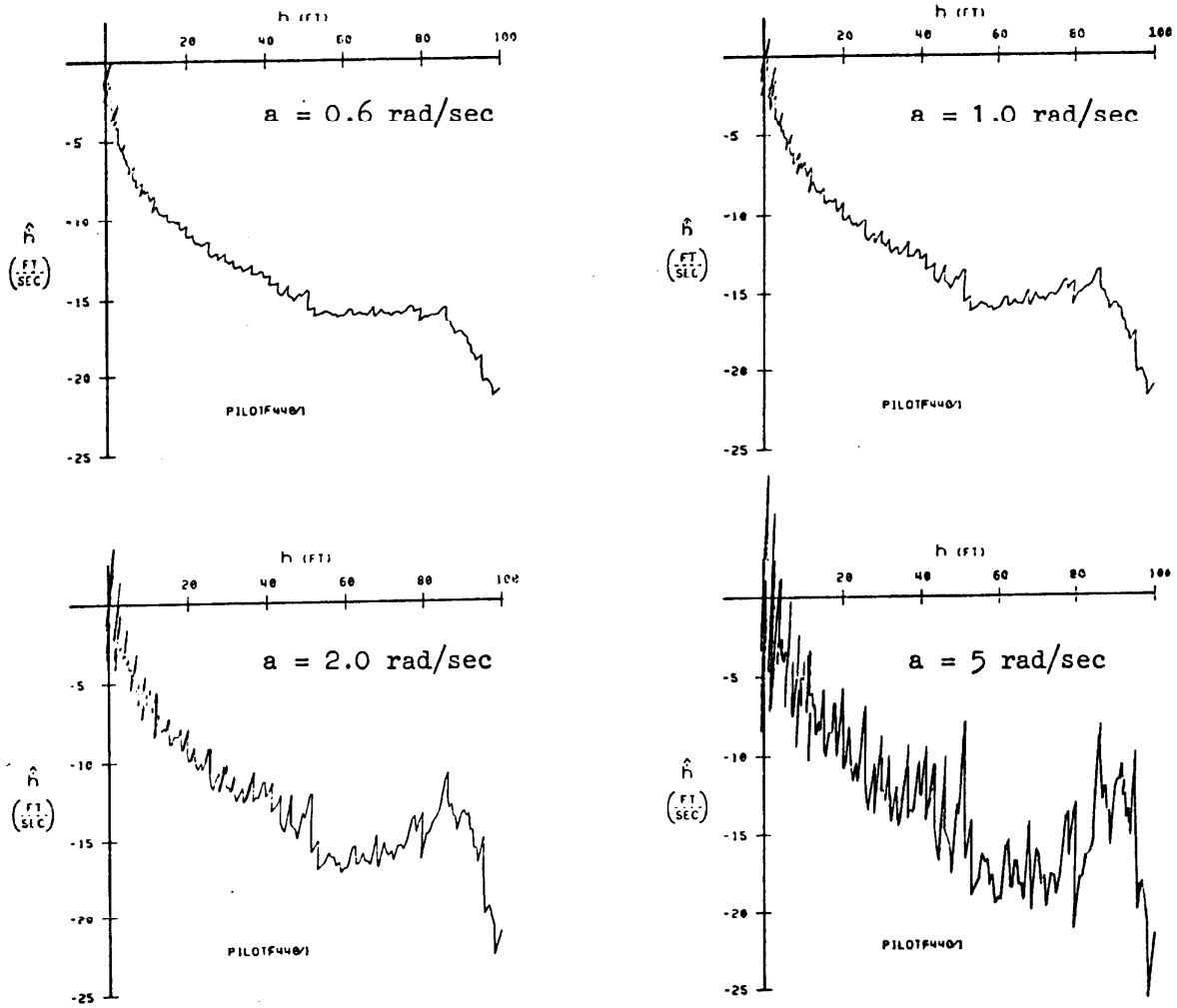

Figure 1. Estimated Sink Rate Versus Altitude for Complementary Filter Break Frequencies, a = 0.6, 1, 2, and 5 rad/sec

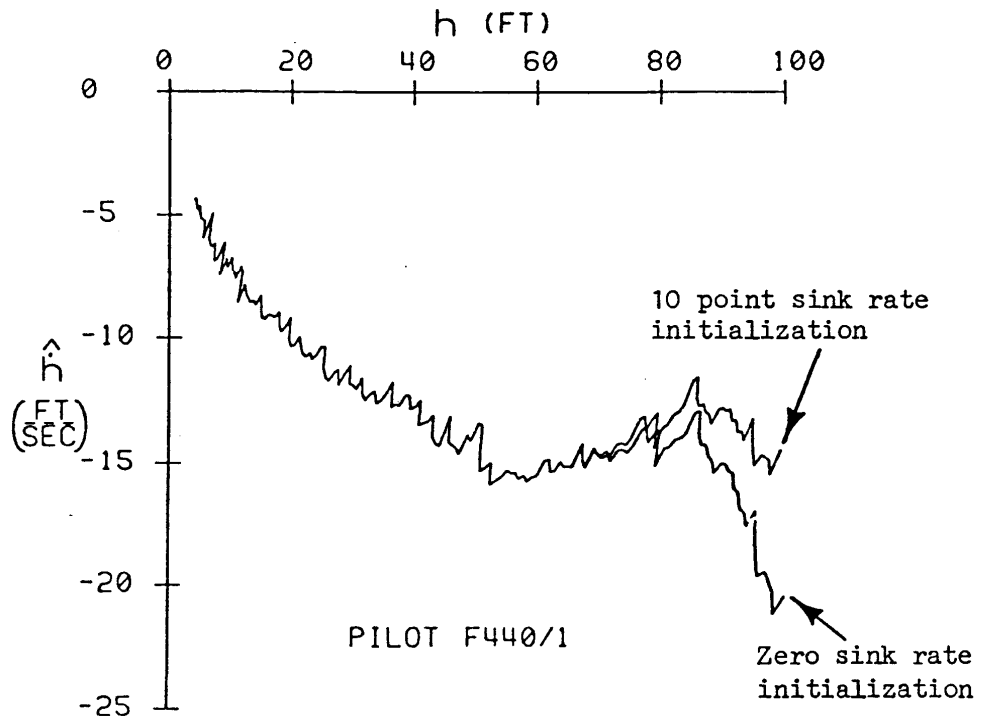

Figure 2. Estimated Sink Rate Versus Altitude with Filter Break Frequency at 1 rad/sec, 0 and 10 Point Sink Rate Initialization, and Termination at Touchdown

or 3). If the data is from simulation, the last two digits of the number indicate the experimental run number on the magnetic tape and the first one or two digits indicate the tape number. For example:

PILOT F404/2

indicates that the data were taken in flight, the pilot identification number is 404, and the landing was the second in the sequence of three.

PILOT S432/1308

indicates that the data were taken on the simulator, the pilot identification number is 432, and the landing was the eighth experimental run on Magnetic Tape 13.

Pitch attitude can be estimated from the two available aircraft states (altitude and vertical acceleration); but, unlike sink rate, the estimation involves the dynamics of the aircraft. The most direct dynamic relationship is the aircraft's sink rate response to pitch attitude. The linearized approximate factor relationship was used as it is a valid approximation in terms of relative time scales of the landing maneuver and the aircraft dynamics. The differential equation is:

$$T_{\theta_2} \ddot{h} + \dot{h} = U\theta \tag{3}$$

where U is the airspeed of the aircraft

T_{θ_2} is the flight path time constant

A number of methods of implementing Eq. 3 were tried. These included direct substitution of the measured vertical acceleration and estimated sink rate, as well as a scheme for differentiating the estimated sink rate to estimate vertical acceleration.

The problem with the first method was that both the measured vertical acceleration and estimated sink rate have high noise-to-signal levels, with the worst being the vertical acceleration. In Eq. 3, T_{θ_2} can be viewed as a weighting coefficient in the computation of pitch attitude. For the DC-10, T_{θ_2} is approximately 1.8 sec. Thus it can be seen that the measured vertical

acceleration is being weighted 1.8 times more heavily than the estimated sink rate. This produced a very unsatisfactory noise-to-signal ratio in the estimated pitch attitude. A possible solution to this problem might be to perform a running polynomial fit to the measured vertical acceleration and the estimated sink rate, or employ some other smoothing scheme before estimating pitch attitude. These were postponed and the second method was tried.

The second method of attitude estimation was to differentiate the estimated sink rate and to filter it to eliminate the noise. Although this method seemed a good candidate due to an apparent frequency separation between the signal and noise (the noise taken as the high frequency oscillations about what can be imagined as a smooth curve in Fig. 2), the resulting signal-to-noise ratio in the estimated pitch attitude was unacceptable. This appears to be a problem implicit in this method; and, in spite of the filtering performed at each step, the more heavily weighted term is the estimated second derivative of measured altitude.

Neither of the attitude estimation schemes proved to be adequate thus were dropped for this study. It is recommended that, in the future, pitch attitude be measured directly along with altitude and acceleration.

Preliminary Data Analysis

This section presents the results of the preliminary analysis performed on the data described in the previous subsections. The purpose of this analysis was to look at the data in some detail so that some initial conclusions could be reached about the pilots' control of the aircraft during the landing maneuver in the aircraft and the simulator. The insight gained here was used as a basis for the detailed modeling described in the next section.

Time Histories. Time history presentations of the landing data can provide certain clues about pilot actions and piloting technique. Consider the examples shown in Fig. 3 for Pilot 432. Figures 3a and 3b were simulator landings and 3c was a check ride landing in the actual aircraft. Figure 3a shows a routine approach with attitude and sink rate maintained down to a nominal flare height of about 40 ft. At that point the column (δ_c) was pulsed rearward at a fairly high frequency (about 7 rad/sec) in order to flare, and a reasonable touchdown sink rate obtained. In the next landing (Fig. 3b) a gentler and more consistent control column action was demonstrated with the flare starting somewhat higher. The approximate frequency of oscillation was about 2.4 rad/sec as determined by the period over several cycles for both the derivative of the z-axis velocity component, $\dot{w}$, (i.e., proportional to angle of attack rate) and the control column. For an actual landing (Fig. 3c), the same pilot performed a comparable landing in terms of sink rate reduction, but the apparent inner-loop frequency of oscillation (which must be inferred from vertical acceleration, h) was lower still, i.e., about 1.3 rad/sec.

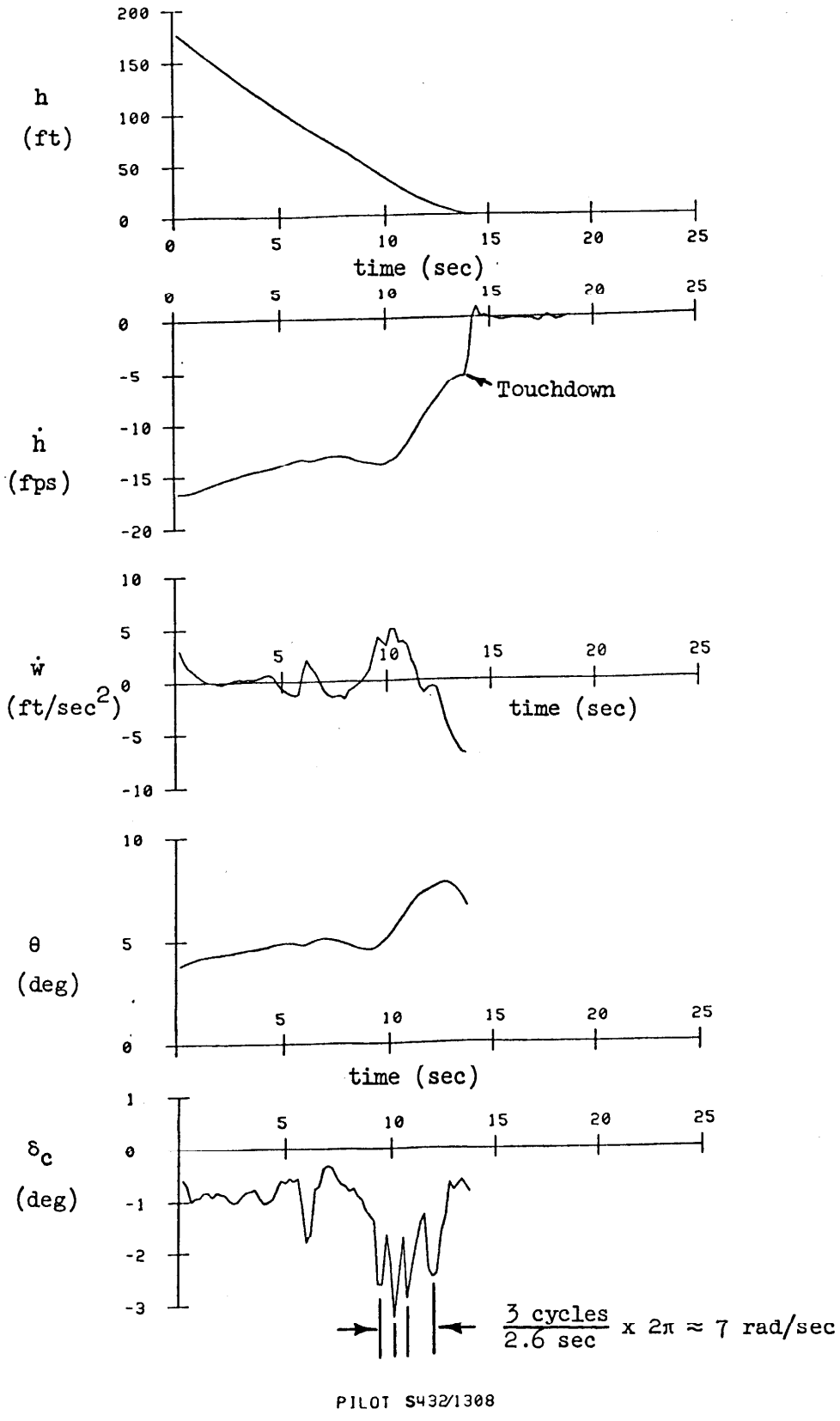

Figure 3. Time Histories for Three Landings by a Simulator-Trained Pilot (two in the simulator and one in the aircraft)
a. First Simulator Landing Made by Pilot 432

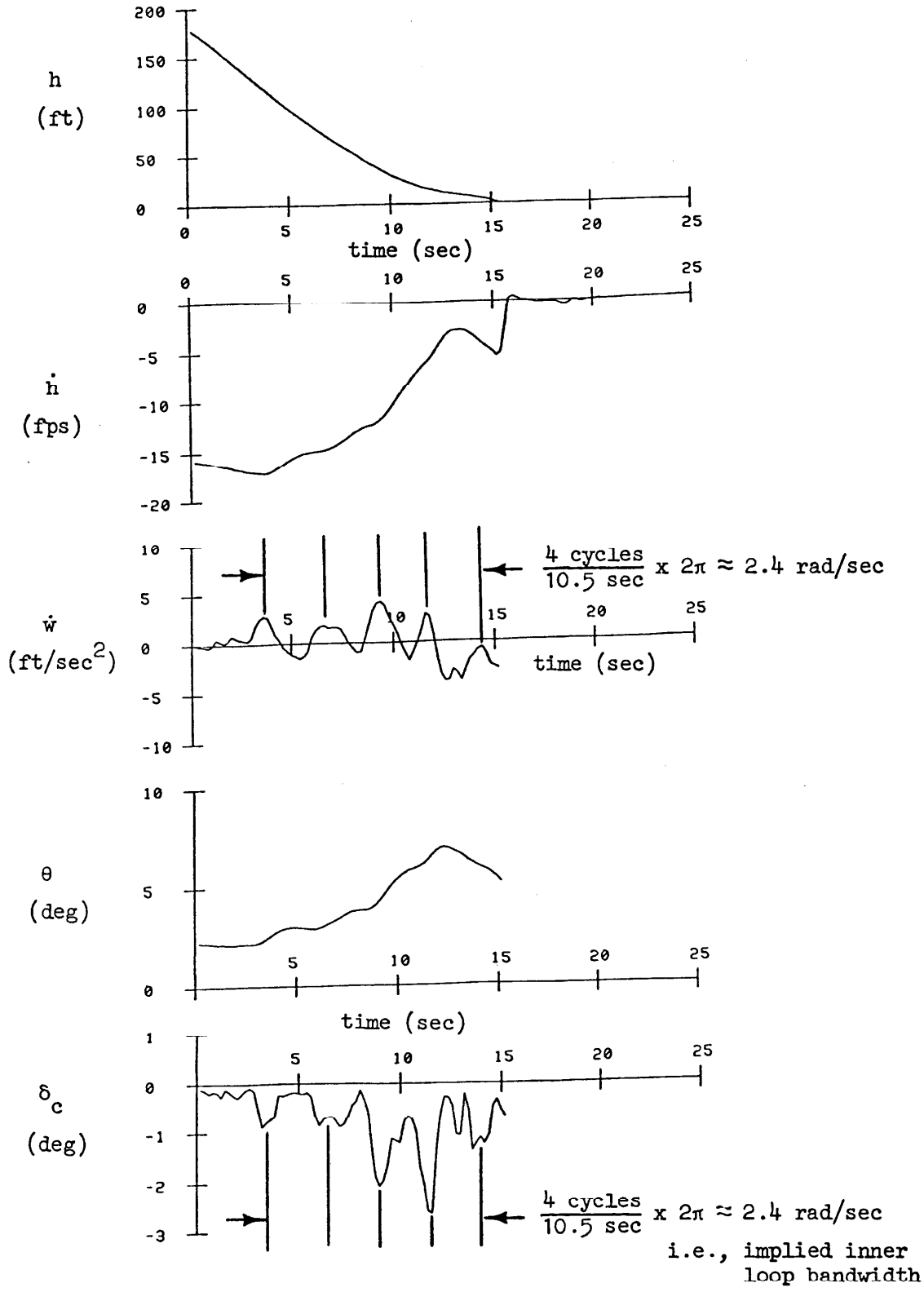

Figure 3 (Continued)
b. Second Simulator Landing Made by Pilot 432

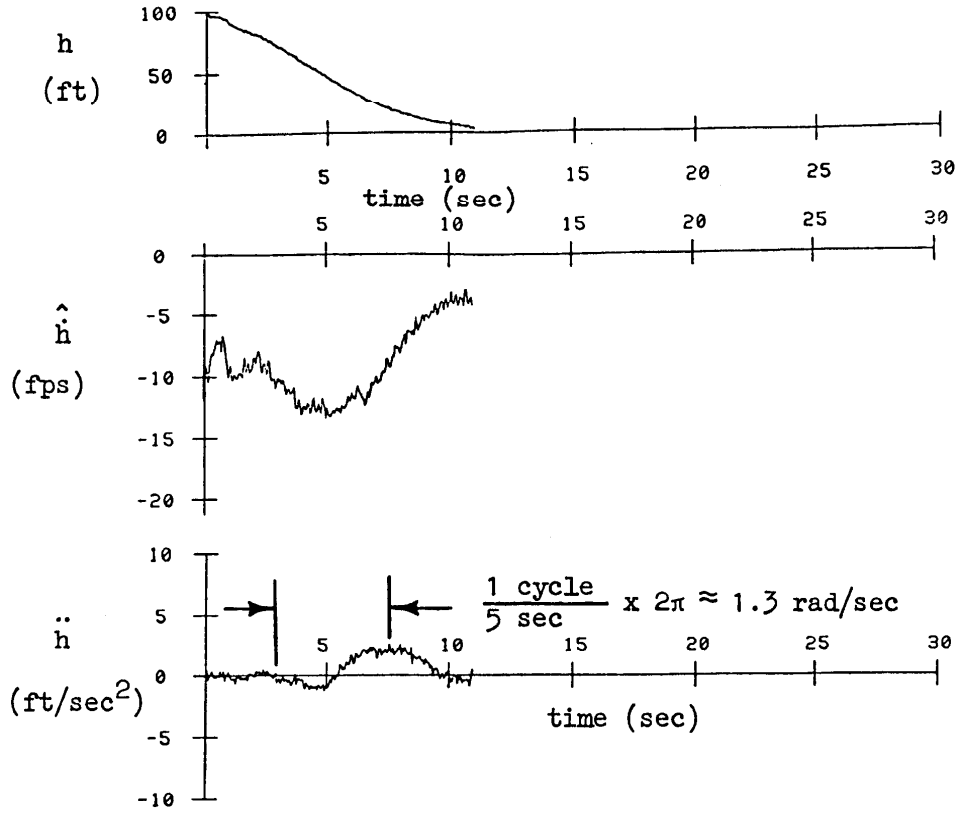

PILOT F432/2

Figure 3 (Concluded)
c. Second Check Ride Landing Made by Simulator-Trained Pilot 432

Examples of the actions of two additional pilots performing actual landings are shown in Figs. 4 and 5. Management of sink rate appears to have varied but inner-loop bandwidth was about the same.

In order to gain more insight into the flare maneuver, per se, (i.e., the flight-path trajectory), it was found useful to consider phase plane representations in addition to time histories.

Phase Plane Plots. Figure 6 shows the phase plane plots that correspond to two of the sets of time histories shown in Fig. 3. Figure 6a is Pilot 432's first simulator landing and 6b, the same pilot's second check ride landing. For the simulator case, a plot of pitch attitude versus height is shown along with the vertical velocity-versus-height phase plane. Both the simulator landing and the flight landing show a phase plane trajectory which spirals inward toward the origin. This final closure with the ground is reflective of second-order system dynamics according to such general control theory texts as Refs. 15 and 16.

One benefit of phase plane information is that effective response parameters can be fairly easily extracted. Some examples are shown in Fig. 7. For a second-order system, the amount of damping is indicated by the tightness of the spiral. Zero damping yields a continuous elliptical trajectory never coming to rest (i.e., never arriving at the origin). Increasing amounts of damping force the response to settle in fewer and fewer cycles. In the case of a terminal maneuver such as a landing, the settling of velocity must be accomplished in a fraction (less than 1/4) of a cycle.

The natural frequency of a system is reflected by the approximate proportion of ellipticity of the phase plane, i.e., the relative extremes in velocity and displacement. For highly damped systems, frequency is related to how steeply the trajectory approaches the origin.

Another feature of phase planes is that they indicate the nature of the response in terms of system order, nonlinearities, and mode switching. This is an important attribute for dealing with an ill- or vaguely-defined system such as the pilot-vehicle combination.

It was not considered necessary to differentiate among height at the pilot, at the cg, or at the radio altimeter antenna (approximately 30 ft ahead of the cg). Assuming a net pitch change of 3 deg there would be less than a 5 ft disparity which is about equal to the uncertainty band in the flight data (e.g., Fig. 6). More precise data might deserve closer scrutiny of this issue, however.

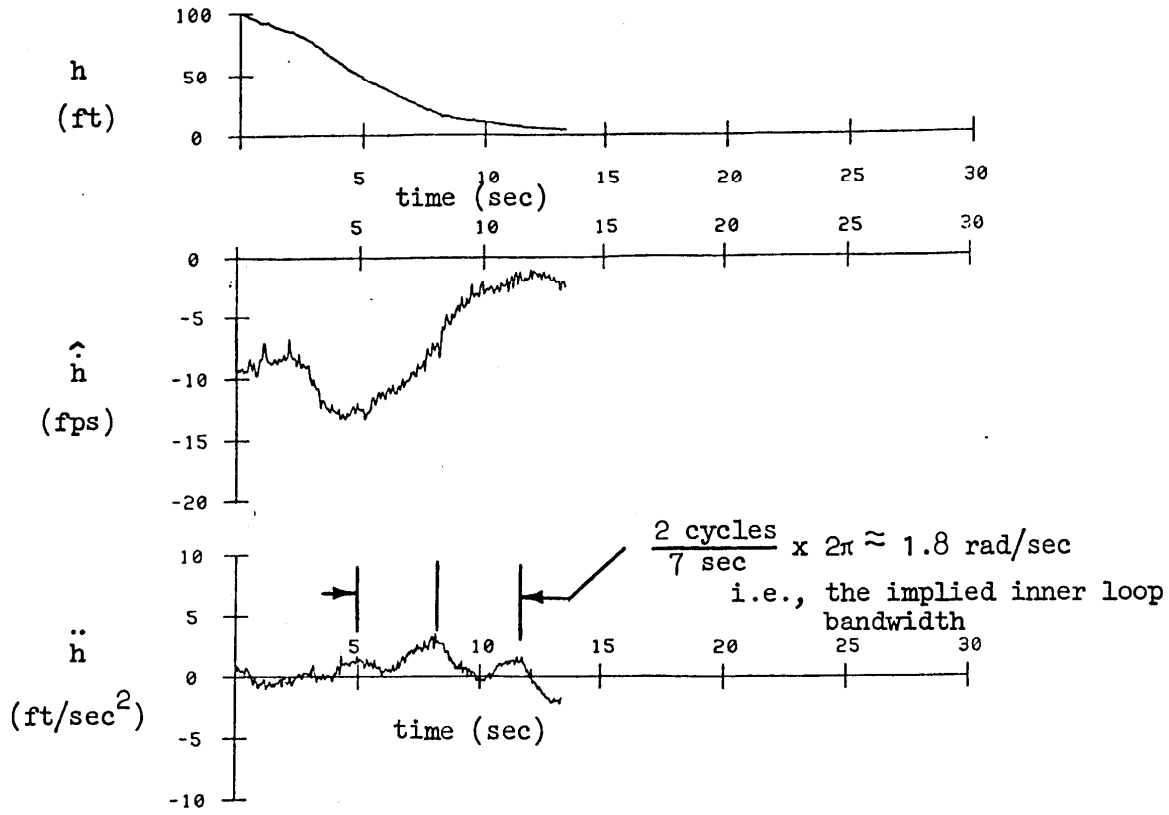

PILOT F404/3

Figure 4. Time Histories for the Third Check Ride Landing by Flight-Trained Pilot 404

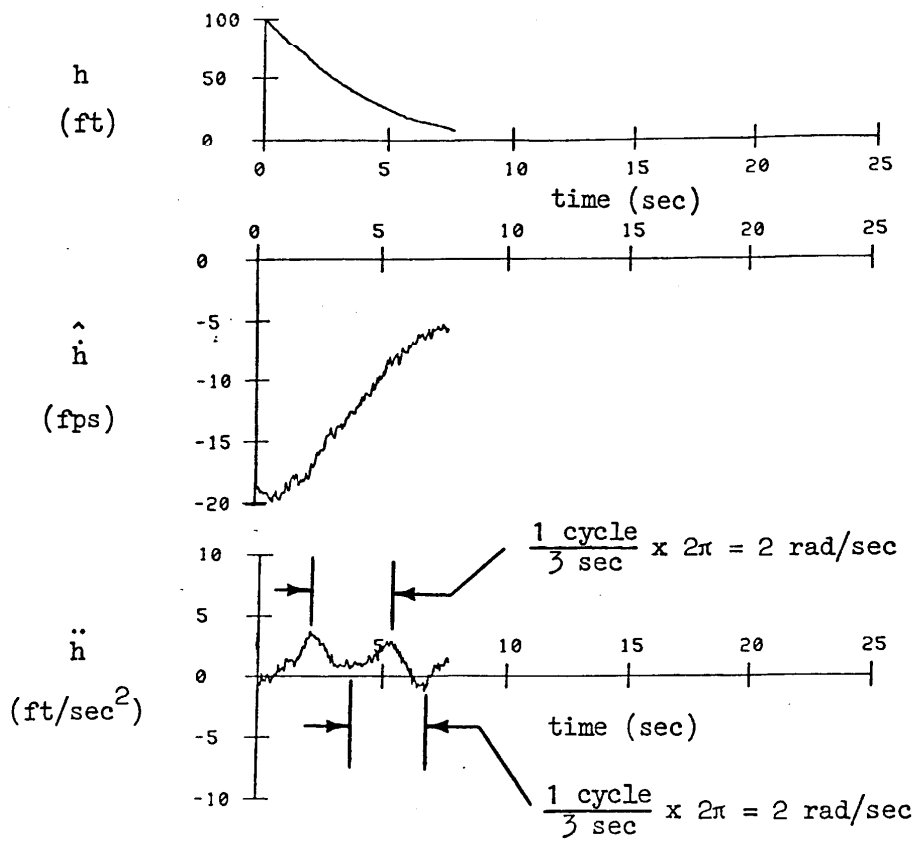

Figure 5. Time Histories for the Second Check Ride Landing by Flight-Trained Pilot 433

a. Simulator Example

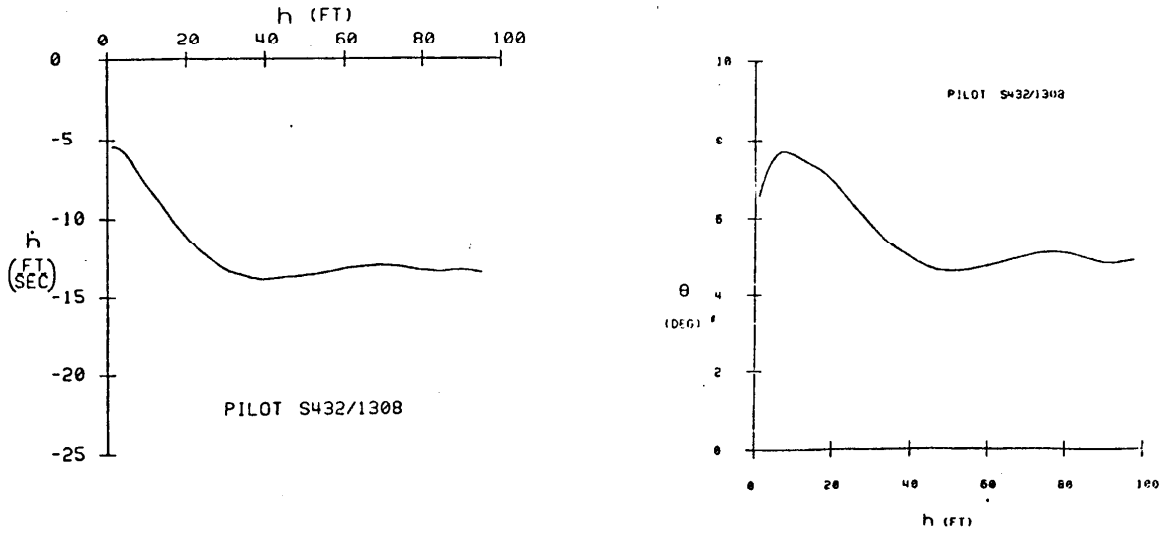

b. Flight Example

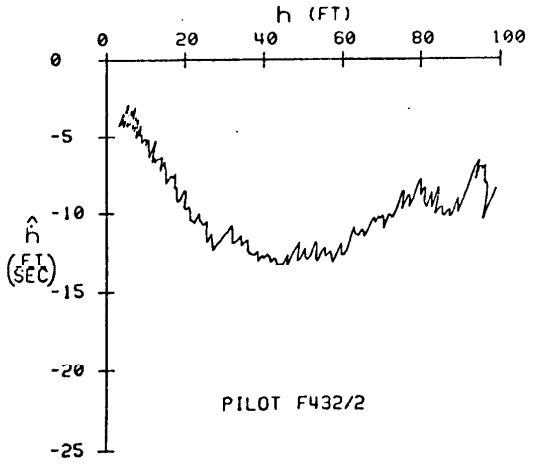

Figure 6. Phase Plane Trajectories for Typical Landings in the Simulator and In Flight

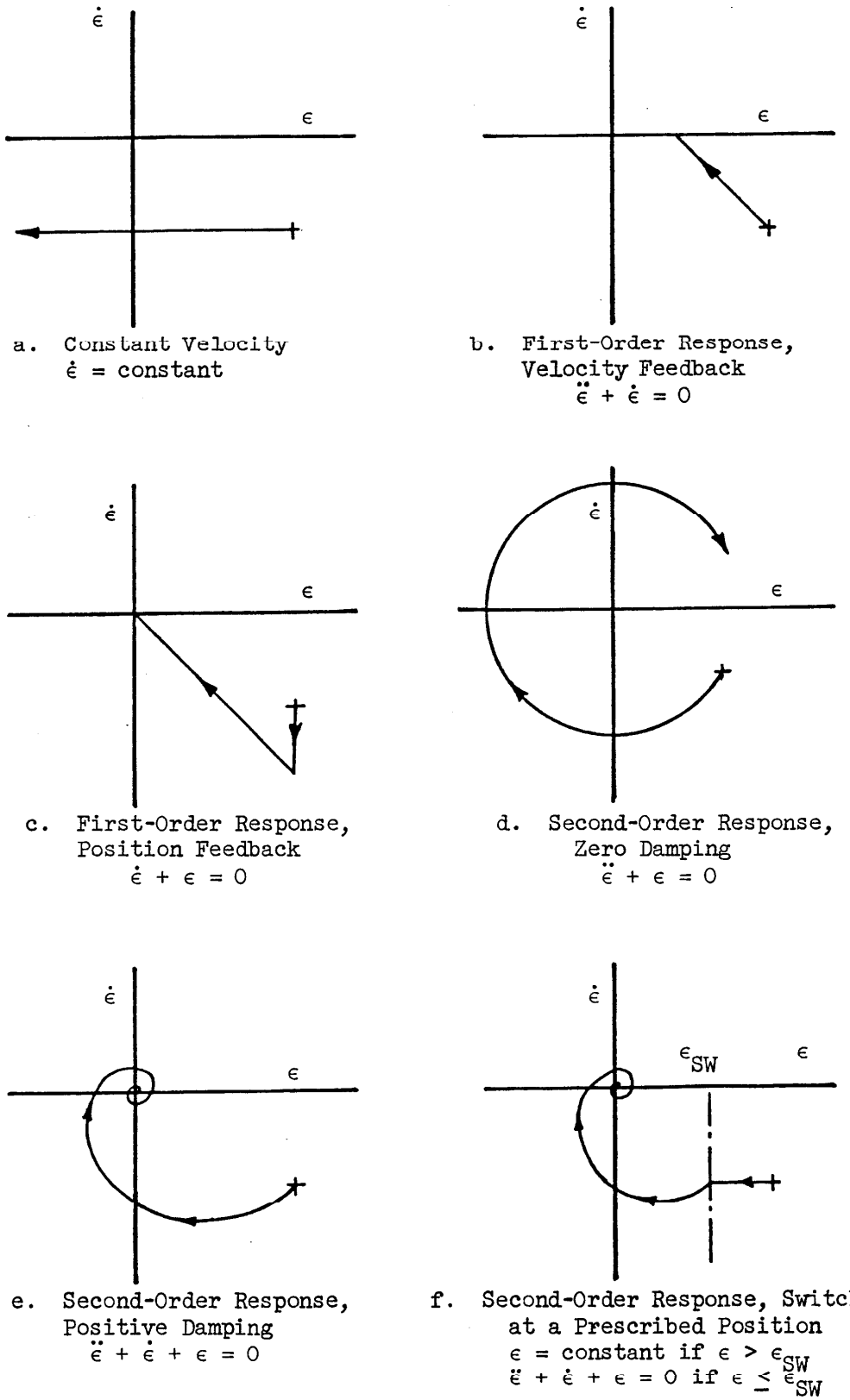

a. Constant Velocity
$\dot{\epsilon}$ = constant

b. First-Order Response, Velocity Feedback
$\ddot{\epsilon} + \dot{\epsilon} = 0$

c. First-Order Response, Position Feedback
$\dot{\epsilon} + \epsilon = 0$

d. Second-Order Response, Zero Damping
$\ddot{\epsilon} + \epsilon = 0$

e. Second-Order Response, Positive Damping
$\ddot{\epsilon} + \dot{\epsilon} + \epsilon = 0$

f. Second-Order Response, Switched on at a Prescribed Position
ϵ = constant if $\epsilon > \epsilon_{SW}$
$\ddot{\epsilon} + \dot{\epsilon} + \epsilon = 0$ if $\epsilon \leq \epsilon_{SW}$

Figure 7. Examples of Phase Plane Trajectories for Various System Dynamics

Flare Model

The objective at this point is to lay the foundations for the analysis of the flight and simulator landing data obtained in this experiment. Specifically a hypothesis for the manual landing maneuver is described which relates the combined pilot-vehicle response measurements, in flight and in the simulator, to the deliberate actions of the pilot. The scope includes not only the psychomotor behavior of the pilot but also the cognitive behavior involved in the pilot's decision as to where to begin the flare maneuver.

Appendix A reviews some existing models of the flare maneuver, considering their strong and weak points. These ideas were taken into account in constructing a revised flare model. The next step was to describe fully the new model, showing how it better explains the recently-acquired landing data as well as encompassing past measurements. The final step in this section will be to discuss a number of performance metrics which arise from the new model formulation. These metrics will then lead to the next section which discusses the formal data analysis of all of the flight and simulator measurements.

Based on the above considerations, a model is proposed of the flare maneuver which covers most, if not all, of the important features noted both in previous models and in the existing data. One important aspect of this proposed model is that there is no added complexity over the other models discussed, in fact there is significant reduction in complexity--so much so that a closed analytic form can be expressed for time histories of altitude, sink rate, normal acceleration, airspeed decay, and touchdown point along the runway. Furthermore it is possible to describe a clear role for the important aircraft properties as well as for the pilot control law properties. This will ultimately aid in developing metrics for analyzing the landing maneuver.

Theoretical Basis. The theoretical basis for the revised model is the assumption of dominant second-order characteristic response which is strongly suggested by the phase planes constructed from flight data. This implies the basic characteristic equation:

$$\ddot{h} + 2\zeta_{FL}\omega_{FL}\dot{h} + \omega_{FL}^2 h = 0 \qquad (4)$$

It is further assumed that this characteristic equation is associated with a pilot-vehicle system having an altitude command loop (outer loop) and that the flare maneuver corresponds to the response from an initial offset with respect to the terminal conditions (i.e., from an initial altitude and sink rate). Thus, analytically, the flare is regarded as an unforced response from a set of initial conditions to a set of desired conditions at touchdown.

In considering the pilot control law implications of a second-order characteristic response, the first step is to examine the aircraft equations of motion, especially with respect to altitude. The complete longitudinal formulation (described in Ref. 17) can be simplified to a second-order, single-axis perturbation form:

$$\ddot{h} + \left(\frac{1}{T_{\theta_1}} + \frac{1}{T_{\theta_2}}\right)\dot{h} + \frac{1}{T_{\theta_1}} \cdot \frac{1}{T_{\theta_2}} h \approx \frac{U}{T_{\theta_2}} \theta \tag{5}$$

Where T_{θ_2} is the dominant first-order lag time constant between a pitch-command, θ, and flight path response,

and T_{θ_1} is the dominant first-order time constant associated with airspeed response.

It can be shown that for operation at or near maximum lift-to-drag ratio, $1/T_{\theta_1} \cdot 1/T_{\theta_2} \approx \omega_p^2$, the phugoid natural frequency squared. In turn, $\omega_p \approx 1\sqrt{2}\, g/U$.

It is instructive to note that the airframe-alone flight path lag, T_{θ_2}, can be expressed in terms of gross weight, W; speed margin above stall, $\mathbb{M}$; and air density, ρ; along with the configuration-dependent parameters: maximum lift coefficient, $C_{L_{max}}$; wing area, S; and lift curve slope, C_{L_α}, i.e.,

$$T_{\theta_2} \approx \frac{\sqrt{2\, C_{L_{max}}\, W/S}}{\sqrt{\rho}\, g\, C_{L_\alpha}\, \mathbb{M}} \tag{6}$$

Thus operationally the amount of flight path lag depends on the square root of gross weight. Hence there is only a small T_{θ_2} variation over a normal range of loadings.

Inference of Pilot Control Strategy. The approach used to infer piloting technique in the landing maneuver was to examine for the difference between a fitted differential equation describing closed-loop motion and the known effective flight path response of the basic airplane. The difference, assuming

negligible atmospheric disturbances, should be the effect of pilot actions and could be interpreted literally as a pilot control law, i.e.,

$$\ddot{h} + 2\zeta_{FL}\omega_{FL}\dot{h} + \omega_{FL}^2 h = 0 \qquad \text{(fitted differential equation of landing maneuver)} \qquad (7)$$

minus

$$\ddot{h} + \left(\frac{1}{T_{\theta_1}} + \frac{1}{T_{\theta_2}}\right)\dot{h} + \omega_p^2 h = \frac{U}{T_{\theta_2}}\theta \qquad \text{(Aircraft flight path equation)} \qquad (8)$$

equals

$$\left(2\zeta_{FL}\omega_{FL} - \frac{1}{T_{\theta_1}} - \frac{1}{T_{\theta_2}}\right)\dot{h} + \left(\omega_{FL}^2 - \omega_p^2\right)h = -\frac{U}{T_{\theta_2}}\theta \qquad \text{(inferred pilot control law)} \qquad (9)$$

Rearranging the result, we obtain

$$\theta = \underbrace{-\frac{\left(\omega_{FL}^2 - \omega_p^2\right)}{U}T_{\theta_2}}_{k_h} h - \underbrace{\frac{2\zeta_{FL}\omega_{FL}T_{\theta_2} - T_{\theta_2}/T_{\theta_1} - 1}{U}}_{k_{\dot{h}}}\dot{h} \qquad (10)$$

or

$$\theta = -k_h h - k_{\dot{h}}\dot{h} \qquad (11)$$

Hence the effective control law should involve an effective feedback of height and vertical velocity. This can be easily seen in graphical terms in Fig. 8

The main value in the above analysis technique is in gaining an appreciation for relative magnitudes of the various pilot and vehicle features at work in the landing maneuver. Certain complications and limitations should be recognized, however.

First there are several of possible ways for the pilot to exhibit the effective height and vertical velocity feedbacks, k_h and $k_{\dot{h}}$. In fact there could be a combination of such alternatives at work involving various perceptual pathways or means of compensation. Figure 9 shows six possible ways in which a vertical velocity equivalent could be established and coupled with a height feedback. The first assumes direct visual perception of vertical velocity either from motion of subtended angular features (e.g., the translation of features which are transversed to the direction of flight) or rotational angular features (e.g., the sides of the runway ahead of the aircraft along the direction of flight). A second possibility, also visual, would be feedback of

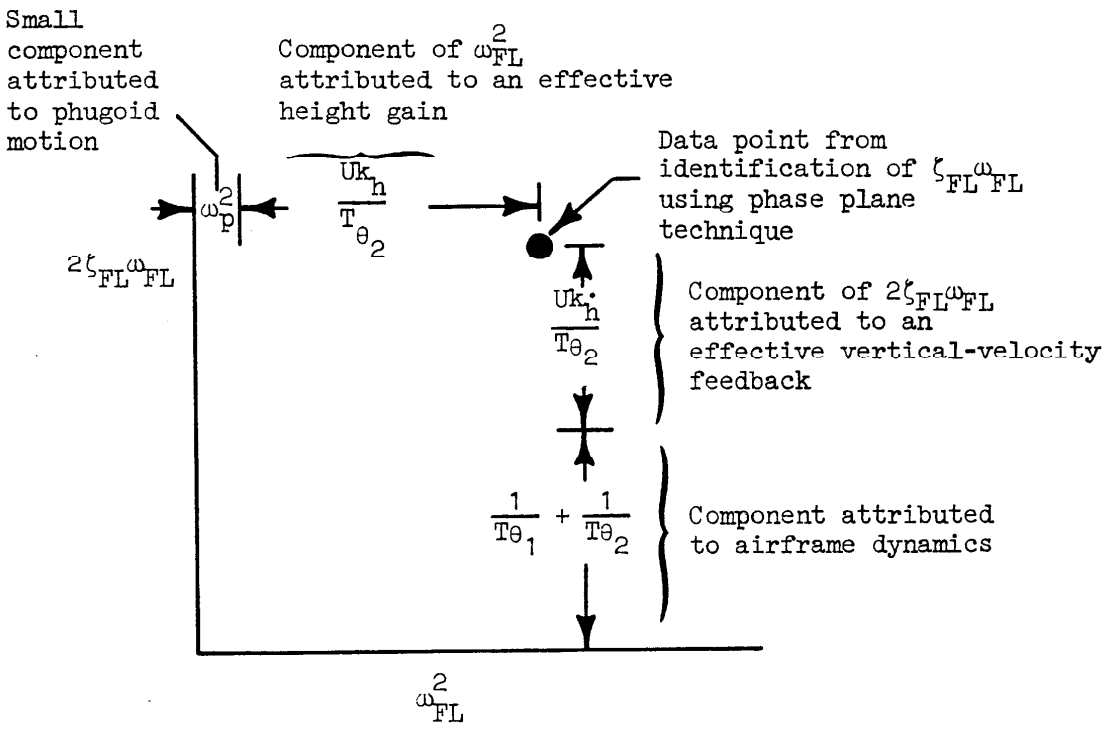

Figure 8. Inference of Effective Height and Vertical Velocity Feedback Gains From a Data Point Plotted As $2\zeta_{FL}\omega_{FL}$ Versus ω_{FL}^2

a. Vertical Velocity Feedback

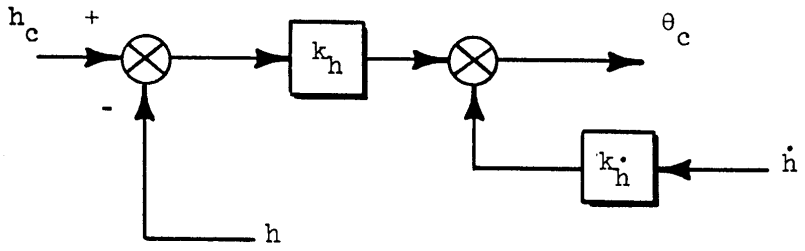

b. Flight Path Angle Feedback

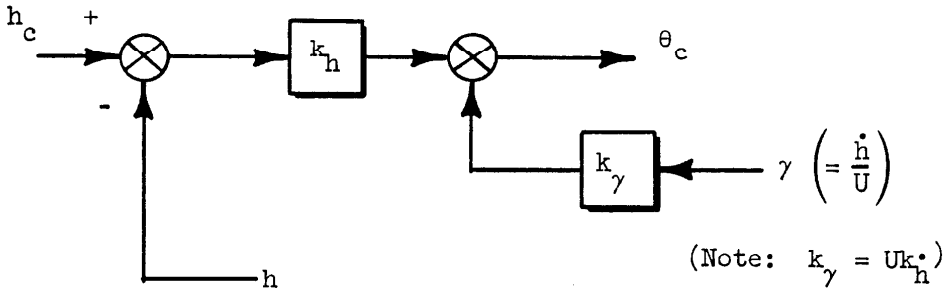

c. Lead-Compensated Height Feedback

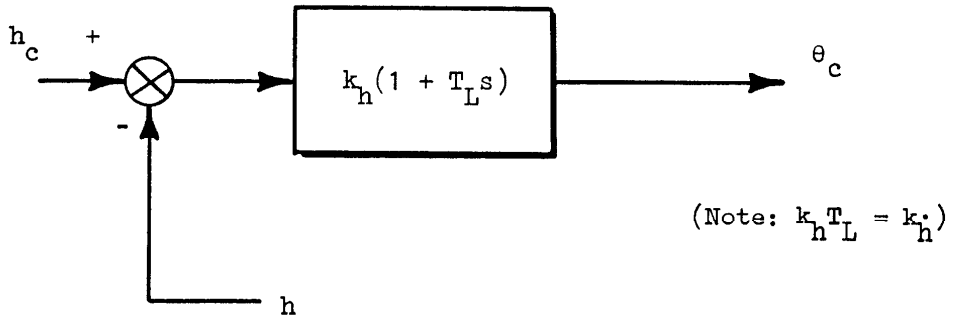

Figure 9. Alternatives for Landing Maneuver Loop Structure

d. First-Order Lead Compensation via Perceptual Preview

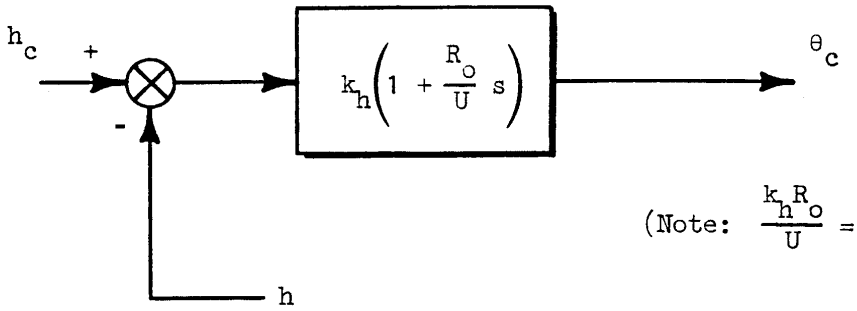

(Note: $\frac{k_h R_o}{U} = k_h T_L = k_{\dot{h}}$)

e. Second-Order Lead Compensation via Perceptual Preview Coupled with a Lagged Pitch Command

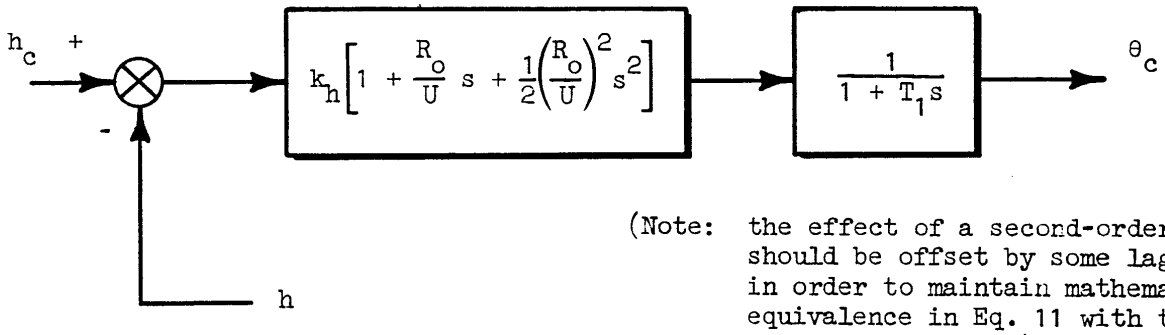

(Note: the effect of a second-order lead should be offset by some lag, T_1, in order to maintain mathematical equivalence in Eq. 11 with the other alternatives)

f. Compensated Vestibular Specific Force Feedback

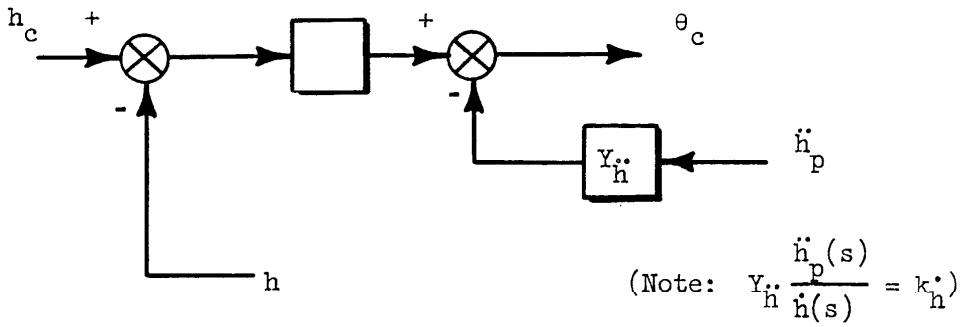

(Note: $Y_{\ddot{h}} \frac{\ddot{h}_p(s)}{\dot{h}(s)} = k_{\dot{h}}$)

(Note also: Y_h represents visual height error gain and lead compensation from any one of cases a through e above. $Y_{\ddot{h}}$ represents vestibular specific force compensation, which may include gain and/or lag compensation to reinforce visual cues.)

Figure 9 (Concluded)

the instantaneous flight path angle which can be detected by perceiving the origin or focus of expansion of streamers (i.e., the point at which there is no relative transverse movement of ground features in the vertical plane). The second possibility is important for another reason: it can be reinforced by the flight path angle symbol in a head-up display. The third and fourth cases involve the pilot-centered generation of a height time derivative, i.e., first-order lead compensation. The third case represents an unspecified computational process in combination with the direct visual perception of altitude; the fourth, a geometric construct based on a preview distance, R_o, in the visual field where the pilot is deriving height information.

A fifth case involves the pilot-centered generation of second-order lead compensation coupled with a first-order lagged (or delayed) pitch attitude command. Second-order lead compensation can be generated in the presence of a curvilinear landing flare (where the focus of expansion no longer exists) by perceiving the inclination of streamers at a preview distance, R_o, in the visual field where the pilot is deriving height information. The instantaneous direction of the flight path in the vertical plane in this case is given by the two (curvilinear) streamers which become horizontal in the left and right peripheral visual fields. A general model for this type of visual field information in horizontal curvilinear flight is presented in Ref. 18. Several possible sources of lag or delay in establishing a change in the pitch attitude will be discussed subsequently. Finally, a sixth possibility would be an acceleration- and/or velocity-like feedback based on vestibular perception of specific force to reinforce the compensation of visual cues from any one of cases a through e in Fig. 9. The relative likelihood of each of these will be discussed in the analysis of the data.

Other complicating factors involve the presence of additional sources of lag beyond those associated with short-term flight-path response (T_{θ_2}) and longer-term flight-path/airspeed response (T_{θ_1} or ω_p). One known source of additional lag is the closed-loop response of pitch attitude following a pilot command. As a rough approximation to the net effect, the inverse closed-loop bandwidth for pitch control, $1/\omega_{c_\theta}$, can be added to the flight path response lag, T_{θ_2}. The goodness of this kind of approximation depends upon the spectral range of interest (relative to $1/T_{\theta_2}$ and ω_{c_θ}) and the amount of spectral separation (the approximation is fairly good for frequencies at or below $1/T_{\theta_2}$ so long as $\omega_{c_\theta} > 3/T_{\theta_2}$).

Another source of lag could be in the pilot's deciding to hold or change the pitch attitude command itself. If we had a time history of pitch attitude, this effective lag would be manifested by the degree to which the pilot is aperiodically "stepping" pitch attitude during the flare. There are indications from other sources (Ref. 19) that pilots will apply an initial step in attitude to start the flare, pause to see the effect on flight path, then apply subsequent attitude steps. This would resemble a sampled-data process, and the consequent lag or delay would thus be associated with the pilot's cognitive and psychomotor processes in commanding pitch attitude.

A summary of the landing model maneuver including the components discussed above is shown in Fig. 10. It will not be possible to identify precisely the various features labeled in Fig. 10 due to the limitations of the data available. It will be possible, however, to derive certain insights based on the nature of "equivalent system" parameters which lump together the pilot and vehicle characteristics just identified. This model is presented next.

The foregoing theoretical development suggests the following:

- The flare maneuver can be described in terms of a closed-loop frequency, ω_{FL}, and damping ratio, ζ_{FL}
- The pilot control strategy should involve the equivalent of height and vertical velocity feedbacks, weighted by gains k_h and $k_{\dot{h}}$, respectively
- Various sources of lag or delay should be expected along with the basic airframe lags, T_{θ_1} and T_{θ_2}.

Taken together, the above considerations suggest the following lumped-parameter model with four undetermined coefficients k_h, T_L, T_I, and k_γ,

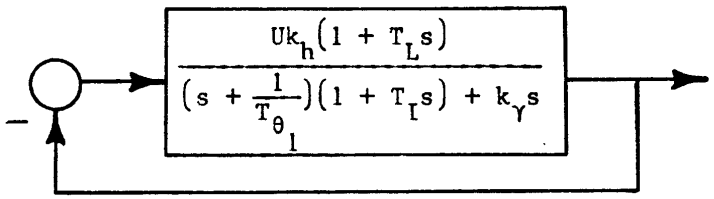

where k_h is the pilot's height feedback gain, the lag time constant T_I subsumes all sources of pilot and airframe lag or delay, excluding the known flight path/airspeed factor, T_{θ_1}, the lead time constant T_L represents the pilot's equivalent vertical velocity feedback-to-height lead ratio, and the gain k_γ weights the pilot's equivalent flight path angle feedback.

If the above lumped-parameter model were to produce a second-order closed-loop response, then the following relationships must exist:

$$2\zeta_{FL}\omega_{FL} = \frac{1}{T_{\theta_1}} + \frac{1}{T_I}\left(1 + k_\gamma - \frac{T_L}{T_{\theta_1}}\right) + T_L\,\omega_{FL}^2 \qquad (12)$$

and

$$\omega_{FL}^2 = \frac{Uk_h}{T_I} + \frac{1}{T_{\theta_1} T_I} \qquad (13)$$

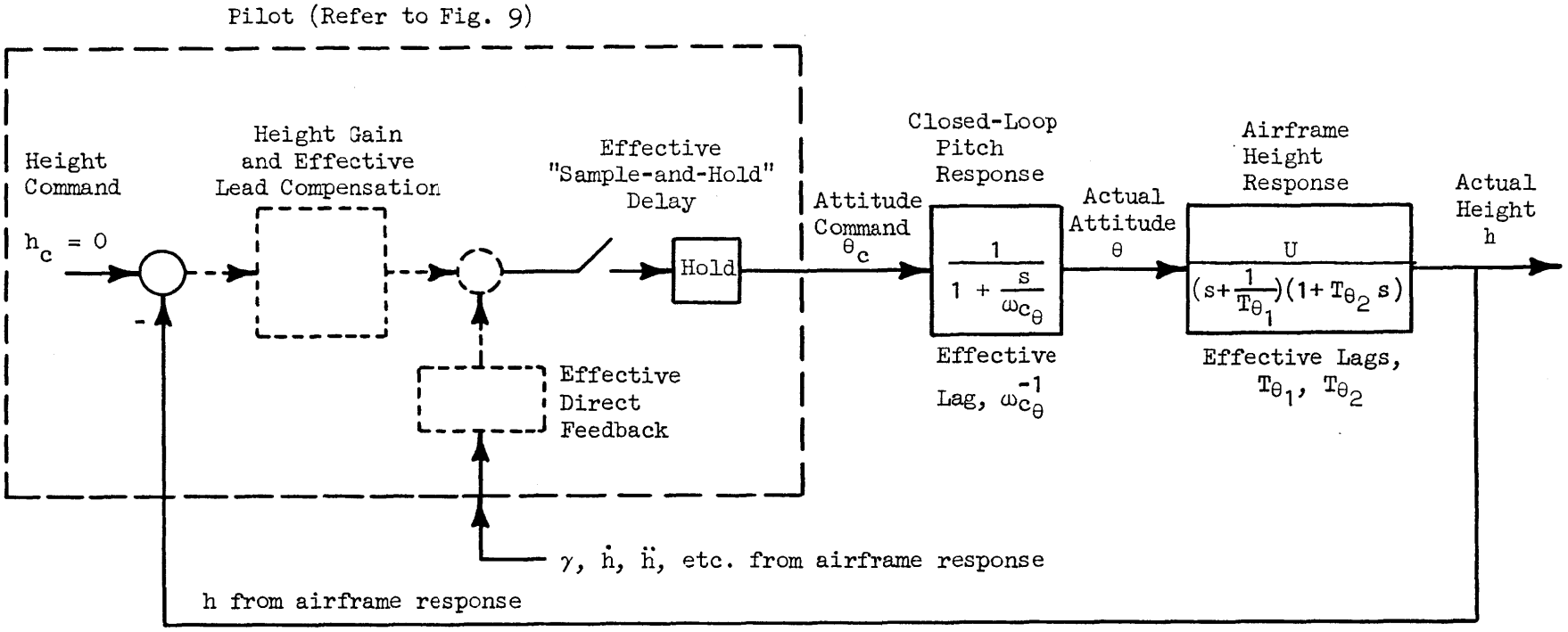

Figure 10. General Model of Landing Maneuver Showing Pilot and Vehicle Components

Hence a data point plotted in the $2\zeta_{FL}\omega_{FL}$ versus ω_{FL}^2 plane would have the properties shown in Fig. 11. Note that for a single data point (only two coordinates, $\zeta_{FL}\omega_{FL}$) there is an ambiguity among k_γ, T_L, and T_I and, as a consequence, k_h. This matter can be resolved, though, if ensembles of landing data are considered. This matter will be reopened shortly when examining the experimental results.

As a final step in the theoretical development of the landing maneuver model, the nature of the maneuver in terms of time history and phase plane solutions will be examined. This will be important in the data reduction process presented shortly.

Recalling the general second-order characteristic response form:

$$\ddot{h} + 2\zeta_{FL}\omega_{FL}\dot{h} + \omega_{FL}^2 h = 0 \tag{14}$$

The following solutions can be found using inverse Laplace transforms:

$$h(t) = \frac{\dot{h}_{TD}}{b} e^{-at} \sin bt \tag{15}$$

$$\dot{h}(t) = \dot{h}_{TD} e^{-at} \left(\cos bt - \frac{a}{b} \sin bt\right) \tag{16}$$

$$\ddot{h}(t) = -2a\dot{h}(t) - \omega_{FL}^2 h(t) \tag{17}$$

where $a \triangleq \zeta_{FL}\omega_{FL}$

$$b \triangleq \omega_{FL}\sqrt{1 - \zeta_{FL}^2}$$

and at touchdown, $t = 0$, $\dot{h} = \dot{h}_{TD}$, and $h = 0$

(Note that in this formulation the flare begins at some negative value for time and runs until touchdown at zero time.)

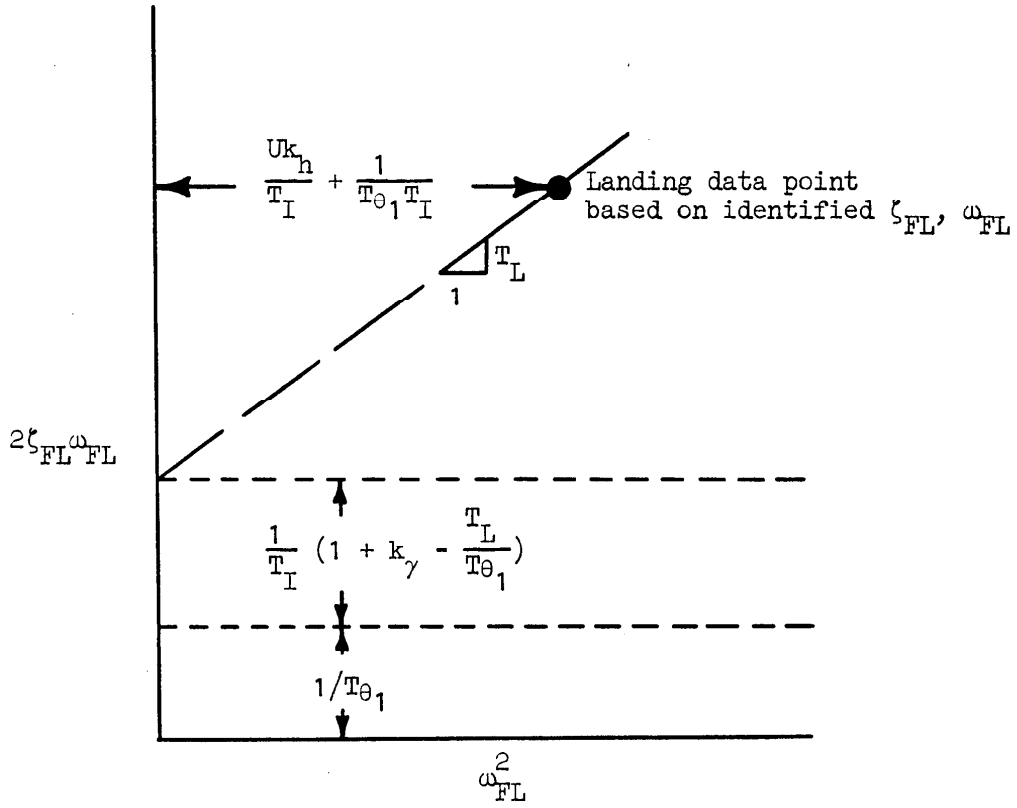

Figure 11. Theoretical Relationships Governing the Coordinates of a Single Landing Data Point Based on Eqs. 12 and 13 in the Text

In view of the earlier stated preference for viewing the acquired landing data in the phase plane domain, consider the above analytic solutions in those terms. Figure 12 shows sink rate versus the flare-height/natural-frequency product both normalized by touchdown sink rate. This view provides some insight to the maneuver, namely, that the reduction of sink rate relative to the maximum sink rate is a strong function of damping ratio. A clearer picture of that can, however, be shown if instead the trajectories are normalized by the maximum sink rate. As Fig. 13 reveals, all of the trajectories are approximately the same shape but stacked according to damping ratio--and proportion of final sink rate reduction. If one last step is taken and the trajectories are superimposed (Fig. 14), then the following statements can be made:

- The shape of the trajectory is mainly a function of ω_{FL}
- The proportion of sink rate reduction is mainly a function of ζ_{FL}

These observations are therefore of considerable value in identifying the effective closed-loop response parameters in the flight and simulator phase planes.

In addition the normalized plot of acceleration versus altitude shown in Fig. 15 indicates that the peak acceleration in the final flare maneuver is approximately independent of damping ratio, i.e., that:

$$\ddot{h}_{max} \approx 0.45\ \omega_{FL}\ |\dot{h}|_{max}$$

However the height at which $\ddot{h}_{max}$ occurs is a strong function of damping--soft landings have an early application of acceleration and hard landings have a late application.

Numerical Descriptions. A number of analytical relationships have been developed for describing the aircraft and the landing maneuver. At this point, it is appropriate to consider them in numerical terms which relate to the data being studied.

Table 1 lists the aircraft model parameters which are representative of the DC-10 based on various sources and estimates. No formal description of the DC-10 was available, but the values should be considered reasonably accurate and applicable to the ranges of conditions encountered in both the flight and simulator landings.

Performance Metrics. The foregoing analytical development now can be used to devise several possible performance metrics which are relevant to the landing maneuver. Again, one is interested in not only the final touchdown condition but also in how it is achieved in terms of piloting technique.

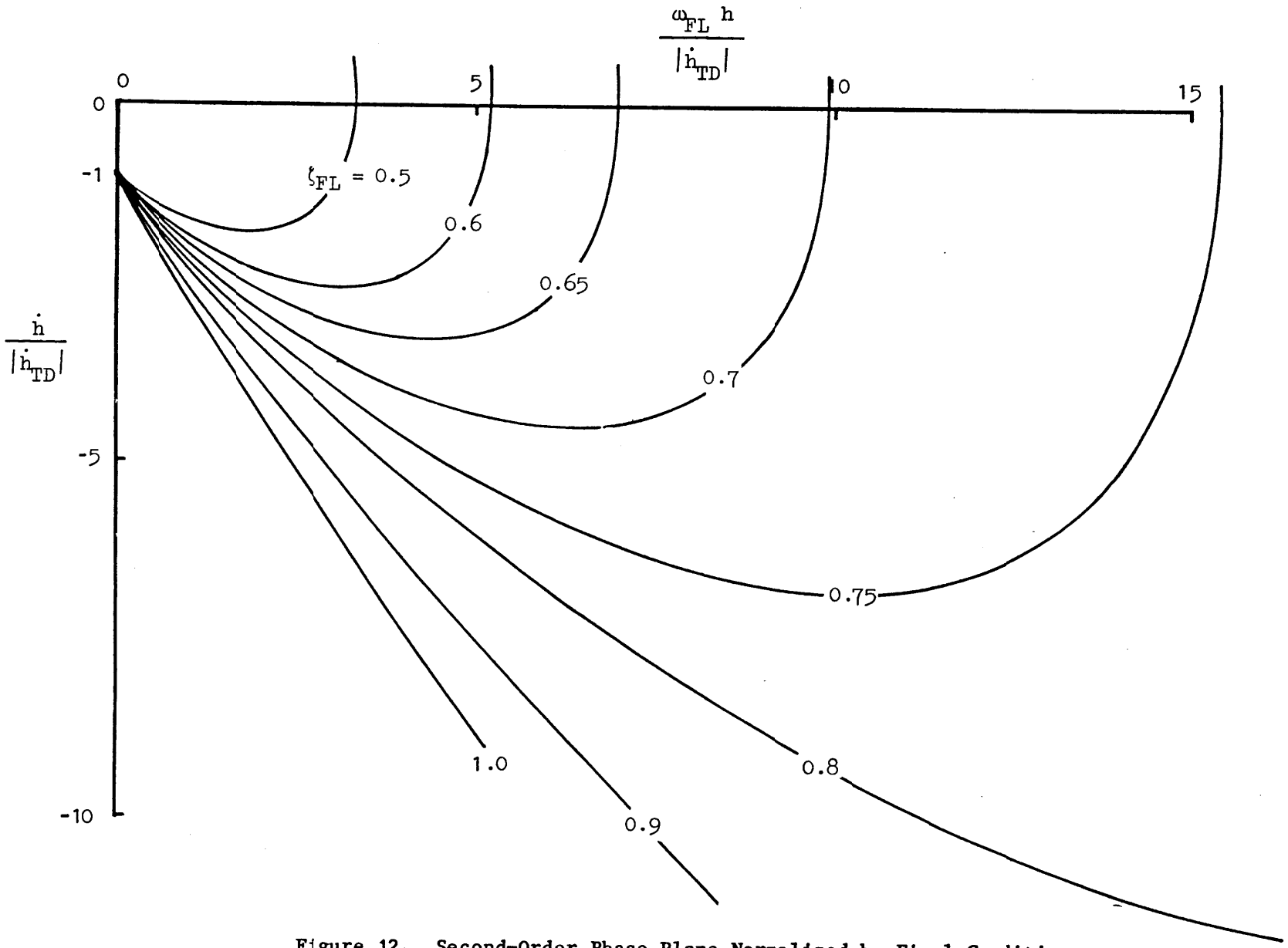

Figure 12. Second-Order Phase Plane Normalized by Final Condition

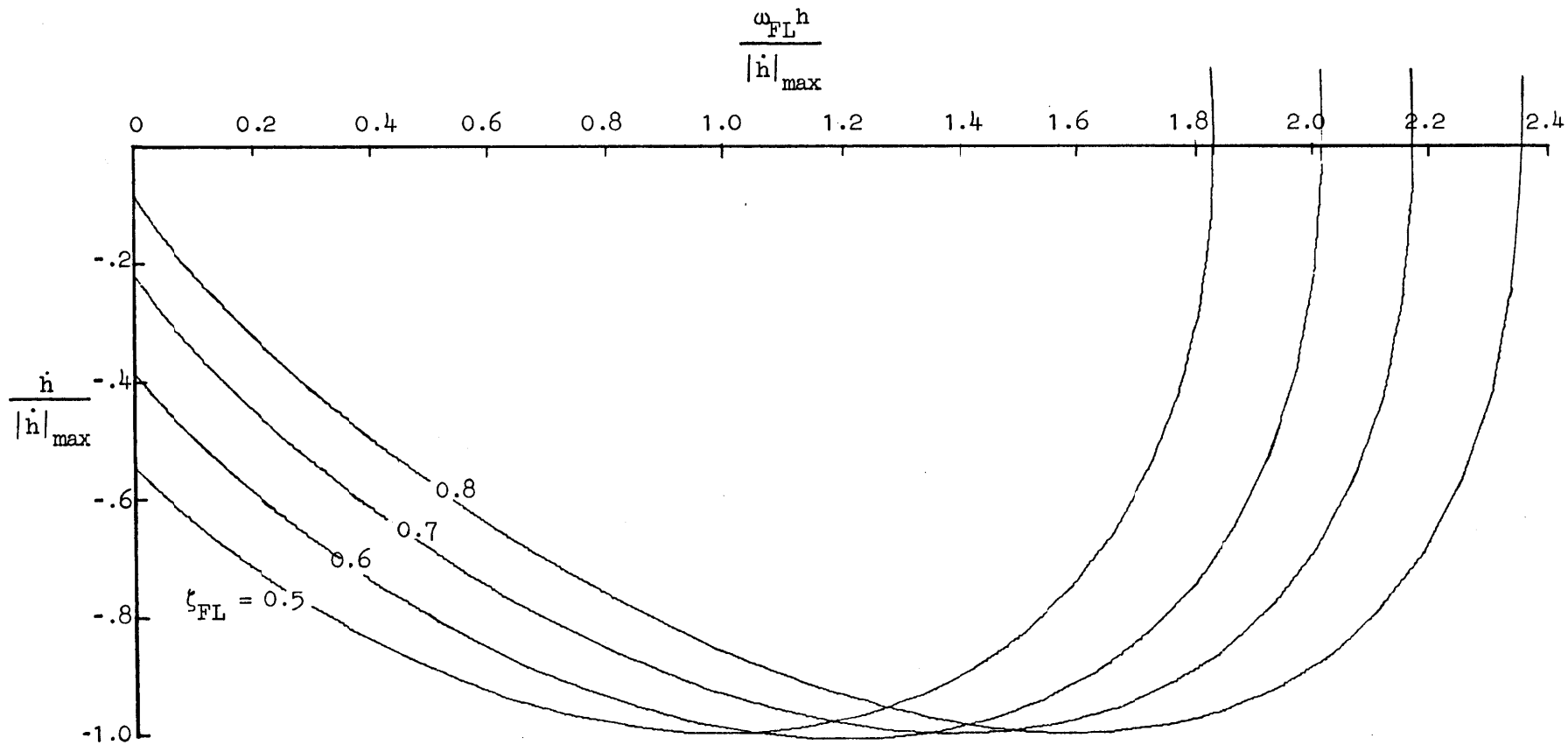

Figure 13. Normalized Second-Order Phase Planes

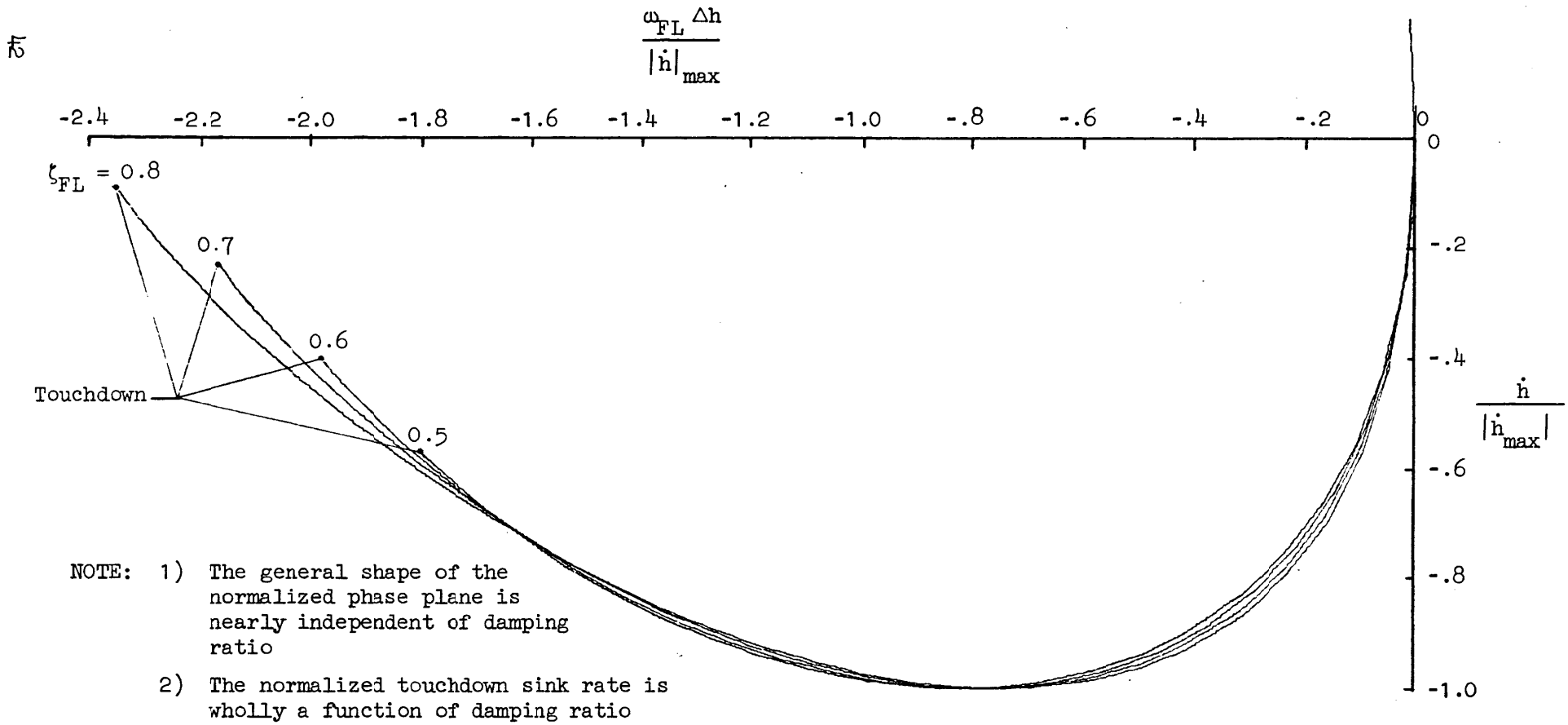

Figure 14. Normalized Second-Order Phase Planes Superimposed

NOTE: The peak normalized acceleration is nearly independent of damping ratio

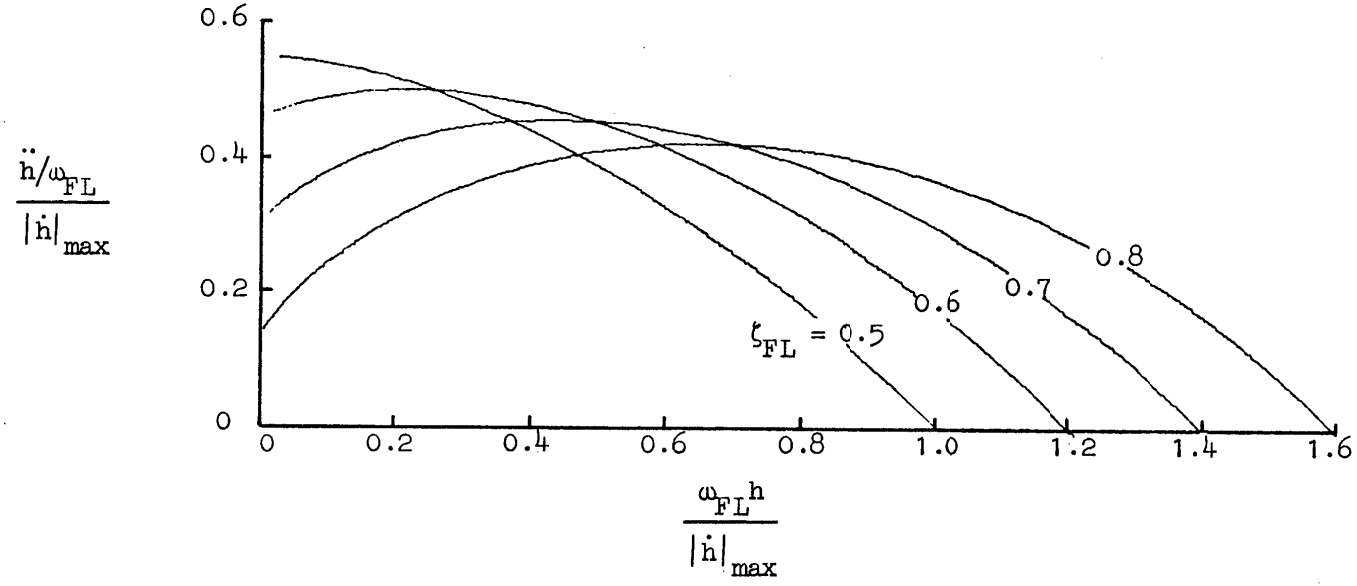

Figure 15. Normalized Acceleration Versus Altitude

TABLE 1

AIRCRAFT PARAMETERS*

Type: DC-10-10

Dimensional Data:

Wing Area, $S = 3861$ ft^2*

Aspect Ratio, $R = 6.8$*

Fuselage Length, $\ell_F = 170.5$ ft*

Pilot Position re c.g. $\approx$ 85 ft†

Tail a.c. re c.g. $\approx$ 64 ft†

Mass Data:

Average Gross Weight, $W \approx 300{,}000$ lb

Pitch Moment of Inertia, $I_y \approx 11 \times 10^6$ slug-ft^2†

Aerodynamic Data (Landing Flaps):

Lift Curve Slope, $C_{L_\alpha} \approx 4.9$/rad†

Maximum Approach Lift-to-Drag ratio, $(L/D)_{max} \approx 7$†

Flight Condition:

Average Approach Speed, $U \approx 130$ kt ≈ 220 ft/sec

Average Approach Sink Rate ≈ -11.5 ft/sec ≈ -690 ft/min

Estimated Dynamic Response Parameters:

Heave Time Constant, $T_{\theta_2} \approx 1.8$ sec

Speed Time Constant, $T_{\theta_1} \approx 13$ sec

Phugoid Frequency, $\omega_p \approx 0.21$ rad/sec

---

* Ref. 20.

† Estimated

First consider the following list of features of the landing maneuver which play a role in determining success or failure, good or bad, safe or unsafe:

- Controllability--compensation for off nominal conditions or disturbances without or within the aircraft

- Precision--tolerances on standards for achieving the desired touchdown point, sink rate, lateral position and drift, heading, and airspeed

- Timing--relative quickness of the maneuver, i.e., fast enough to: (a) avoid excessive airspeed decay while airborne and (b) get close enough to perceive usable height and vertical velocity information

  --but slow enough to maintain good control of pitch attitude.

- Limits--stay within runway confines, aircraft structure limits, and acceptable passenger comfort and opinion

- Excess Control Capacity (Workload)--preserve a margin of capacity to attend to other control axes, cope with emergencies or disturbance upsets, maintain communication within the cockpit.

Several conventional metrics exist which address the above features. Some are based on control theory, others on subjective opinion. A general list applicable to a variety of piloting tasks, including the landing maneuver, is given in Table 2. Carrying the sequence to a more definitive level, Table 3 then gives a set of various theoretical and empirical relationships for various metrics. Many of these are restatements from earlier sections of this report.

One significant implication of the above lists of task features and performance metrics is that there are many ways to quantify the various aspects of the landing maneuver. Some parameters are more esoteric than others, but all have a degree of relevance depending upon one's area of interest--loop structure, overall response, aerodynamics, etc. For example, the sink rate reduction ratio, h_{TD}/h_{max}, would have clear meaning to the pilot, instructor, or observer. The ratio can also be translated into a closed-loop damping ratio or to phase margin in order to consider stability. Damping ratio, in turn, can be related to effective loop gains in order to consider perceptual pathways. Therefore it is not the intent to pick a "most-favored" parameter or metric, rather it is to make the inter-relationships clear and use what is most convenient or meaningful for a given situation.

TABLE 2

METRICS WHICH DESCRIBE FEATURES OF A PILOTING TASK

FEATURE	CORRESPONDING METRICS
Controllability	Phase margin, closed-loop damping ratio, effective feedback gains, pilot opinion
Precision	Variance of state variables during the maneuver and at the end, pilot and observer's opinion
Timing	Closed-loop bandwidth, crossover frequency, natural frequency, damped frequency, effective feedback gains (especially height)
Limits	Absolute maxima and minima of final states, cumulative probability of exceedence
Excess Control Capacity	Effective controlled element type, phase margin, slope of frequency response amplitude at crossover, pilot opinion

TABLE 3

THEORETICAL AND EMPIRICAL RELATIONSHIPS AMONG METRICS

Closed-Loop Damping Ratio, ζ_{FL}

$$\zeta_{FL} = 0.83 - 0.6 \frac{\dot{h}_{TD}}{\dot{h}_{max}}$$ (empirical fit to second-order response model--see Fig. 18)

Closed-Loop Natural Frequency, ω_{FL}

$$\omega_{FL} = 1.6 \frac{\dot{h}_{max}}{\Delta h_1}$$ (see Fig. 12)

Where Δh_1 is the virtual height to flare from maximum sink rate to level flight

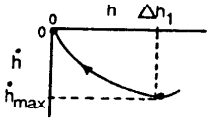

$$\omega_{FL} = 2.4 \frac{\dot{h}_{max}}{\Delta h_2}$$ (see Fig. 12)

Where Δh_2 is the virtual height to make an s-shaped flare starting and ending in level flight (width of a phase plane half cycle).

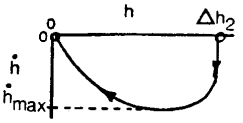

Closed-Loop Damped Frequency, b

$$b = \omega_{FL}\sqrt{1 - \zeta_{FL}^2}$$ (definition of damped frequency)

Height-to-Attitude Transfer Function, $\frac{h}{\theta}(s)$

$$\frac{h}{\theta}(s) = \frac{U}{\left(s + \frac{1}{T_{\theta_1}}\right)\left(T_{\theta_2} s + 1\right)}$$ (see Ref. 17 and Table 1)

Airframe Response Parameters

$$\omega_p^2 = \frac{2g^2}{U^2}$$

$$T_{\theta_2} = \frac{2m}{\rho S C_{L_\alpha} U}$$ (see Ref. 17 and Table 1)

$$T_{\theta_1} = \frac{1/T_{\theta_2}}{\omega_p^2}$$

RESULTS

The results of the analysis of this training experiment are divided into three main parts:

- Nominal piloting technique for the landing maneuver
- Training effectiveness of flight versus simulator
- Simulator fidelity and validity.

In each case performance and piloting technique are considered and the cause-effect relationships discussed.

Phase Plane Trajectories

The starting point for the data analysis is the set of phase plane trajectories for all of the flight-trained and simulator-trained subjects. A complete set of applicable phase planes are provided for each pilot in a chronological sequence. The plots are further classified, first according to the pilot's training background and, second according to the approximate goodness of the landing in terms of touchdown sink rate. On this latter count, the landings were divided mainly on the basis of whether they exceeded 5 ft/sec. (Recall that the design-limit touchdown sink rate of the DC-10 is 10 ft/sec.) The phase plane trajectory classification will now be described in more specific terms.

The phase plane trajectories for all of the flight-trained subjects are shown in Fig. 16. As described earlier, the only trajectories available for the flight-trained subjects were for the three NASA check ride landings--no data were recorded for the training landings. The flight-trained subjects are further divided in terms of their apparent success. Group FA consists of all of those flight-trained pilots who demonstrated landings with touchdown sink rates of 5 ft/sec or less along with no obvious tendency to float or with no obvious height misjudgment tendency. (Two landings in this group slightly exceed 5 ft/sec, but the generally consistent performance exhibited by the pilots involved did not warrant exclusion.) Group FC, in Fig. 16, are those subjects who did not fall within the landing criteria just described.

Phase plane trajectories for the simulator-trained pilots are shown in Fig. 17. Data for the training-phase simulator landings are followed by the three actual landings for the NASA check ride. (The actual landings are easily distinguished from the simulator landings by the smoothness of the simulator trajectories.) The pilots in the simulator-trained group are further divided into three subgroups: SA, SB, and SC. As with the flight-trained pilots, the

a. Group FA (Check ride landings consistently less than 5 ft/sec)

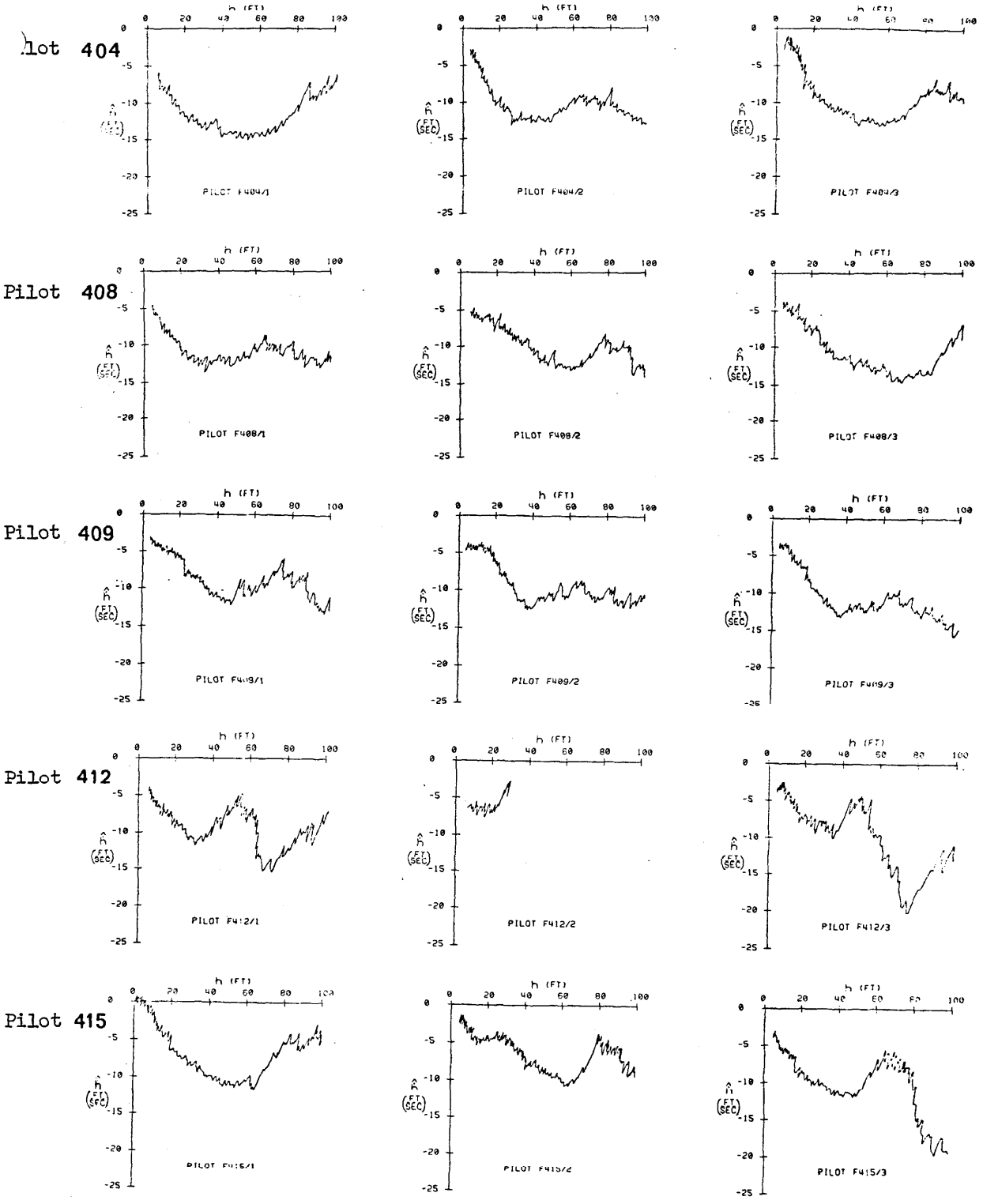

Figure 16. Landing Trajectory Phase Planes for Flight-Trained Subjects

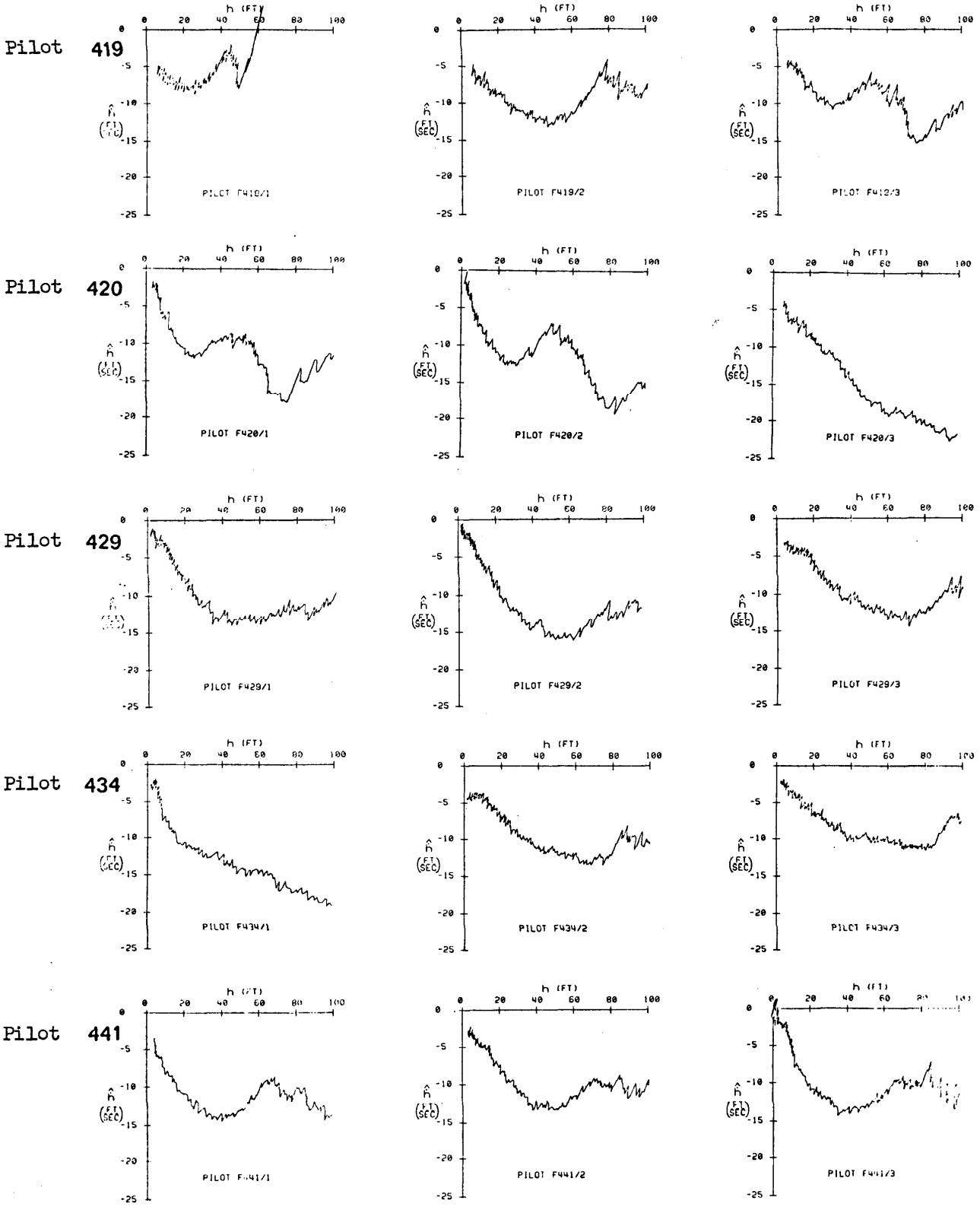

Figure 16. (Continued)

b. Group FC (Check ride landings harder than 5 ft/sec or height misjudgment tendencies)

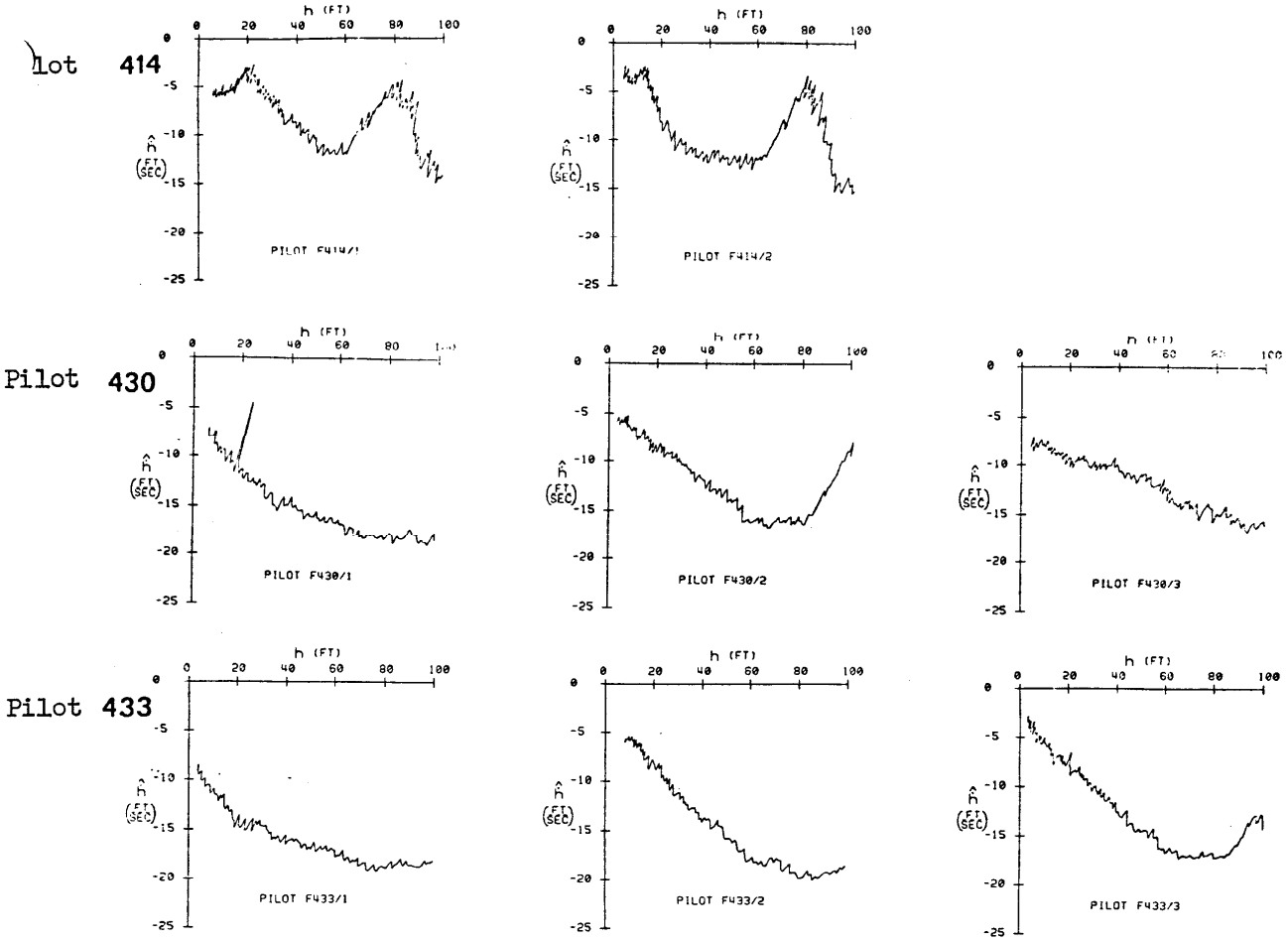

Figure 16. (Concluded)

a. Group SA (Check ride landings consistently less than 5 ft/sec)

Pilot 413

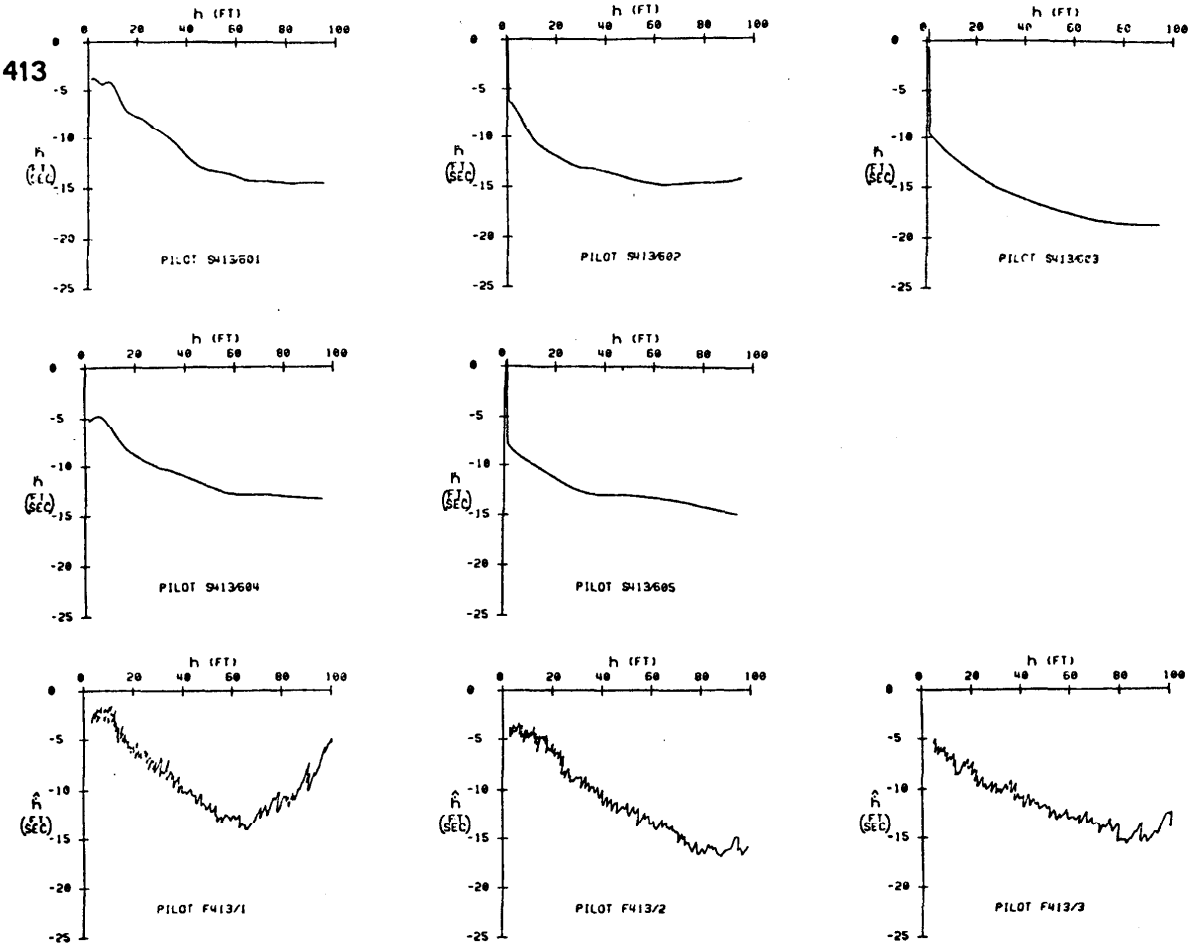

Figure 17. Landing Trajectories for Simulator-Trained Subjects (Simulator Training Plus NASA Check Ride Cases)

Group SA (Continued)

Pilot 418

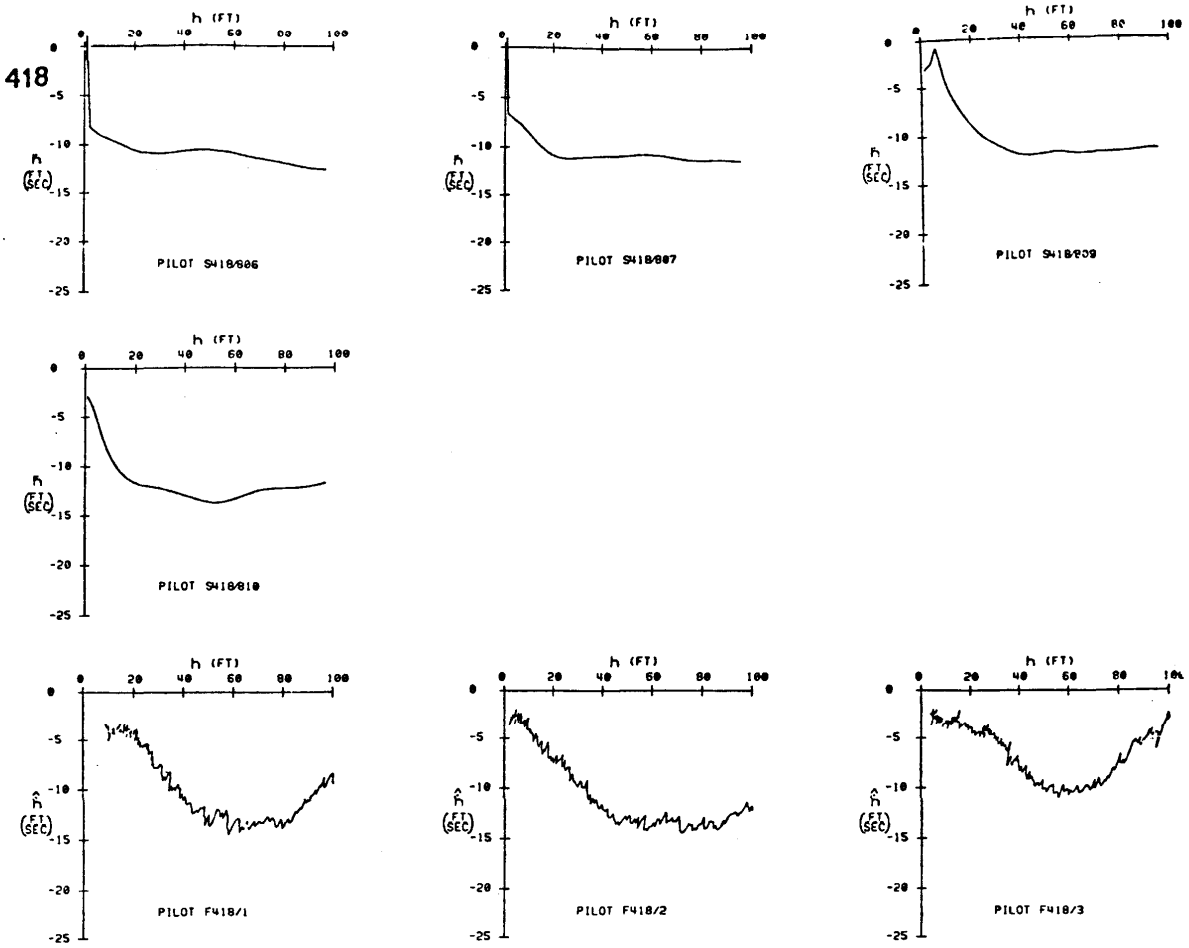

Figure 17. (Continued)

Group SA (Continued)

Pilot 421

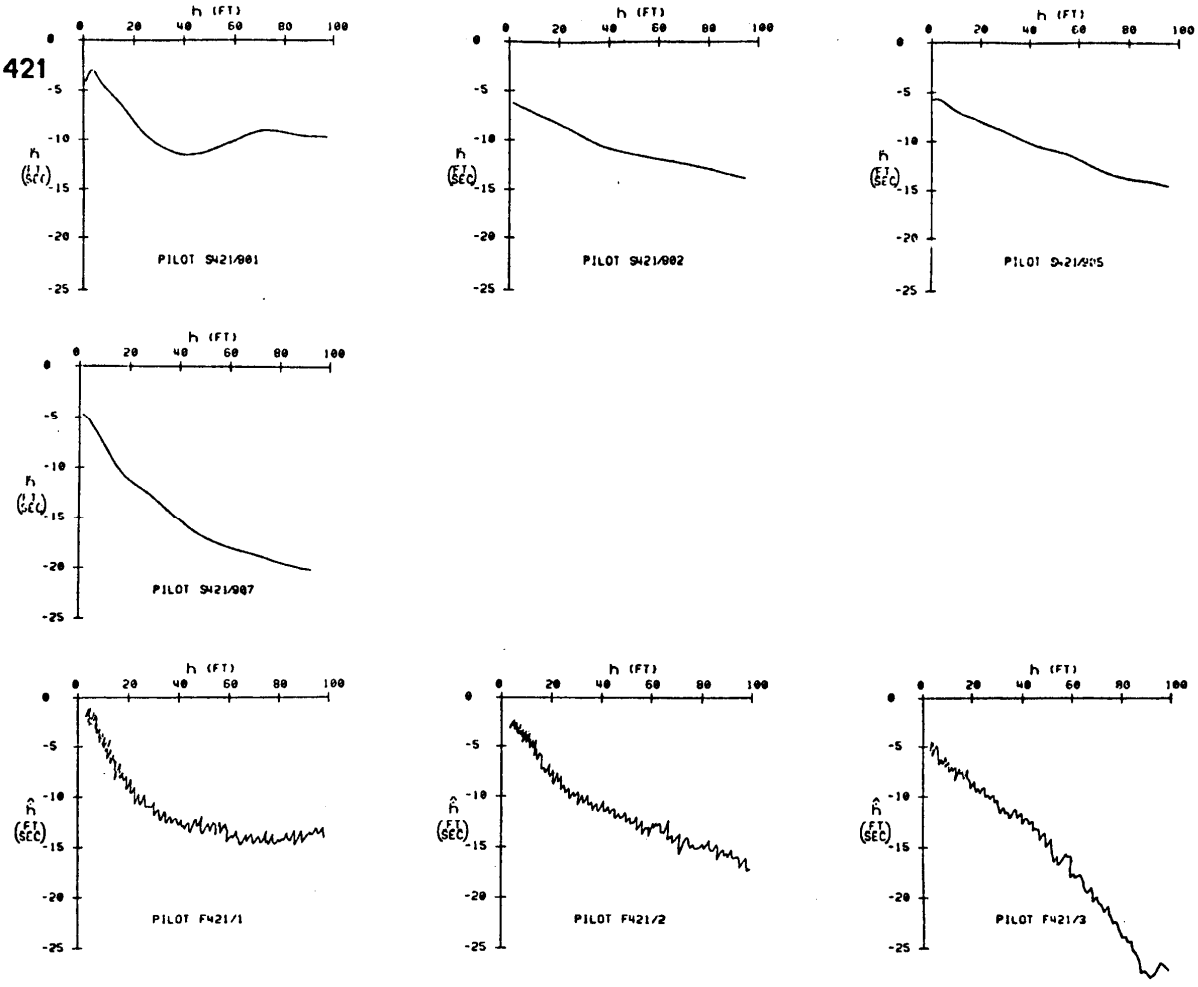

Figure 17. (Continued)

Group SA (Continued)

Pilot 423

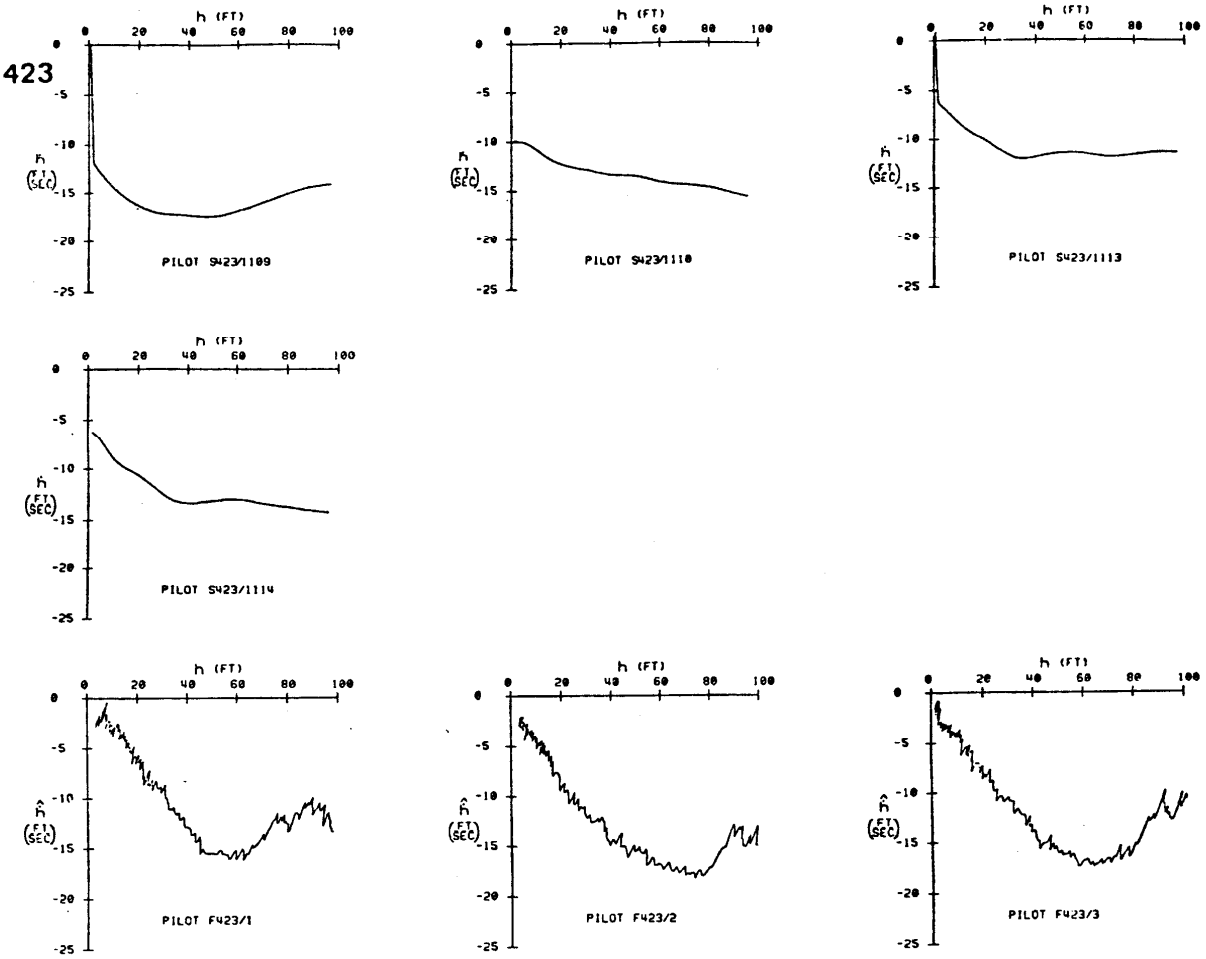

Figure 17. (Continued)

Pilot 424

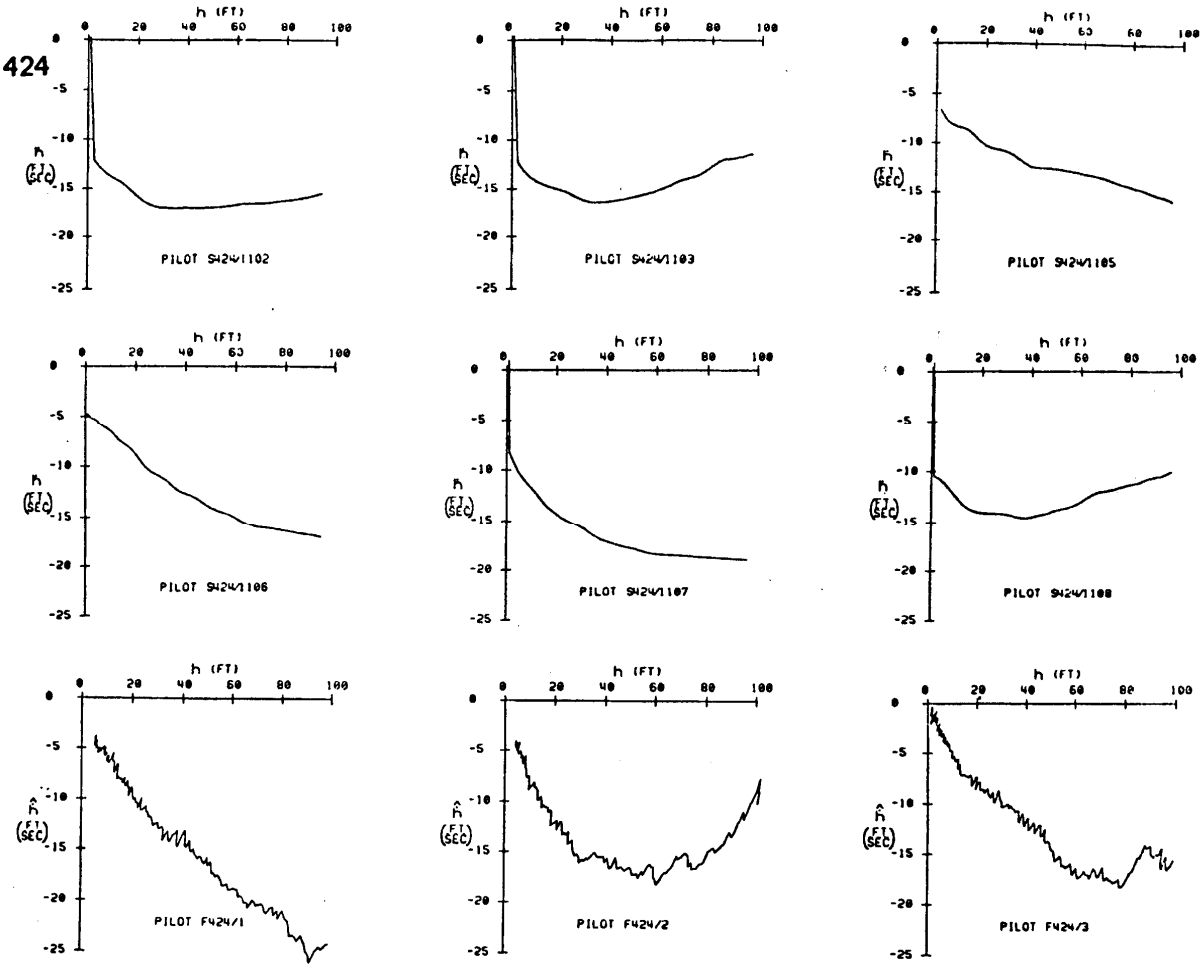

Pilot 432

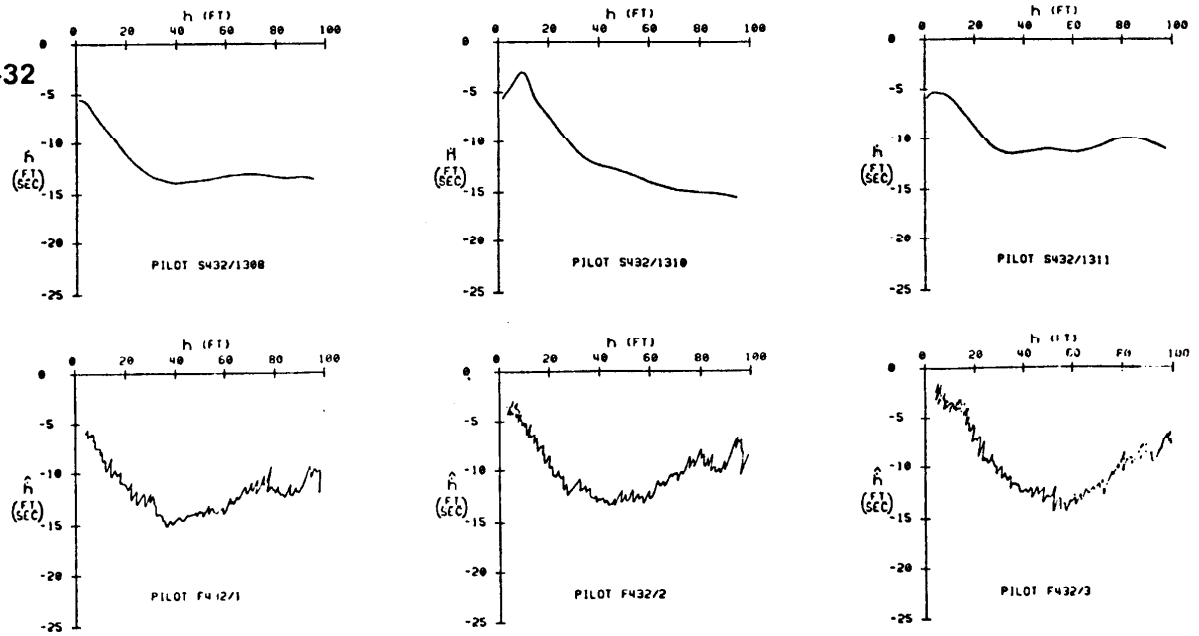

Figure 17. (Continued)

Group SA (Continued)

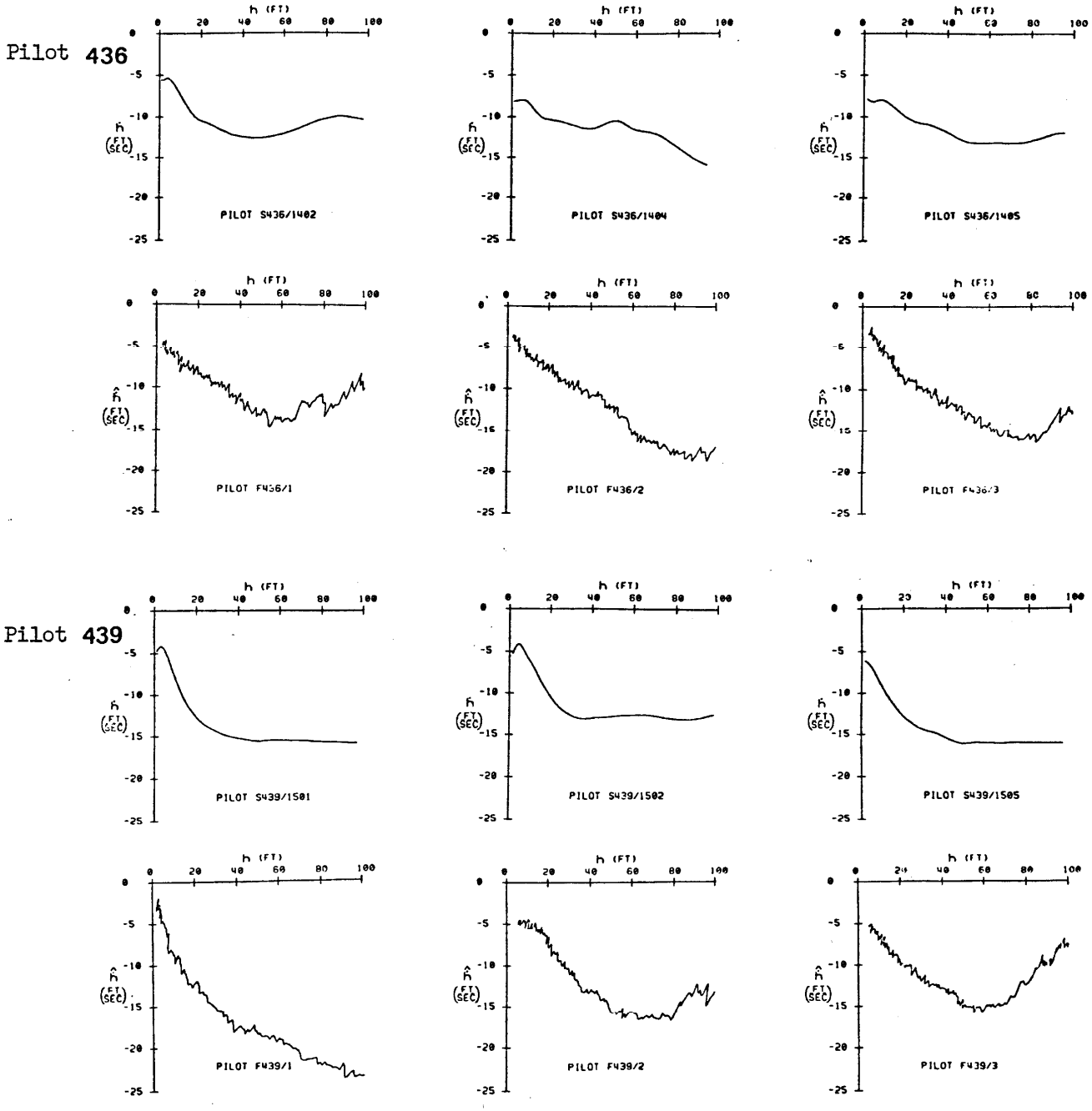

Figure 17. (Continued)

Group SA (Concluded)

Pilot 443

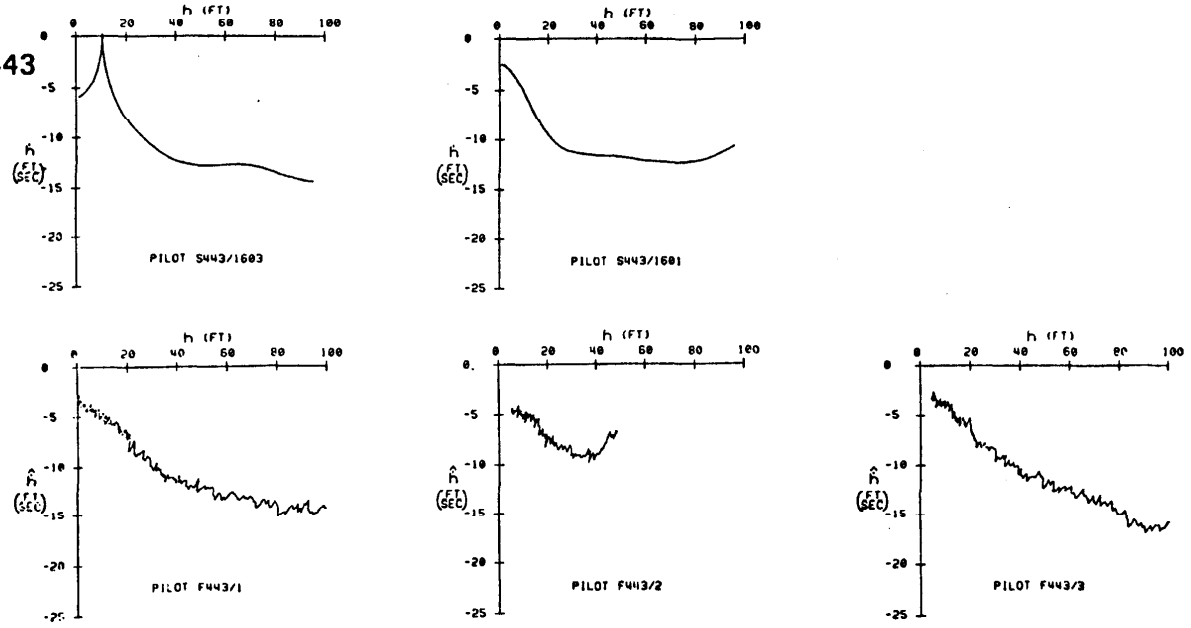

Figure 17. (Continued)

b. Group SB (First check ride landing harder than 5 ft/sec but followed by continual improvement)

Pilot 402

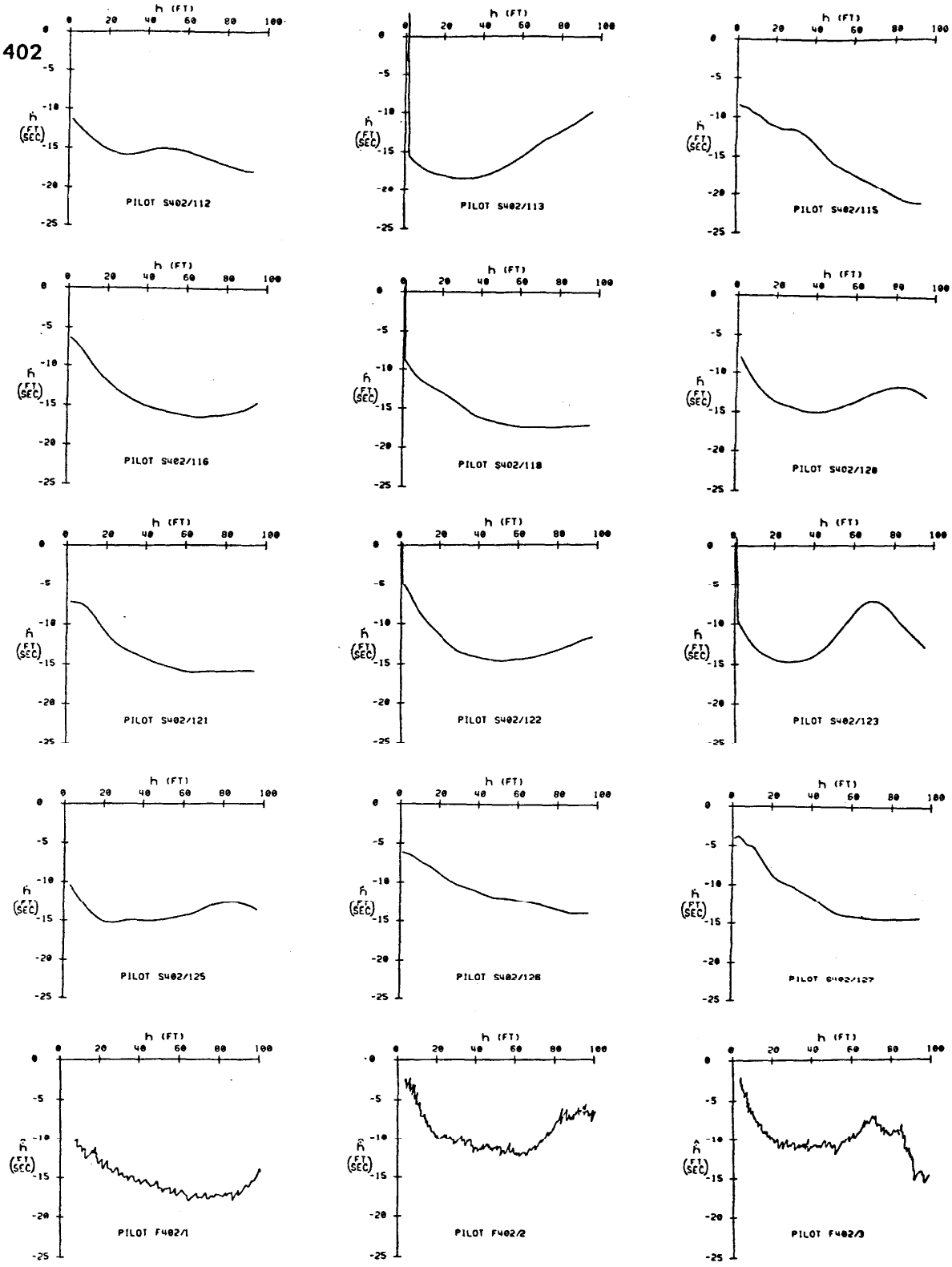

Figure 17. (Continued)

Pilot 403

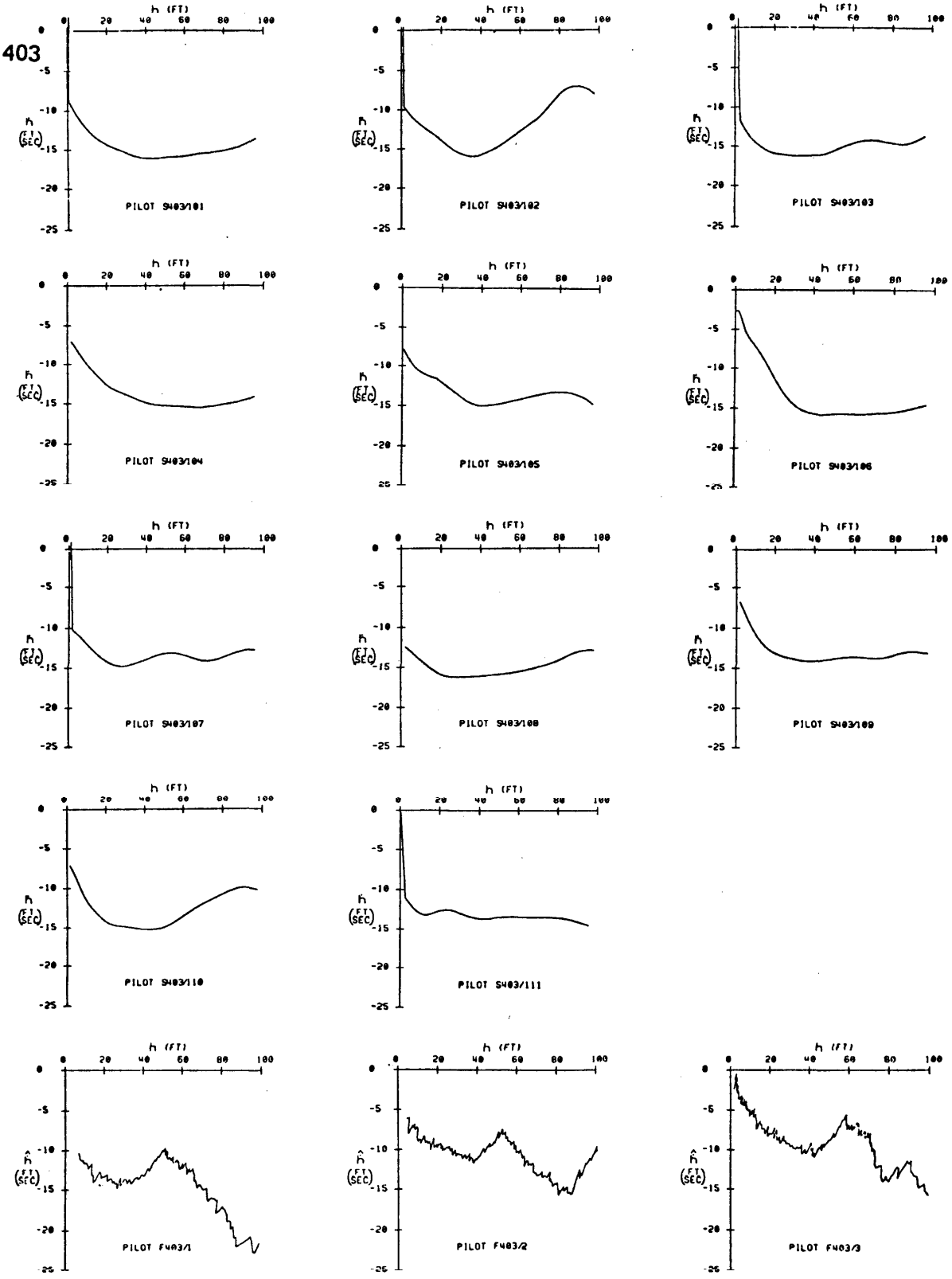

Figure 17. (Continued)

Group SB (Continued)

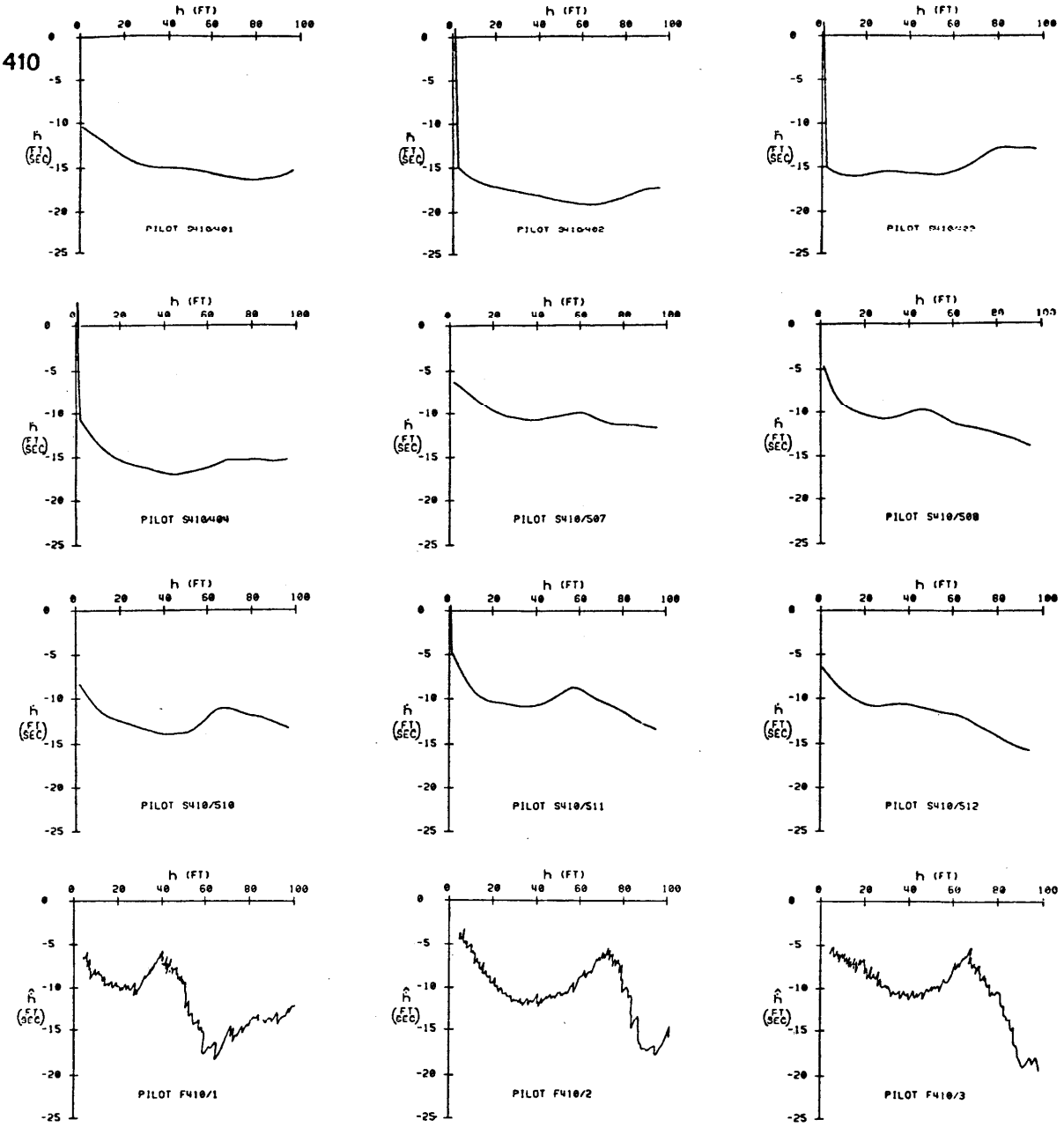

Figure 17. (Continued)

Pilot 417

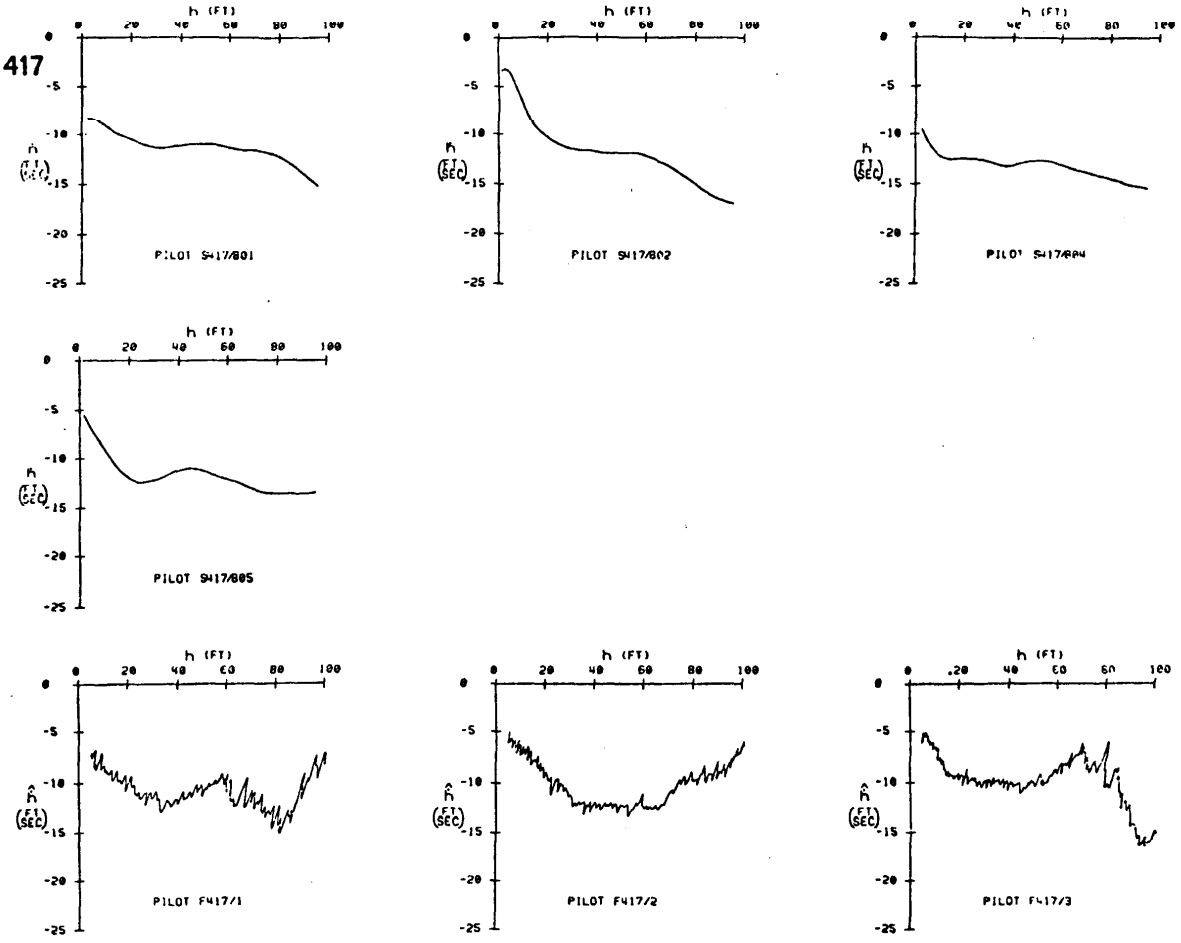

Figure 17. (Continued)

Group SB (Continued)

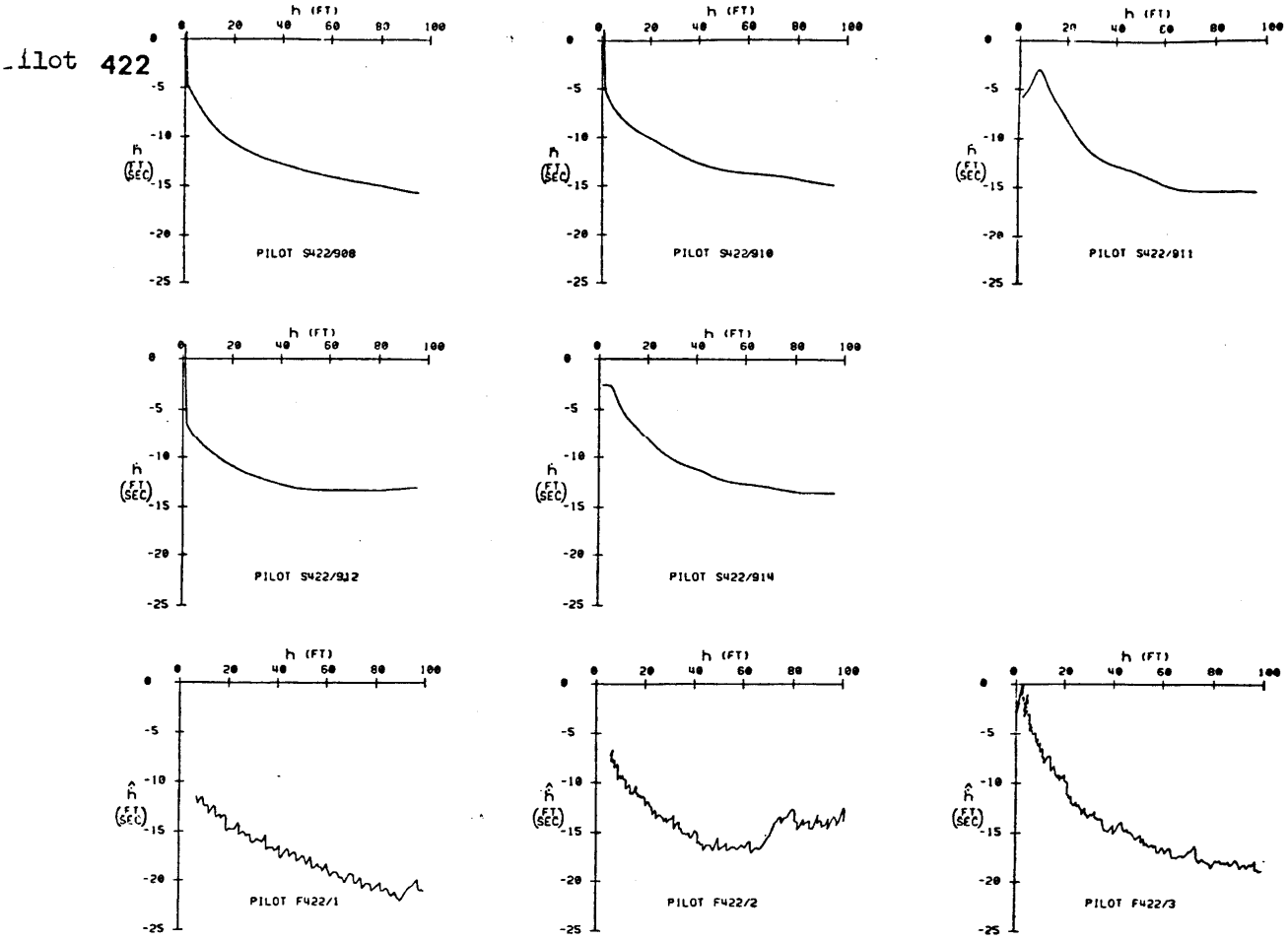

Figure 17. (Continued)

Pilot 431

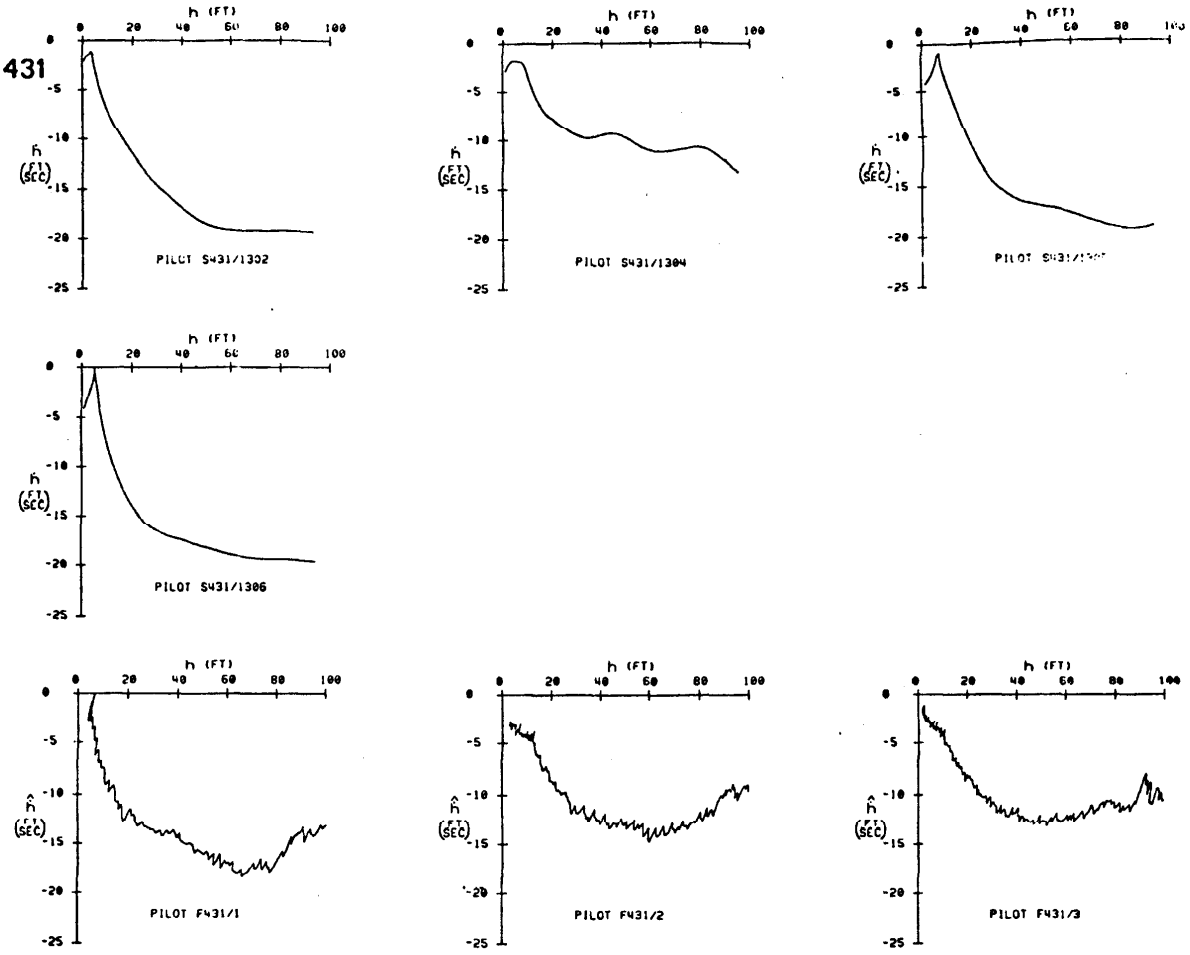

Figure 17. (Continued)

c. Group SC (Check ride landings inconsistent — no discernible improvement)

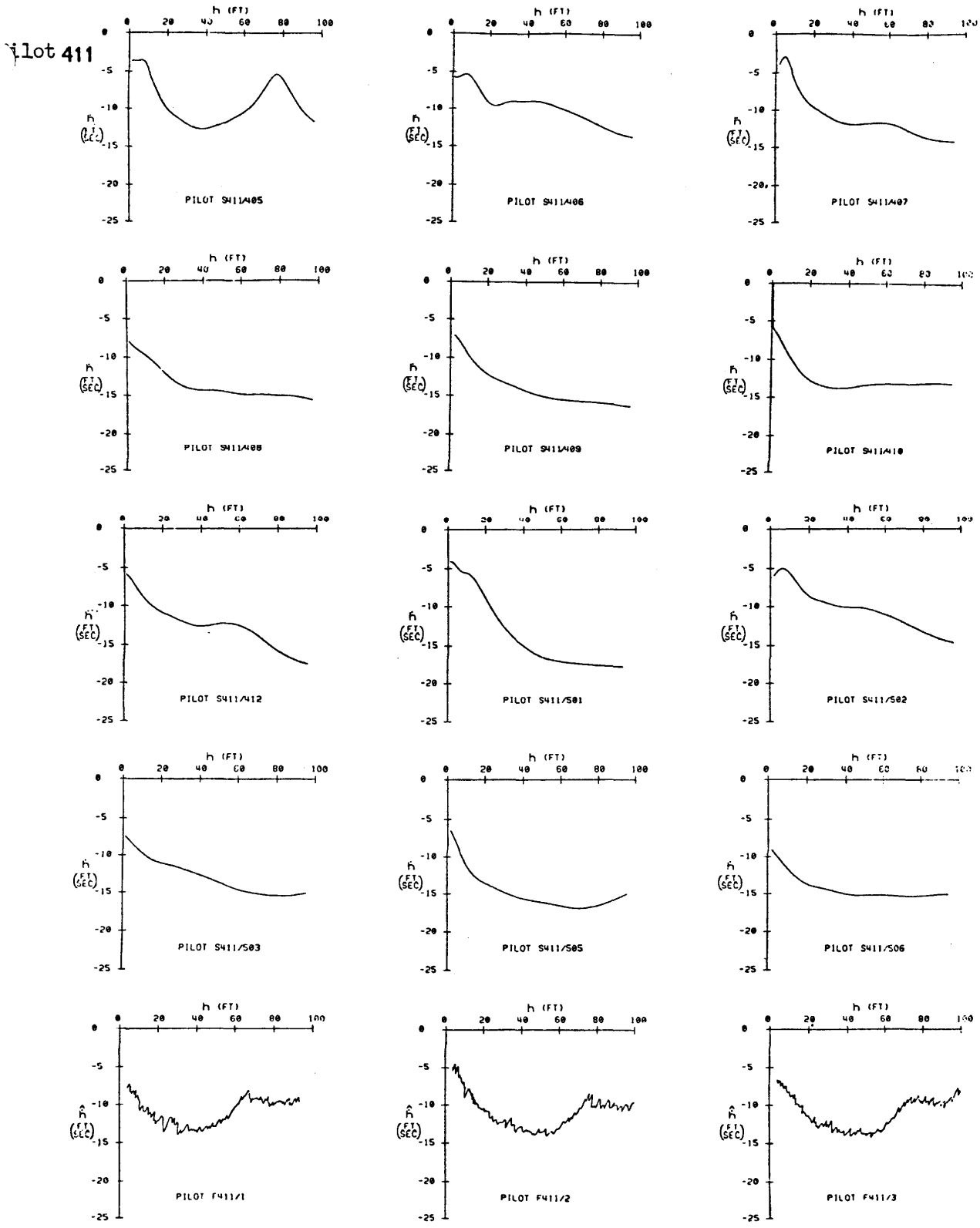

Figure 17. (Continued)

Group SC (Continued)

Pilot 416

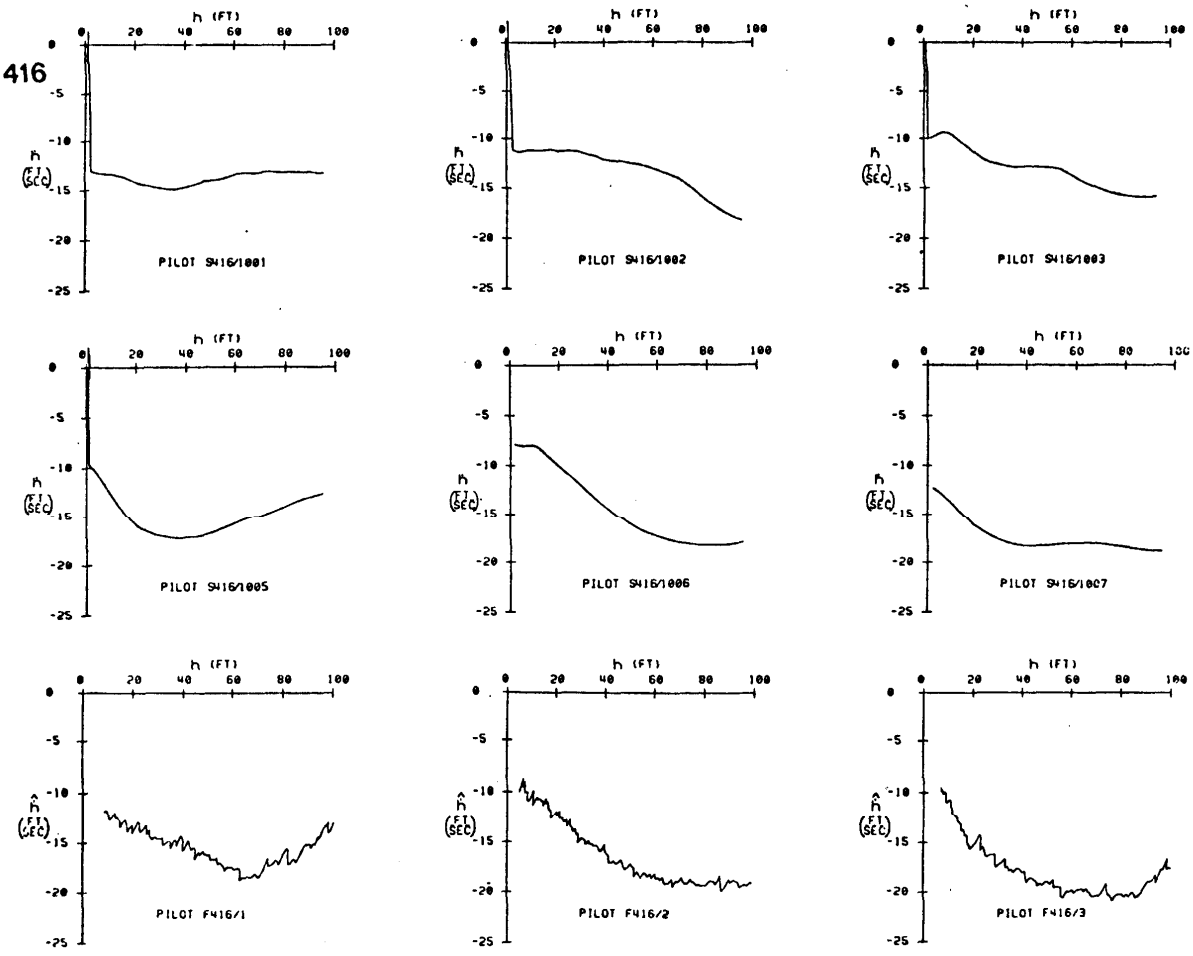

Pilot 435

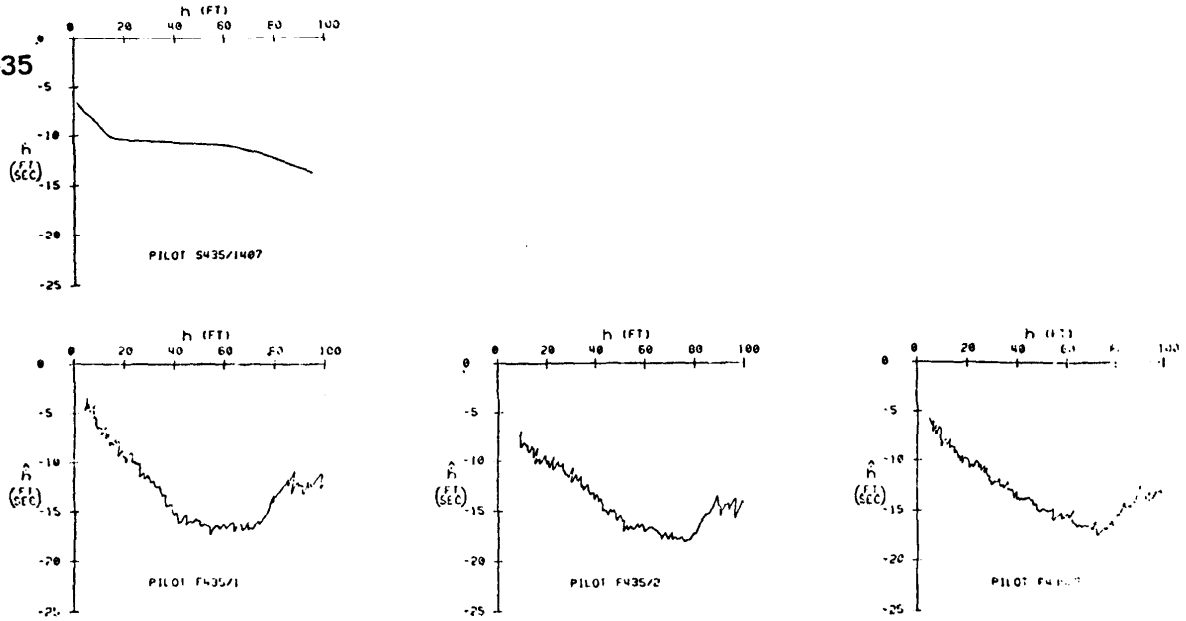

Figure 17. (Continued)

Group SC (Concluded)

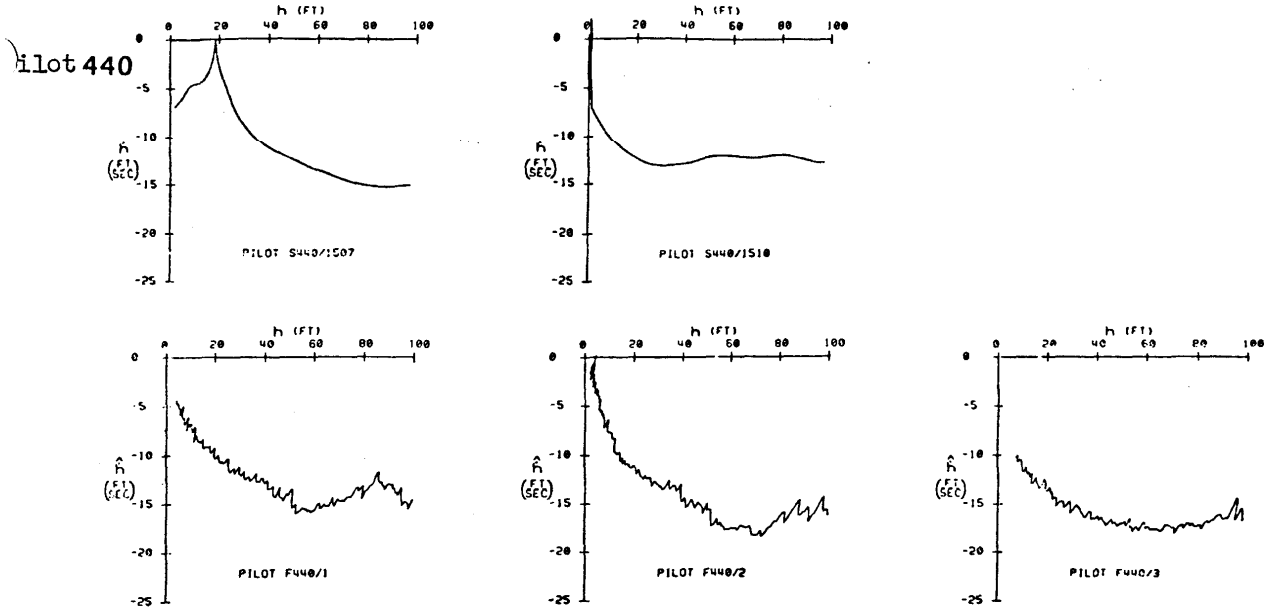

Figure 17. (Concluded)

groupings are made on the basis of approximate landing success for the NASA check ride. All of those subjects in Group SA demonstrated touchdown sink rates of 5 ft/sec or less and are therefore comparable with the flight-trained group, FA. Group SB consists of those pilots whose initial check ride landing was in excess of 5 ft/sec but whose subsequent landings consistently improved to a level of less than 5 ft/sec. Group SB, therefore, exhibited some degree of learning during the NASA check ride itself, i.e., the trainees' first exposure to the actual flight vehicle. Group SC is composed of those simulator-trained pilots who consistently exhibited landings in excess of 5 ft/sec or exhibited other undesirable tendencies such as excessive float. Thus Group SC is the simulator-trained counterpart of Group FC.

To summarize, the groupings of phase plane trajectories are made first in terms of training background (i.e., flight-trained versus simulator-trained) and second in terms of a rough measure of landing performance. These groupings will be convenient in the subsequent interpretation of results.

The main data reduction procedure applied to the phase plane trajectories was the identification of the effective second-order response parameters, i.e., the damping ratio, ζ_{FL}, and natural frequency, ω_{FL}. Each of these parameters was extracted manually using the following guides and criteria.

Effective damping ratio can be related to the ratio of the touchdown sink rate to the maximum sink rate, h_{TD}/h_{max}, as shown in the previous section. The theoretical relationship shown in Fig. 18 was the primary basis for extraction of effective damping ratio from the data. In most cases the phase plane trajectory features corresponding to maximum sink rate and touchdown sink rate are reasonably clear. For some landings, however, the maximum sink rate is not obvious; and, in those cases, a cut-and-try match was made using special transparent overlays of second-order response trajectories. The estimated goodness of fit for ζ_{FL} is ± 0.02 based on ± 0.5 ft/sec discrimination of sink rate.

The effective natural frequency can be obtained in a number of ways. Where possible, transparent overlays of trajectories such as those shown in Fig. 19 were used to match natural frequency. The portion of the trajectory from maximum sink rate to touchdown was the most prominent feature matched. The steepness of the phase plane during the sink rate reduction is, of course, directly related to natural frequency of the maneuver. In some cases it was possible to use the gross dimensions of the phase plane as they relate to an ideal trajectory, i.e., the ratio of maximum sink rate to the height at maximum sink rate. The estimated goodness of fit for ω_{FL} is ± 0.05 rad/sec based on the 0.1 rad/sec increments used for overlay templates. In general the precision of the matches is better than the dispersions in characteristics exhibited by the pilots themselves.

Table 4 lists the identified parameters for each case. Following interpretation, these parameters provide one with reasonably clear indications of the nominal piloting technique used during the flare maneuver, the effects of training between the simulator and aircraft, and the apparent simulator fidelity for the landing maneuver.

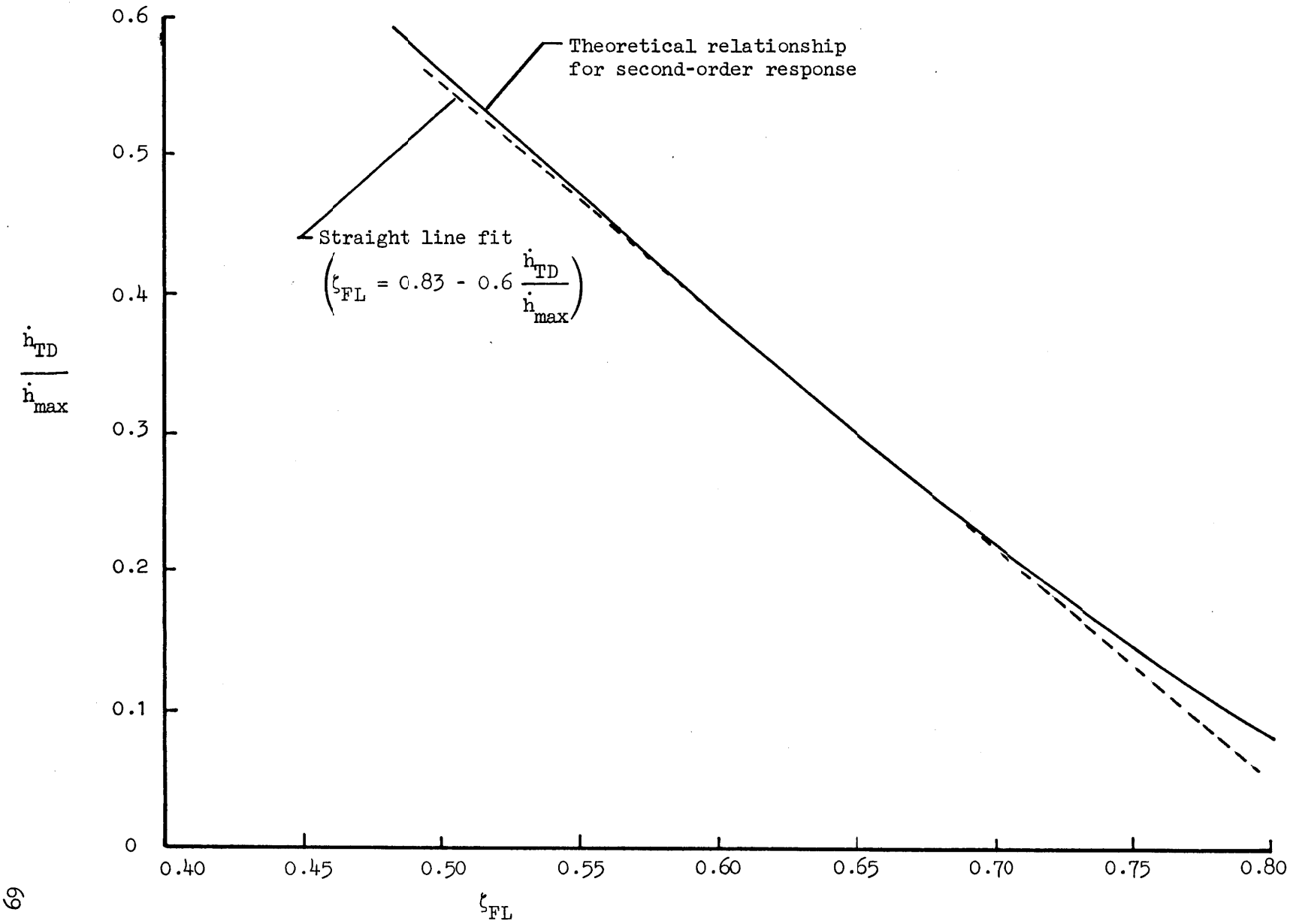

Figure 18. **Relationship Between Sink Rate Reduction Ratio and Damping Ratio**

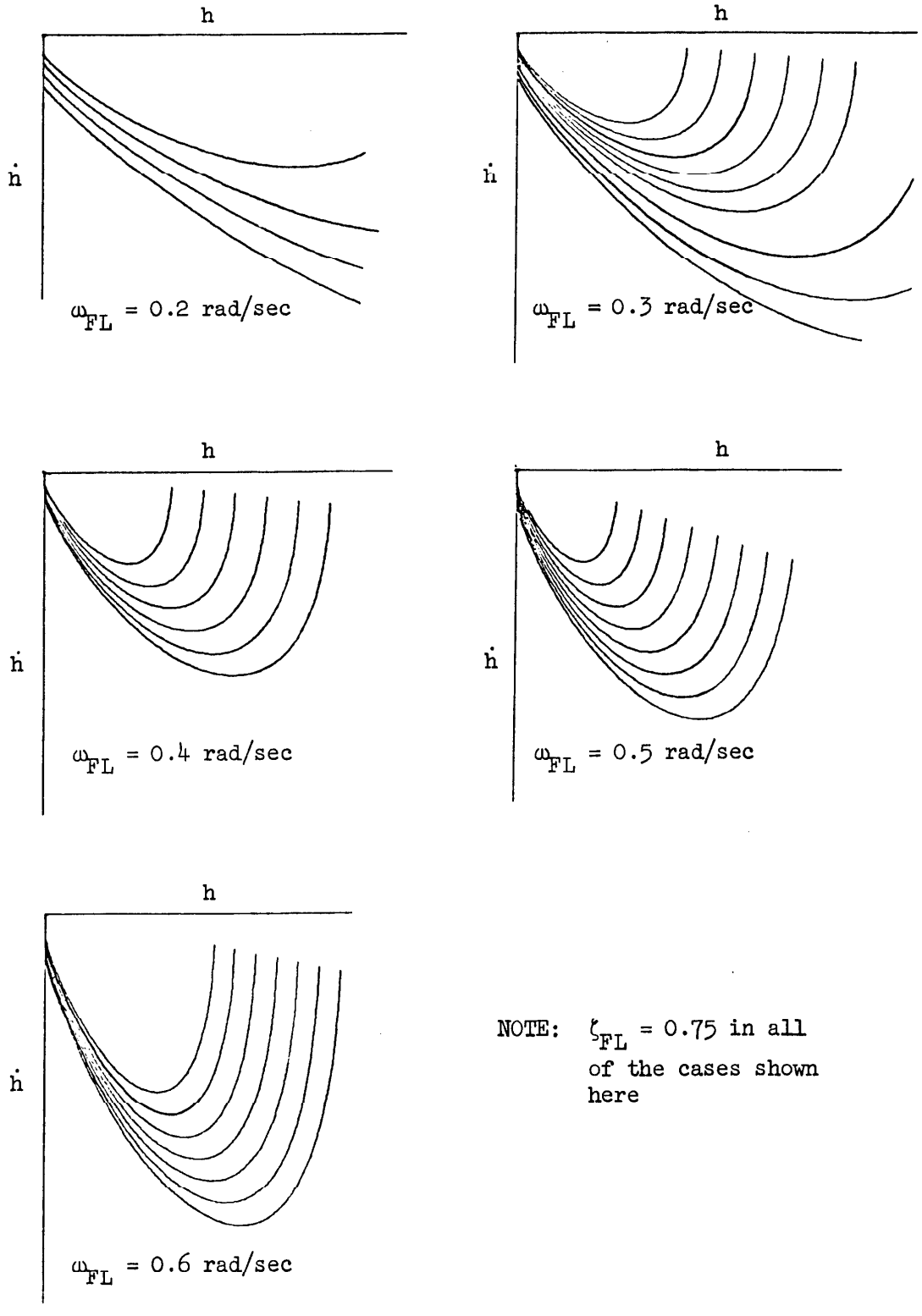

Figure 19. Families of Phase Plane Trajectories Used to Overlay and Identify Natural Frequency

TABLE 4

IDENTIFIED FLARE MANEUVER PARAMETERS

Group/ Pilot	$\frac{\dot{h}_{TD}}{\dot{h}_{max}}$	ζ_{FL}	ω_{FL}	$\zeta_{FL}\omega_{FL}$	ω_{FL}^2
GROUP FA					
F404/1	0.42	0.58	0.4	0.23	0.16
2	0.22	0.7	0.5	0.35	0.25
3	0.20	0.71	0.47	0.33	0.22
F408/1	0.35	0.62	0.4	0.25	0.16
2	0.38	0.60	0.3	0.18	0.09
3	0.26	0.67	0.3	0.20	0.09
F409/1	0.23	0.69	0.37	0.26	0.14
2	0.35	0.62	0.5	0.31	0.25
3	0.26	0.67	0.46	0.31	0.21
F412/1	0.33	0.63	0.5	0.32	0.25
3	0.33	0.63	0.5	0.32	0.25
F415/1	0	0.9	0.4	0.36	0.16
2	0.22	0.7	0.3	0.21	0.09
3	0.28	0.66	0.4	0.26	0.16
F419/1	0.60	0.48	0.3	0.14	0.09
2	038	0.60	0.37	0.22	0.14
3	0.47	0.55	0.5	0.28	0.25
F420/1	0.16	0.74	0.6	0.44	0.36
2	0.16	0.74	0.6	0.44	0.36
3	0.19	0.72	0.3	0.22	0.09
F429/1	0.12	0.77	0.46	0.35	0.21
2	0.06	0.82	0.47	0.39	0.22
3	0.23	0.69	0.35	0.24	0.12
F434/1	0.22	0.7	0.4	0.28	0.16
2	0.33	0.63	0.3	0.19	0.09
3	0.20	0.71	0.3	0.21	0.09
F441/1	0.23	0.69	0.5	0.35	0.25
2	0.20	0.71	0.5	0.36	0.25
3	0	0.9	0.5	0.45	0.25
GROUP FC					
F414/1	0.20	0.68	0.4	0.27	0.16
2	0.25	0.71	0.4	0.28	0.16
F430/1	0.38	0.6	0.3	0.18	0.09
2	0.35	0.62	0.2	0.12	0.04
3	0.45	0.56	0.2	0.11	0.04
F433/1	0.42	0.58	0.36	0.21	0.13
2	0.25	0.68	0.39	0.27	0.15
3	0.18	0.73	0.35	0.26	0.12
GROUP SA					
S413/601	0.25	0.68	0.26	0.18	0.07
602	0.45	0.56	0.23	0.13	0.05
603	0.51	0.53	0.18	0.10	0.03
604	0.38	0.6	0.28	0.17	0.08
605	0.62	0.47	0.16	0.08	0.03
F413/1	0.25	0.68	0.3	0.20	0.09
2	0.22	0.7	0.26	0.18	0.07
3	0.35	0.62	0.21	0.13	0.04
S418/806	0.77	0.43	0.2	0.08	0.04
807	0.6	0.48	0.4	0.19	0.16
809	0.25	0.68	0.55	0.37	0.30
810	0.22	0.7	0.31	0.22	0.10
F418/1	0.25	0.68	0.4	0.27	0.16
2	0.19	0.72	0.3	0.22	0.09
3	0.22	0.7	0.4	0.28	0.16
S421/901	0.25	0.68	0.48	0.33	0.23
902	0.47	0.55	0.23	0.13	0.05
905	0.47	0.55	0.23	0.13	0.05
907	0.25	0.68	0.33	0.22	0.11
F421/1	0.11	0.78	0.4	0.31	0.16
2	0.15	0.75	0.3	0.23	0.09
3	0.15	0.75	0.2	0.15	0.04

TABLE 4 (Continued)

Group/ Pilot	$\frac{\dot{h}_{TD}}{\dot{h}_{max}}$	ζ_{FL}	ω_{FL}	$\zeta_{FL}\omega_{FL}$	ω_{FL}^2
S423/1109	0.69	0.44	0.3	0.13	0.09
1110	0.67	0.45	0.2	0.08	0.04
1113	0.52	0.52	0.33	0.17	0.11
1114	0.47	0.55	0.33	0.18	0.11
F423/1	0.16	0.74	0.5	0.37	0.25
2	0.14	0.76	0.3	0.23	0.09
3	0.06	0.82	0.4	0.33	0.16
S424/1102	0.8	0.4	0.3	0.12	0.09
1103	0.8	0.4	0.3	0.11	0.09
1105	0.45	0.56	0.2	0.11	0.04
1106	0.30	0.65	0.26	0.17	0.07
1107	0.49	0.54	0.25	0.14	0.06
1108	0.8	0.4	0.24	0.10	0.06
F424/1	0.16	0.74	0.4	0.30	0.16
2	0.16	0.74	0.4	0.30	0.16
3	0.06	0.82	0.36	0.30	0.13
S432/1308	0.40	0.59	0.5	0.30	0.25
1310	0.30	0.65	0.4	0.26	0.16
1311	0.52	0.52	0.5	0.26	0.25
F432/1	0.42	0.58	0.5	0.29	0.25
2	0.31	0.64	0.4	0.26	0.16
3	0.19	0.72	0.4	0.29	0.16
S436/1402	0.45	0.56	0.5	0.28	0.25
1404	0.56	0.5	0.2	0.10	0.04
1405	0.62	0.47	0.2	0.09	0.04
F436/1	0.36	0.61	0.3	0.18	0.09
2	0.22	0.7	0.2	0.14	0.04
3	0.20	0.71	0.2	0.14	0.04
S439/1501	0.30	0.65	0.36	0.23	0.13
1502	0.40	0.59	0.52	0.31	0.27
1505	0.38	0.60	0.41	0.25	0.17
F439/1	0.08	0.8	0.38	0.30	0.14
2	0.28	0.66	0.4	0.26	0.16
3	0.33	0.63	0.36	0.23	0.13
S443/1601	0.22	0.7	0.48	0.34	0.23
1603	0	0.9	0.52	0.47	0.27
F443/1	0.22	0.7	0.2	0.14	0.04
2	0.50	0.53	0.43	0.23	0.18
3	0.15	0.75	0.2	0.15	0.04
GROUP SB					
S402/112	0.8	0.4	0.5	0.20	0.25
113	0.8	0.4	0.5	0.18	0.25
115	0.40	0.59	0.2	0.12	0.04
116	0.38	0.6	0.4	0.24	0.16
118	0.52	0.52	0.2	0.10	0.04
120	0.54	0.51	0.5	0.26	0.25
121	0.47	0.55	0.4	0.22	0.16
122	0.31	0.64	0.4	0.26	0.16
123	0.69	0.44	0.5	0.22	0.25
125	0.78	0.41	0.6	0.25	0.36
126	0.43	0.57	0.2	0.11	0.04
127	0.28	0.66	0.5	0.33	0.25
F402/1	0.58	0.49	0.3	0.15	0.09
2	0.22	0.7	0.3	0.21	0.09
3	0.22	0.7	0.3	0.21	0.09
S403/101	0.56	0.5	0.36	0.18	0.13
102	0.6	0.48	0.45	0.22	0.20
103	0.8	0.4	0.6	0.24	0.36
104	0.47	0.55	0.4	0.22	0.16
105	0.54	0.51	0.4	0.20	0.16
106	0.15	0.75	0.6	0.45	0.36
107	0.75	0.42	0.5	0.21	0.25
108	0.8	0.4	0.3	0.12	0.09
109	0.49	0.54	0.6	0.32	0.36
110	0.47	0.55	0.3	0.17	0.09
111	----	----	0	0	0
F403/1	0.8	0.4	0.4	0.16	0.16
2	0.52	0.52	0.27	0.14	0.07
3	0.10	0.79	0.4	0.32	0.16

TABLE 4 (Concluded)

Group/ Pilot	$\frac{\dot{h}_{TD}}{\dot{h}_{max}}$	ζ_{FL}	ω_{FL}	$\zeta_{FL}\omega_{FL}$	ω_{FL}^2
S410/401	0.67	0.45	0.2	0.09	0.04
402	0.8	0.4	0.2	0.07	0.04
403	----	----	0	0	0
404	0.67	0.45	0.5	0.23	0.25
507	0.58	0.49	0.2	0.10	0.04
508	0.43	0.57	0.6	0.34	0.36
510	0.62	0.47	0.35	0.16	0.12
511	0.43	0.57	0.6	0.34	0.36
512	0.67	0.45	0.4	0.18	0.16
F410/1	0.60	0.48	0.45	0.22	0.20
2	0.30	0.65	0.4	0.26	0.16
3	0.51	0.53	0.3	0.16	0.09
S417/801	0.8	0.4	0.3	0.12	0.09
802	0.25	0.68	0.6	0.41	0.36
804	0.8	0.4	0.15	0.05	0.02
805	0.38	0.6	0.6	0.36	0.36
F417/1	0.62	0.47	0.4	0.19	0.16
2	0.40	0.59	0.3	0.18	0.09
3	0.47	0.55	0.3	0.17	0.09
S422/908	0.30	0.65	0.35	0.23	0.12
910	0.33	0.63	0.3	0.19	0.09
911	0.36	0.61	0.4	0.24	0.16
912	0.49	0.54	0.3	0.16	0.09
914	0.19	0.72	0.26	0.19	0.07
F422/1	0.58	0.49	0.3	0.15	0.09
2	0.43	0.57	0.3	0.17	0.09
3	0	0.9	0.29	0.26	0.09
S431/1302	0.12	0.77	0.5	0.39	0.25
1304	0.22	0.7	0.5	0.35	0.25
1305	0.22	0.7	0.65	0.46	0.42
1306	0.22	0.7	0.65	0.46	0.42
F431/1	0.12	0.77	0.6	0.46	0.36
2	0.19	0.72	0.4	0.29	0.16
3	0.12	0.77	0.4	0.31	0.16
GROUP SC					
S411/405	0.28	0.66	0.43	0.28	0.18
406	0.60	0.48	0.2	0.09	0.04
407	0.31	0.64	0.45	0.29	0.20
408	0.51	0.53	0.3	0.16	0.09
409	0.43	0.57	0.4	0.23	0.16
410	0.43	0.57	0.51	0.29	0.26
412	0.45	0.56	0.33	0.18	0.11
501	0.23	0.69	0.4	0.28	0.16
502	0.30	0.65	0.2	0.13	0.04
503	0.49	0.54	0.3	0.16	0.09
505	0.36	0.6	0.3	0.18	0.09
506	0.60	0.48	0.26	0.12	0.07
F411/1	0.58	0.49	0.4	0.20	0.16
2	0.35	0.62	0.4	0.25	0.16
3	0.49	0.54	0.4	0.22	0.16
S416/1001	----	----	0	0	0
1002	----	----	0	0	0
1003	0.65	0.46	0.2	0.09	0.04
1005	0.54	0.51	0.45	0.23	0.20
1006	0.47	0.55	0.34	0.19	0.12
1007	0.75	0.43	0.35	0.15	0.12
F416/1	0.69	0.44	0.2	0.09	0.04
2	0.52	0.52	0.3	0.16	0.09
3	0.47	0.55	0.4	0.22	0.16
S435/1407	0.8	0.4	0.5	0.20	0.25
F435/1	0.20	0.71	0.43	0.31	0.18
2	0.40	0.59	0.33	0.19	0.11
3	0.31	0.64	0.32	0.20	0.11
S440/1507	0.47	0.55	0.37	0.20	0.14
1510	0.67	0.45	0.4	0.18	0.16
F440/1	0.28	0.66	0.4	0.26	0.16
2	0	0.9	0.4	0.36	0.16
3	0.58	0.49	0.24	0.12	0.06

Interpretation of Ensemble Data Results

A second step to analyzing the landing data is to consider common trends shown by individual pilots or groups of pilots. This is crucial to resolving the ambiguity among flight path feedback gain, k_γ, effective vertical velocity-to-height feedback lead ratio, T_L, and pilot-vehicle lag, T_I, discussed earlier.

In those few cases where a single pilot performed a fairly large number of landings, an important trend is discernible. This is illustrated in Fig. 20.

In all of the Fig. 20 cases, there is a general trend which fits the form $2\zeta_{FL}\omega_{FL}\, c_o + c_1\, \omega_{FL}^2$. In fact, for three of the four pilots, this trend appears rather strong, and it can be therefore reasonably justified in extending the lumped lag-lead model of Eqs. 12 and 13 to the landing data in general. The main inference being made in doing so is that the pilot is adjusting the amount of effective vertical velocity feedback commensurate with the height feedback--that the two feedbacks track one another rather than being independent. Such behavior is equivalent to lead-compensated height feedback and is represented by the parameter T_L (see Fig. 9c,d). Two consequent implications would be that only a height feedback is at work, perhaps with preview distance, R_o, and that a vertical velocity feedback, per se, is not involved.

Table 5 summarizes the ensemble data analysis results for the various groups of interest.

Piloting Technique. In analyzing piloting technique, the focus will be on those data which are most indicative of a skilled pilot familiar with the aircraft in question. The best set of data in that respect is considered to be for the flight-trained pilots who exhibited reasonably good and consistent reductions in sink rates. Therefore Group FA is considered as being most representative of exemplary piloting technique in the absence of other data.

The performance involved in the nominally good landings of Group FA can be expressed in various ways. The most common performance metric is perhaps touchdown sink rate, and its cumulative probability distribution is shown in Fig. 21. As indicated, the distribution is essentially Gaussian with a mean slightly greater than 3 ft/sec. It should be recalled, however, that this probability distribution is somewhat conditional because the grouping was itself based chiefly on sink rate performance. Nevertheless this will prove to be a useful point of reference with other groups. Further there is a clear tendency to achieve a moderate, positive rate of sink at landing thus avoiding both floating and hard landings.

Figure 22 shows the identified closed-loop parameters for each of the landings in Group FA. Note that most landings ranged in natural frequency from 0.3 to 0.5 rad/sec and in damping ratio from 0.55 to 0.75. The two landings having damping ratios of 0.9 involved substantial floating and as such should not

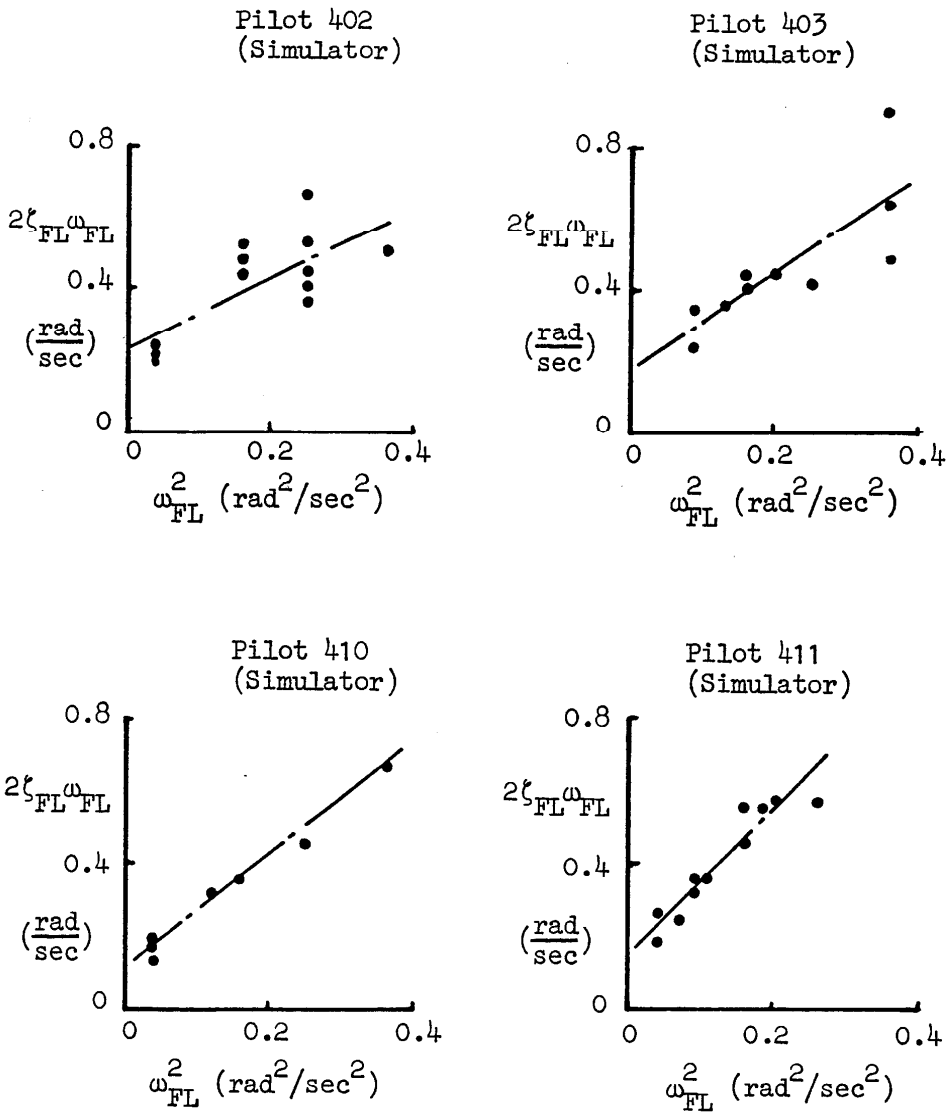

Note: Plotted points represent individual landings and line represents the linear regression of those landings.

Figure 20. Ensemble Data for Four Individual Pilots Having a Large Number of Landings

TABLE 5

SELECTED LANDING MANEUVER STATISTICS FOR VARIOUS PILOT GROUPS

Group	n Pilots	n Landings	$\bar{\omega}_{FL} \pm \sigma_{\omega}$	$\bar{\zeta}_{FL} \pm \sigma_{\zeta}$	$\overline{\omega^2_{FL}} \pm \sigma_{\omega^2}$	$\overline{2\zeta_{FL}\omega_{FL}} \pm \sigma_{2\zeta\omega}$	Regression Line* C_o	C_1	R	$s_{2\zeta\omega}$	Remarks
Actual DC-10											
Flight Trained											
FA	10	29	0.42 ± 0.09	0.68 ± 0.09	0.19 ± 0.08	0.58 ± 0.16	0.24	1.9	0.88	0.08	Consistently "good" landings
FC	3	8	0.33 ± 0.08	0.65 ± 0.06	0.11 ± 0.05	0.46 ± 0.14	0.13	2.70	0.96	0.03	Some hard landings or height misjudgment
FA + FC	13	37	0.40 ± 0.10	0.68 ± 0.09	0.17 ± 0.08	0.54 ± 0.17	0.11	2.0	0.91	0.04	
Simulator-Trained											
SA	9	27	0.34 ± 0.09	0.70 ± 0.07	0.12 ± 0.06	0.48 ± 0.14	0.24	2.0	0.89	0.06	Consistently "good" landings re sink rate
SB	6	18	0.36 ± 0.08	0.62 ± 0.14	0.13 ± 0.07	0.44 ± 0.16	0.18	1.9	0.82	0.09	First landing hard but subsequent improvement
SC	4	12	0.35 ± 0.07	0.60 ± 0.12	0.13 ± 0.05	0.44 ± 0.15	0.08	2.8	0.85	0.08	Poor landirgs with no consistent improvement
SA + SB + SC	19	57	0.35 ± 0.08	0.65 ± 0.12	0.13 ± 0.06	0.46 ± 0.15	0.20	2.0	0.83	0.08	
SB (Landing #1)	6	6	0.41 ± 0.11	0.52 ± 0.13	0.18 ± 0.10	0.44 ± 0.24	0.04	2.3	0.96	0.06	First checkride landing for SB
SB (Landing #2)	6	6	0.33 ± 0.06	0.63 ± 0.08	0.11 ± 0.04	0.42 ± 0.11	0.12	2.8	0.95	0.03	Second checkride landing for SB
SB (Landing #3)	6	6	0.33 ± 0.05	0.67 ± 0.16	0.11 ± 0.04	0.48 ± 0.14	0.10	3.3	0.86	0.06	Third checkride landing for SB
DC-10 Simulator											
Simulator Trained											
SA	9	34	0.33 ± 0.12	0.57 ± 0.11	0.12 ± 0.09	0.38 +	0.12	2.1	0.93	0.07	
SB	6	45	0.40 ± 0.17	0.54 ± 0.11	0.20 ± 0.12	0.46	0.16	1.5	0.87	0.10	Simulator training runs
SC	4	21	0.32 ± 0.14	0.54 ± 0.08	0.13 ± 0.07	0.38	0.18	1.6	0.84	0.07	
Selected Individuals											
Pilot 402 (SB)	1	12	0.41 ± 0.14	0.52 ± 0.09	0.18 ± 0.10	0.42 ± 0.14	0.24	1.0	0.72	0.09	
Pilot 403 (SB)	1	11	0.41 ± 0.18	0.51 ± 0.10	0.22 ± 0.11	0.46 ± 0.18	0.18	1.3	0.81	0.10	Ensemble data for single pilots having eight or more landings
Pilot 410 (SB)	1	8	0.34 ± 0.21	0.48 ± 0.06	0.17 ± 0.14	0.38 ± 0.21	0.12	1.5	0.99	0.02	
Pilot 411 (SC)	1	12	0.34 ± 0.10	0.58 ± 0.07	0.12 ± 0.07	0.40 ± 0.14	0.16	2.0	0.94	0.04	

*Regression line defined in $2\zeta_{FL}\omega_{FL}$ versus ω^2_{FL} with sample correlation coefficient R and standard error of estimate $s_{2\zeta\omega}$.

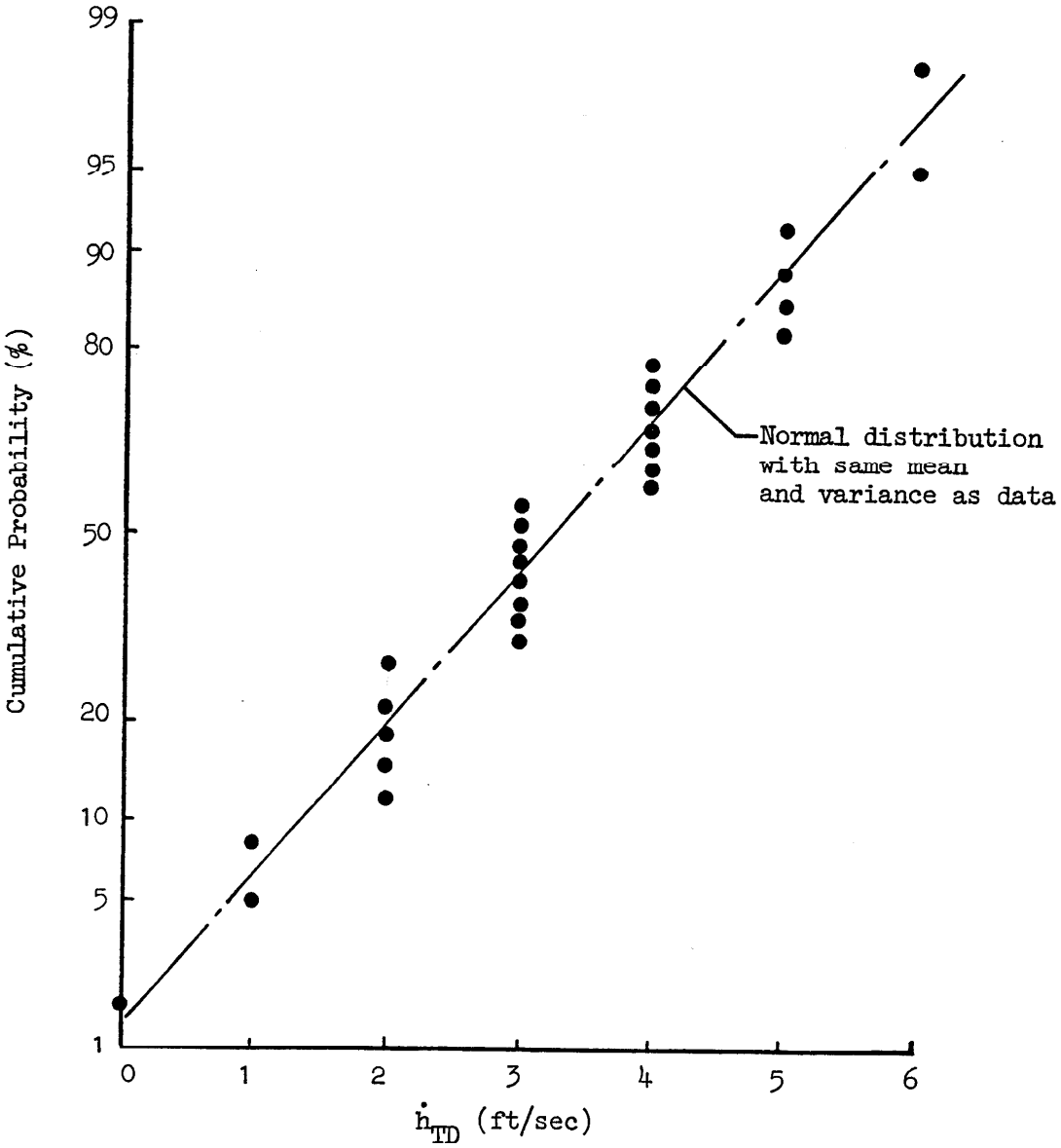

Figure 21. Distribution of Landing Sink Rate for Pilots in Group FA

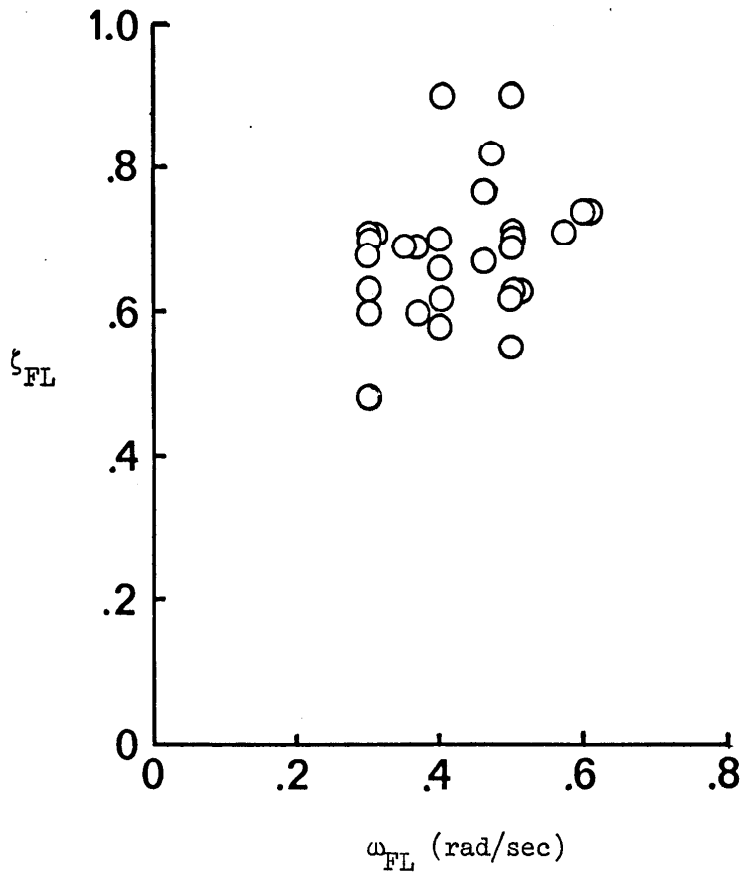

Figure 22. Closed-Loop Performance Representative of Skilled Pilots

necessarily be regarded as desirable. At the other extreme the very low damping ratios corresponded to somewhat hard touchdowns (with velocity 6 ft/sec) for this group.

It is important to note the operating ranges of ζ_{FL} and ω_{FL} demonstrated by Group FA. These are shown in the cumulative probability plots in Figs. 23 and 24. First, ζ_{FL} appears normally distributed over a range naturally bounded by insufficient and excessive sink rate decay. Shaded boundaries are shown for sink-rate-decay ratios of 0.5 and 0.05 which, when applied to a nominal approach sink rate of 10 ft/sec, correspond to $\dot{h}_{TD}$ = 5 ft/sec at one extreme and 0.5 ft/sec at the other.

A similar treatment is presented for ω_{FL} data; however, the distribution appears more nearly uniform. The boundaries shown in this case are the frequencies corresponding to overly-timid and overly-aggressive flare control. The lower bound corresponds to a margin of about three times $1/T_{\theta_1}$ which is the point at which flight path response is cancelled by airspeed decay. The hazard is the loss of airspeed margin while, at the same time, not effectively decreasing sink rate. The upper bound shown corresponds to airframe heave damping, $1/T_{\theta_2}$. An ω_{FL} higher than about 1.5 $1/T_{\theta_2}$ would involve an attitude change without a commensurate change in sink rate, i.e., the point at which aggressive pitch control does not affect flight path.

The FA-Group data are plotted in "technique-related" terms in Fig. 25. From this it is possible to infer how the closed-loop response is obtained or what are the effective pilot feedback gains.

Along with the individual landing data from Group FA, a curve corresponding to optimum closed-loop damping ratio, ζ_{FL} = 0.7, and a linear regression line are both superimposed. According to the regression-line analysis discussed earlier, if we assume for the moment that flight path angle gain k_γ = 0, the FA pilots exhibit an effective lag (with $1/T_I$ = 0.19/sec) and lead (with T_L = 1.86 sec) which correspond well to the optimum closed-loop damping ratio parabola.

The effective lag observed with k_γ = 0, T_I = 5.3 sec, is substantially greater than the lags previously estimated, i.e., $T_{\theta_2} \approx$ 1.8 sec (Table 1) and $\omega_{c_\theta}^{-1} \approx$ 0.5-1 sec (as shown in the preliminary data analysis). Hence the residual lag should be about 1.5 sec. If gain $k_\gamma > 0$, this residual lag can be > 1.5 sec. Nevertheless, at 1.5 sec this residual lag is so large as to suggest that the null hypothesis, k_γ = 0, is preferable. Resolution of the ambiguity in k_γ and the source of this residual lag must await the collection of pitch attitude, pitch rate, and control displacement data from further flight and simulator tests. At the same time this lag, whatever its source, provides near-optimum compensation and should not be considered as undesirable.

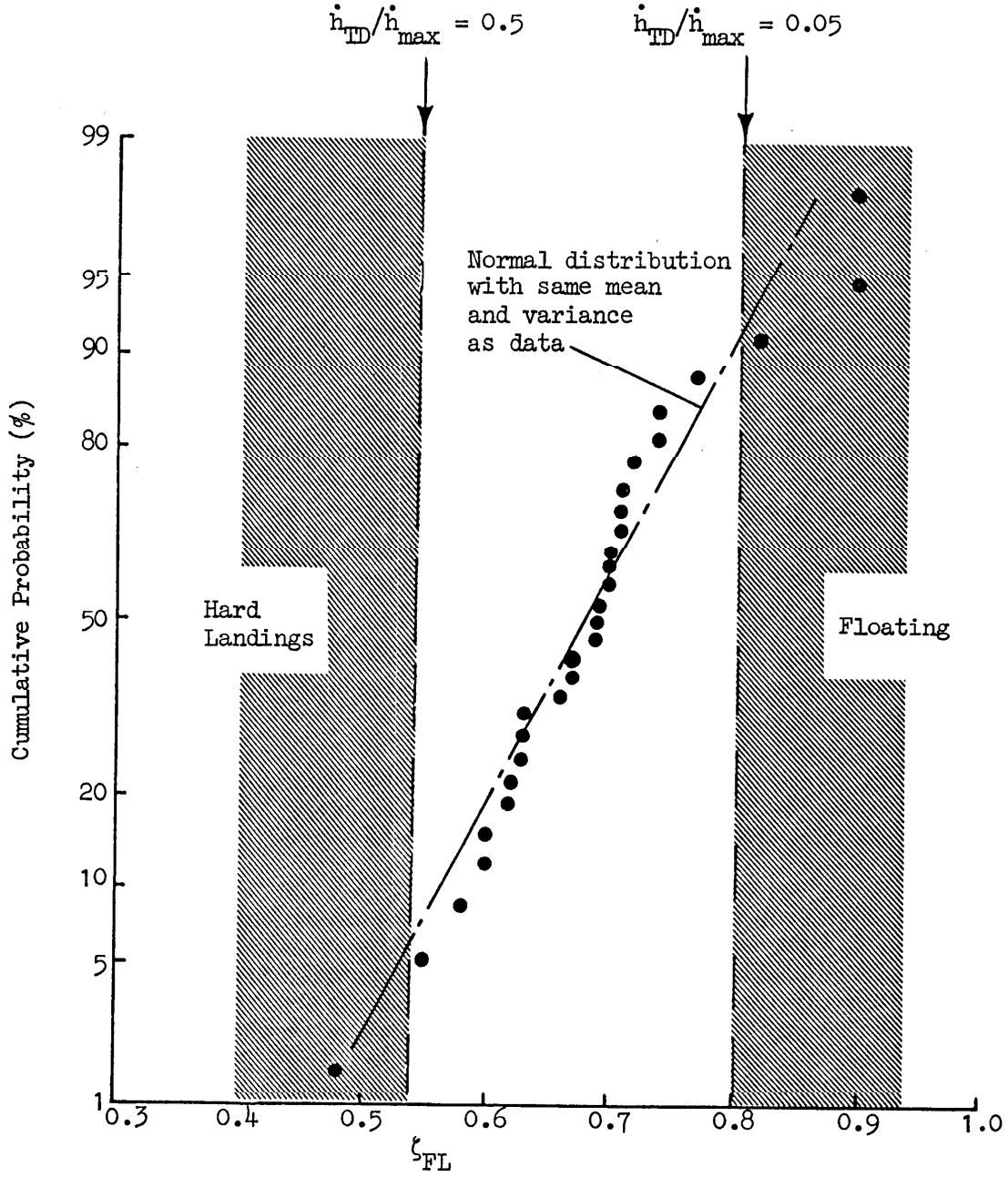

Figure 23. Cumulative Probability of Damping Ratio for Skilled Pilots (Group FA)

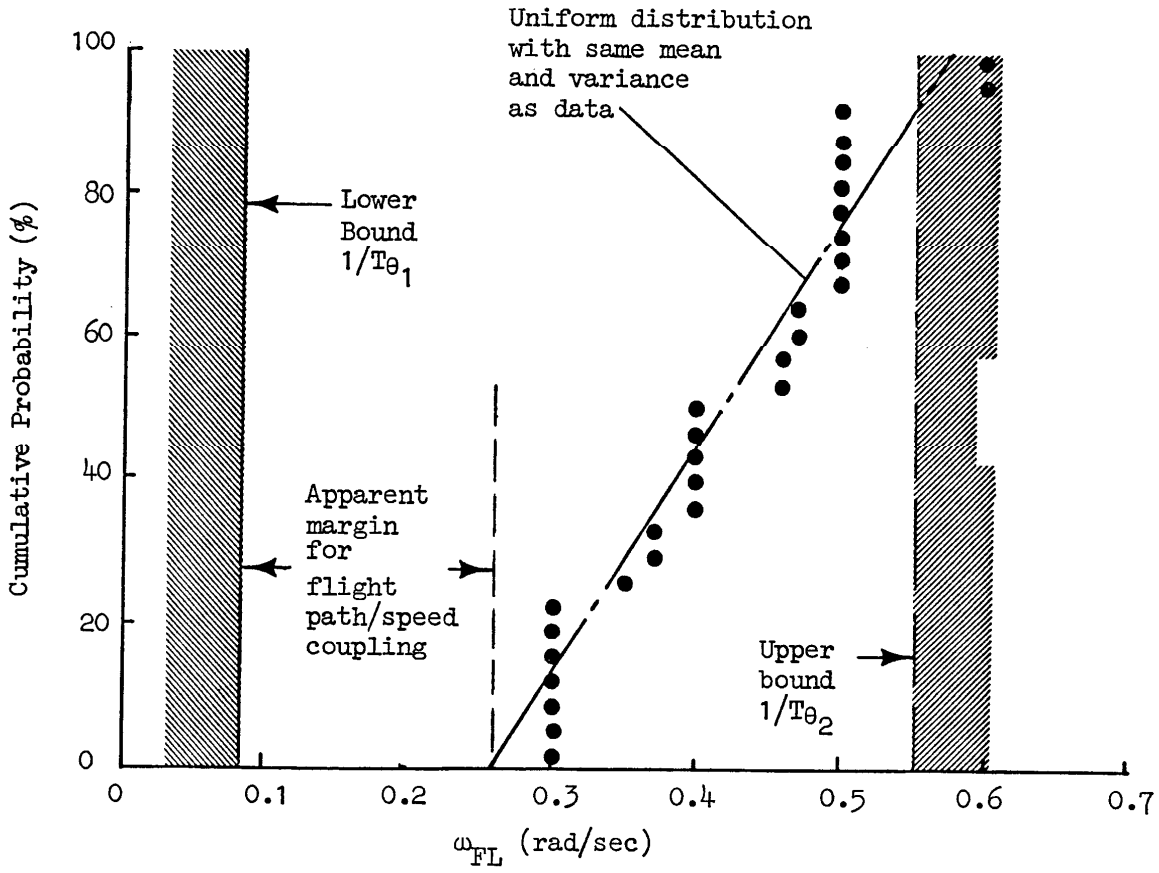

Figure 24. Cumulative Probability of Closed-Loop Frequency for Skilled Pilots (Group FA)

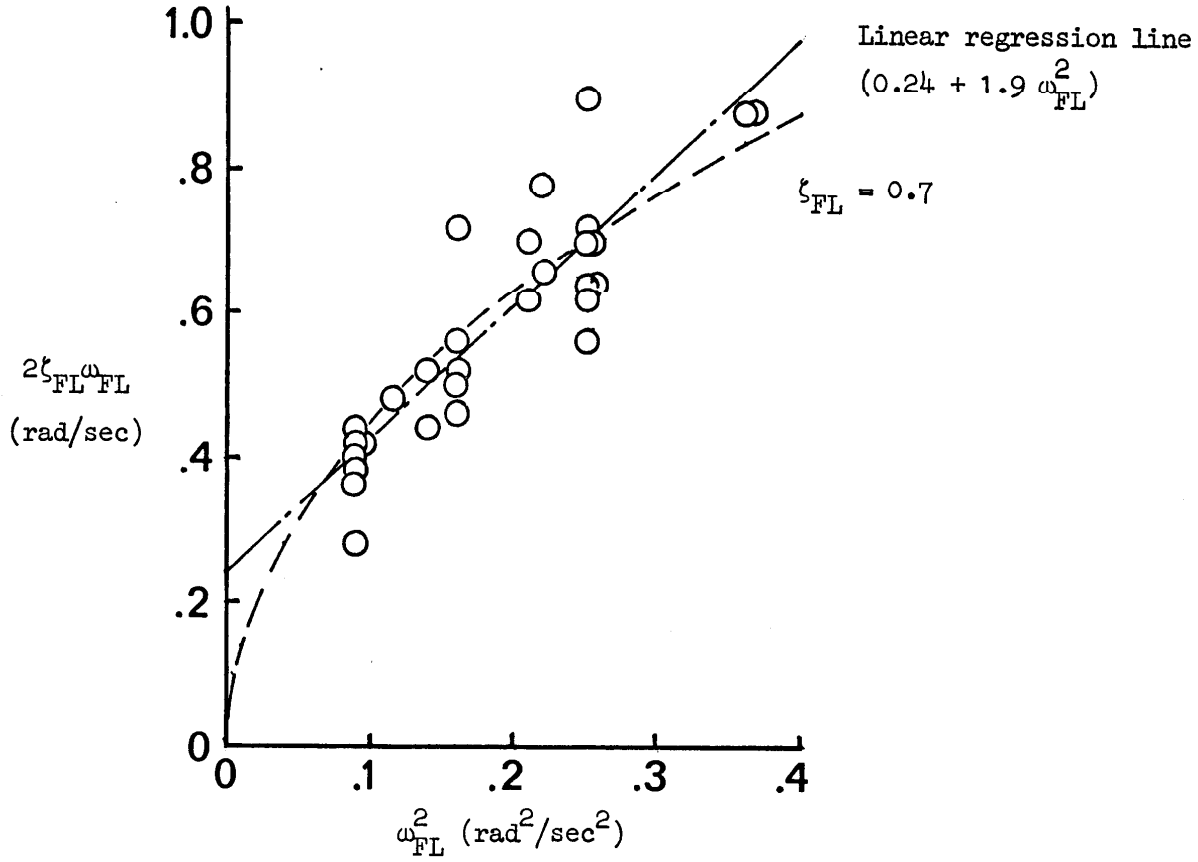

Figure 25. Closed-Loop Technique for Skilled Pilots (Group FA)

The inferred lead compensation, T_L, of 1.9 sec for Group FA was also near-optimum. This appears to be the primary "vertical velocity feedback" mechanism and suggests that vertical velocity information might be tied to lead-compensated height perception rather than through a separate visual or motion channel. It is possible that such height compensation derives from the geometrical properties connected with the pilot's focus of attention. This is commonly referred to as a "preview distance" and is equal to $T_L \cdot U$, in this case about 400 ft.

An important aspect of the flare model arises when one attempts to decompose the effective lag-lead dynamics into respective pilot and aircraft components. As mentioned above, the effective lag, T_I, can be attributed to various sources (airframe T_{θ_2}, pilot-vehicle ω_{c_θ}, and a residual lag). If each of these sources is taken to be an individual first order lag or delay, then the simple first-order lead, T_L, by itself is inadequate in producing an important feature of the ensemble data results. Namely, an increasing pilot gain, k_h (which increases ω_{FL}), will not produce the observed increasing $2\zeta_{FL}\omega_{FL}$ in Fig. 20. To produce the observed relationship in Fig. 20 requires that the actual lead compensation be higher than first order. Thus the second-order lead possibilities suggested in Fig. 9 appear more likely. Recall that either visual or vestibular pathways (Fig. 9e or 9f) could fulfill this requirement for higher than first-order lead compensation.

To summarize, then, in order to decompose the effective lag-lead flare model into individual pilot and vehicle components which are consistent with the observed gain-varying features of the dynamics in Fig. 20, one must deduce that higher than first-order lead compensation is required of the pilot. This could conceivably be furnished by the visual perception model (Fig. 9e) suggested in Ref. 18 or by vestibular feedbacks (Fig. 9f) via the utricular system as suggested in Ref. 7.

One particularly interesting feature in the piloting technique demonstrated in many of the actual landings (not only those of Group FA but for all subjects) is the "duck-under" or "push-over" just prior to the flare portion of the landing. Figure 26 shows a typical case in which the landing maneuver control law behavior appears to begin at about 75 ft, followed by an increase in sink rate, and finally a flare beginning at about 50 ft.

A NASA research pilot examining the data suggested that the duck-under tendency is a natural and common action intended to alter the point of touchdown. This technique could be deemed appropriate by the pilot when following an electronic glide slope which intercepts the runway at a conservative distance from runway threshold. Additional discussion of this maneuver can be found in Refs. 21 and 22.

The implication of the above observation is that there is, in effect, an outer loop around the landing maneuver loop structure considered thus far.

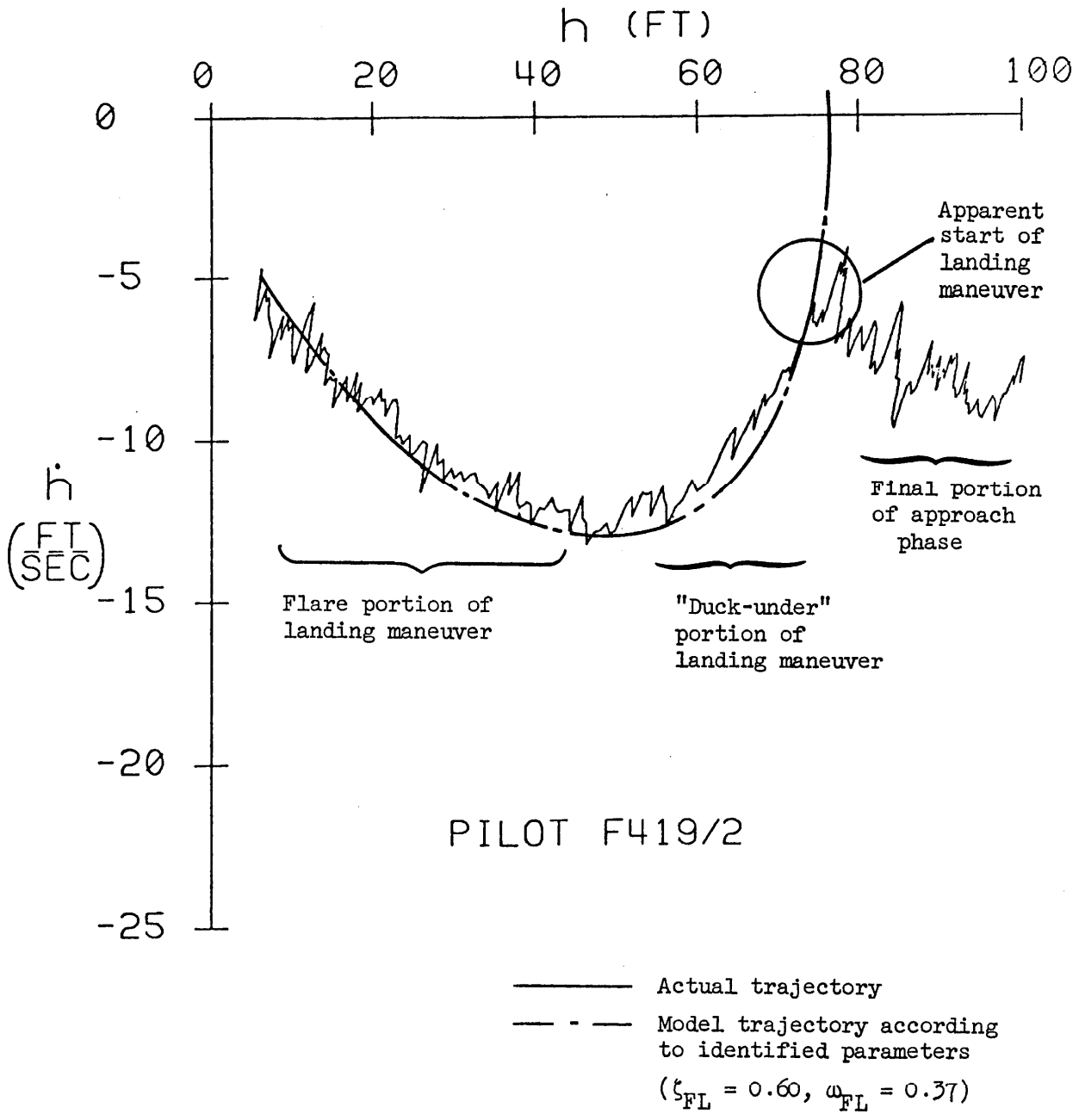

Figure 26. Typical Landing Maneuver Performed in the Actual Aircraft

That loop involves the aim point relative to the runway threshold or touchdown zone. In terms of the pilot model, it appears that the initiation height of the landing maneuver, h_{FL}, is selected according to the runway intercept of the nominal flight-path-angle vector. This would tend to explain the wide variation in h_{FL} in the landing data. Unfortunately measurements of height versus distance along the runway axis were not available.

In order to illustrate the general effect of flare height on touchdown point, consider Fig. 27. For nominal values of closed-loop response parameters and ILS geometry, it can be seen how an increase in h_{FL} above the nominal range of 30 to 40 ft tends to move the touchdown point closer to the threshold. For h_{FL} above 30 to 40 ft, in fact, the relationship between x_{TD} and h_{FL} is approximately linear.

The nominal piloting technique observed in Group FA pilots is summarized in Fig. 28

Training Effectiveness

Training effectiveness judged only on the basis of overt landing performance can be misleading. For example, Fig. 29 shows the combined cumulative probability distribution of the flight-trained pilots (Groups FA and FC) against those simulator-trained (Groups SA, SB, and SC). The difference, while discernible, is not particularly great. On the other hand, if each group is considered separately, then performance is more effectively partitioned (Fig. 30) and each distribution appears fairly Gaussian. Moreover there is a simulator-trained group (SA) which looks nearly identical to the good flight-trained group (FA), and an inferior flight-trained group (FC), comparable to the corresponding simulator-trained cases (SB and SC). This breakdown is, however, still incomplete without considering other aspects of performance and piloting technique such as are summarized in the regression analysis depicted in Fig. 31. Hence the following analysis will consider the various performance and technique metrics discussed previously in conjunction with Fig. 11. The inset in Fig. 31 describes again the theoretical interpretation of each regression line in terms of the metrics of piloting technique represented by regression coefficients C_0 and C_1 in Table 5.

The effects of training clearly favor those pilots transitioning in the actual airplane of whom 77 percent (Group FA) demonstrated near-optimum technique and superior performance. Two of the remaining three flight-trained pilots (in Group FC) exhibited deficiencies in terms of aggressiveness in flaring and excessive lag or delay which they could not adequately compensate. The third FC pilot exhibited satisfactory closed-loop response parameters but appeared to suffer from height misjugment during the flare.

The simulator-trained pilots showed varying degrees of difficulties. Of those pilots, the best group (SA) composed 47 percent of the total and was nearly identical to FA in terms of touchdown sink rate performance and in the

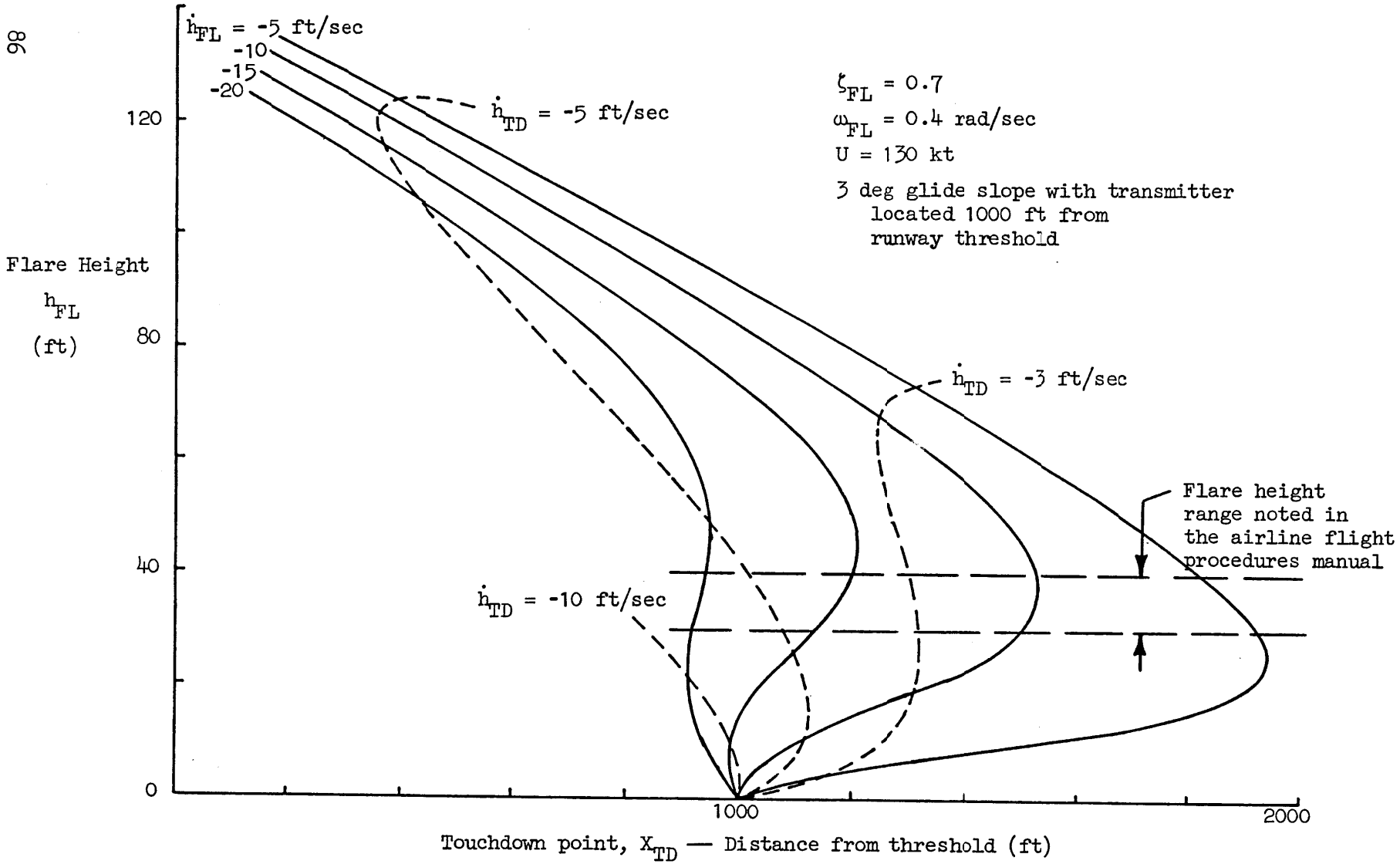

Figure 27. Relationship Between Flare Height and Touchdown Point

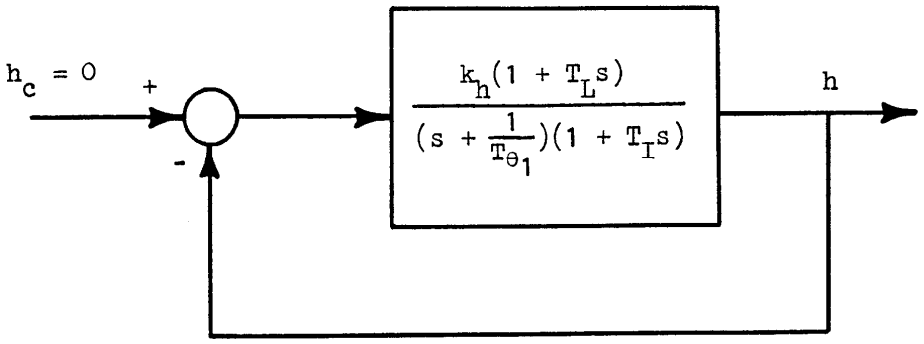

k_h is variable such that

$0.25 < \omega_{FL} < 0.55$

$T_L = 1.9$ sec

$T_I = 5.3$ sec

Figure 28. Summary of Nominal DC-10 Piloting Technique (Group FA)

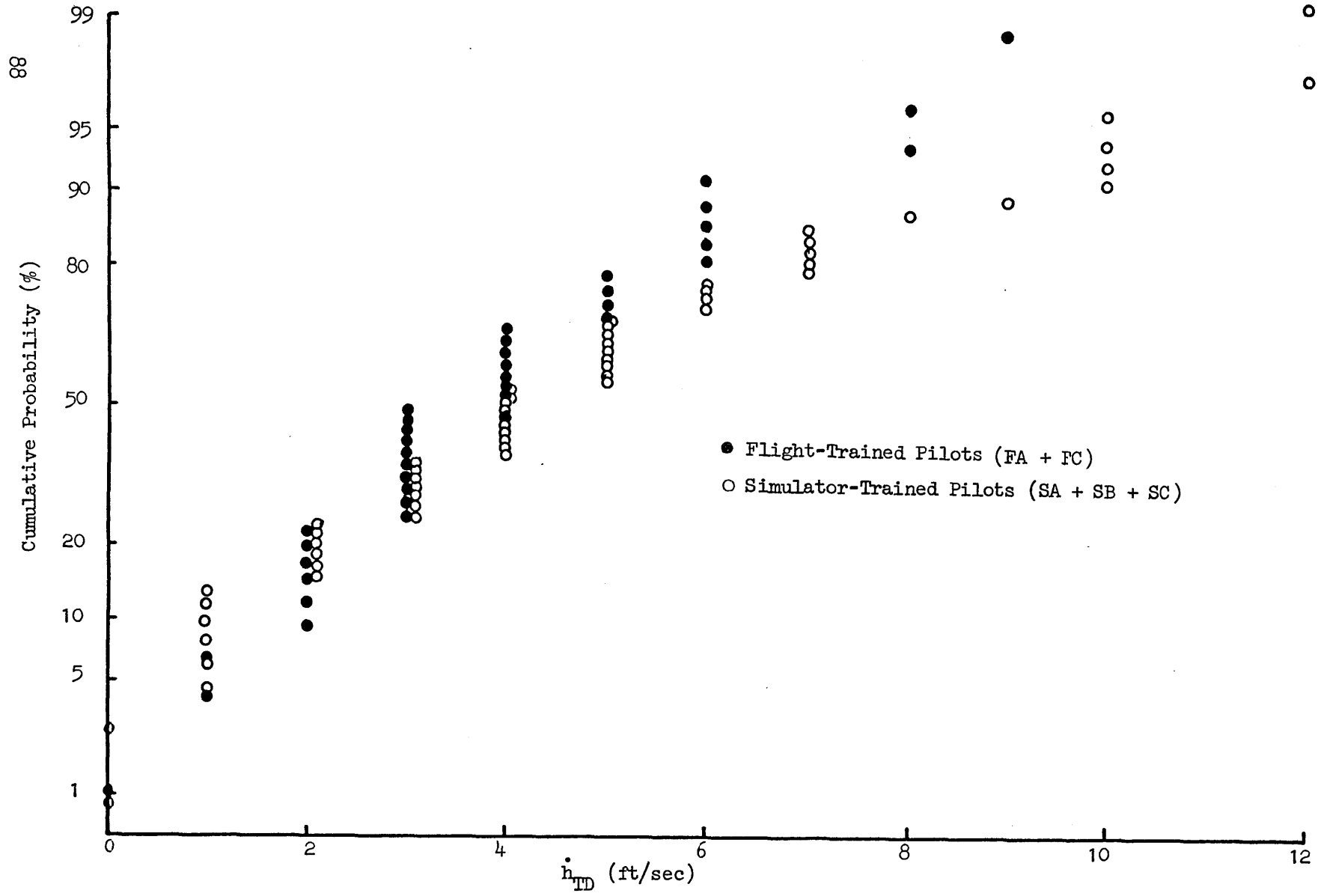

Figure 29. Cumulative Landing Sink Rate Probability Distributions Pooled According to Training Medium

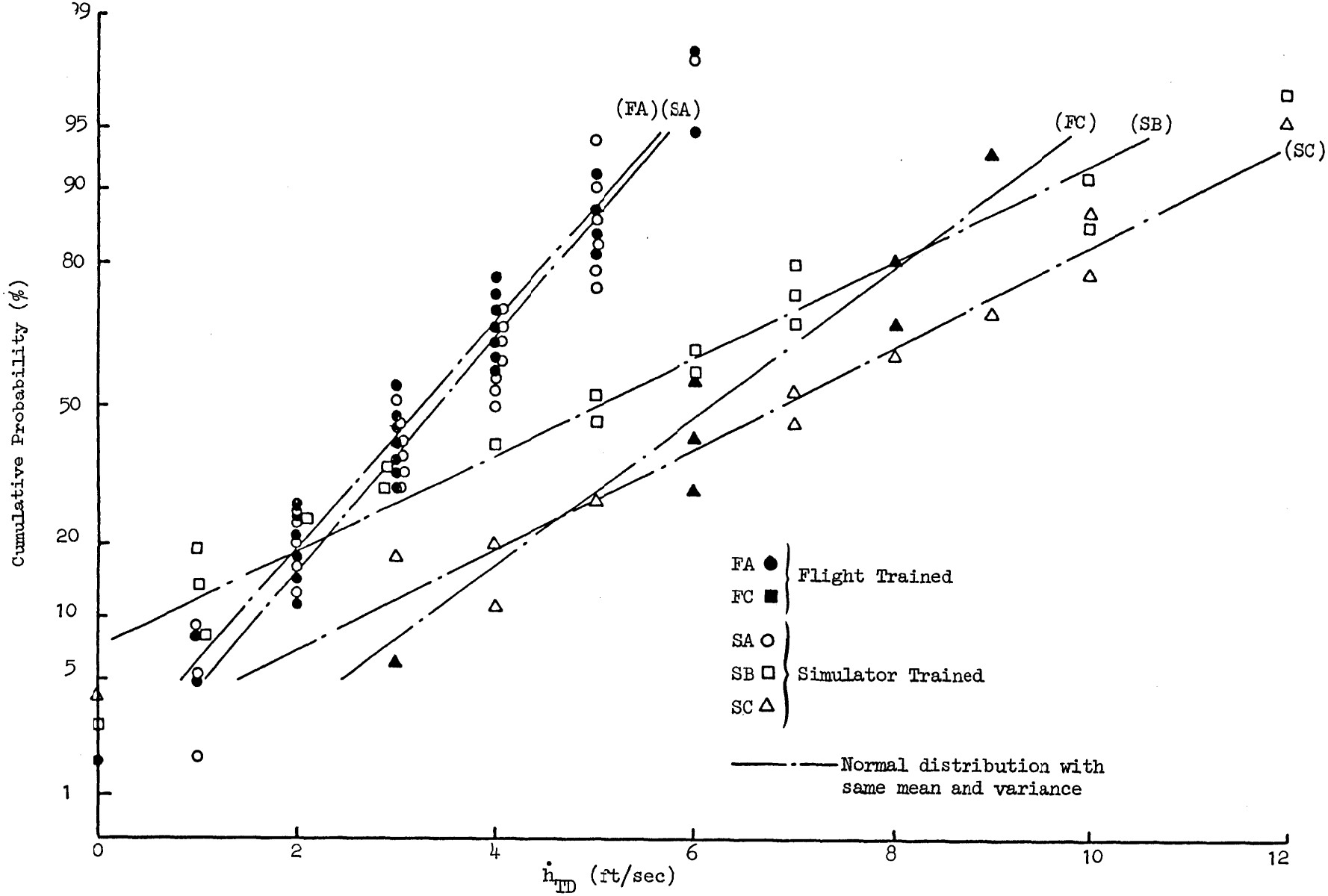

Figure 30. Cumulative Landing Sink Rate Distributions of Individual Groups During Checkride Landings

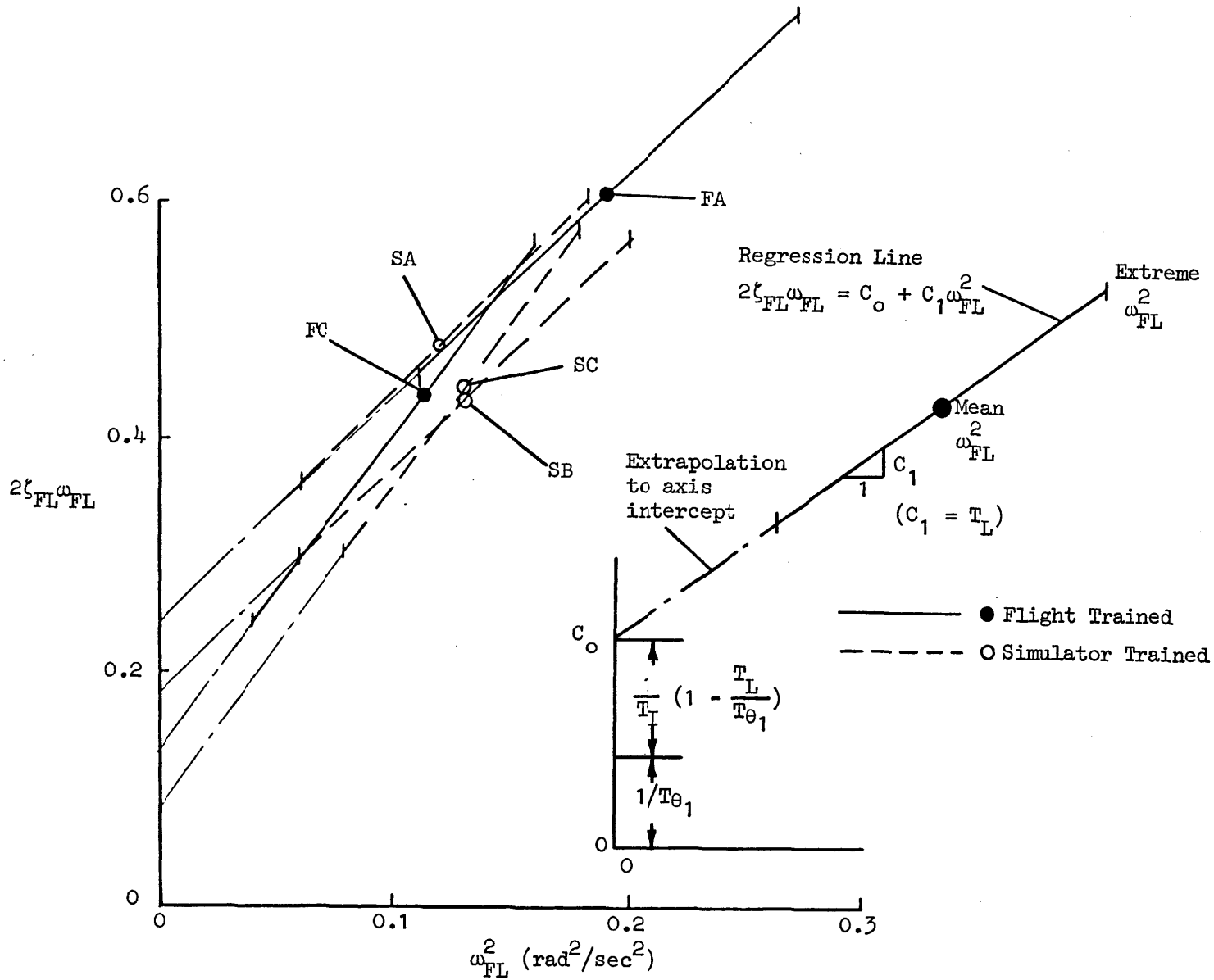

Figure 31. Summary of Regression Analysis for all Flight Data

amount of effective lag and lead compensation. The main difference rested in the lack of aggressiveness by most SA pilots which, according to Fig. 32, showed up as a shift downward in the distribution of closed-loop natural frequency. The consequence would be a greater loss of speed margin during the flare maneuver by SA pilots than with the more aggressive technique exhibited by FA pilots.

For the remaining 53 percent of simulator-trained pilots (SB and SC) landing performance was substantially poorer with median touch down sink rates of 5 to 7 ft/sec and extremes in excess of 10 ft/sec. These two groups, originally distinguished on the basis of improvement during the three checkride landings or the lack thereof, showed a basic difference in piloting technique. Group SB differed from Group SA in terms of more effective lag (T_I). Group SC exhibited vastly more of this same lag quality along with increased but nevertheless inadequate lead compensation. It should be noted from Table 5 that the Group SB learning trend over the three actual landings could be tracked in terms of the reduction in overall lag (increase in C_o) and the increased amount of lead compensation (increased C_1) to counter that lag. The second and third checkride landings for SB, in fact exhibit improved lag and lead coefficients roughly comparable to those of Group FC; furthermore SB's landing sink rate performance, per se, was satisfactory (< 5 ft/sec).

The effects of training for each of the five groups of pilots are summarized in Table 6. Only Group FA exhibited consistency in all respects: good touchdown sink rate performance, aggressiveness in the flare maneuver, optimum compensation, and minimal effective lag. This group included 77 percent of the flight-trained pilots. The "good" simulator-trained group (SA) included only 43 percent of the pilots using that medium, and while performance and technique compared favorably to FA, there was less aggressiveness shown in the flare by SA. Consequently a greater loss of speed margin could be expected during the sink rate reduction by SA. Inspection of individual pilots within SA did, however, reveal five who exhibited proficiency in technique comparable to FA (i.e., pilots F418, F423, F424, F432, F439). It is particularly noteworthy that the one quality shared by the poorer performing groups (FC, SB, and SC) was excessive lag.

Simulator Fidelity and Validity

The experimental results have important implications on (a) the fidelity of the training simulator in terms of adequate perceptual effects and consequent pilot behavior and (b) the validity of the simulator performance if transferred to a flight situation.

The same analysis method used for determining control strategy in the actual DC-10 was also applied to the simulator results. Differences between simulator and flight were observed from direct comparisons using the simulator-trained pilots: Groups SA, SB, and SC.

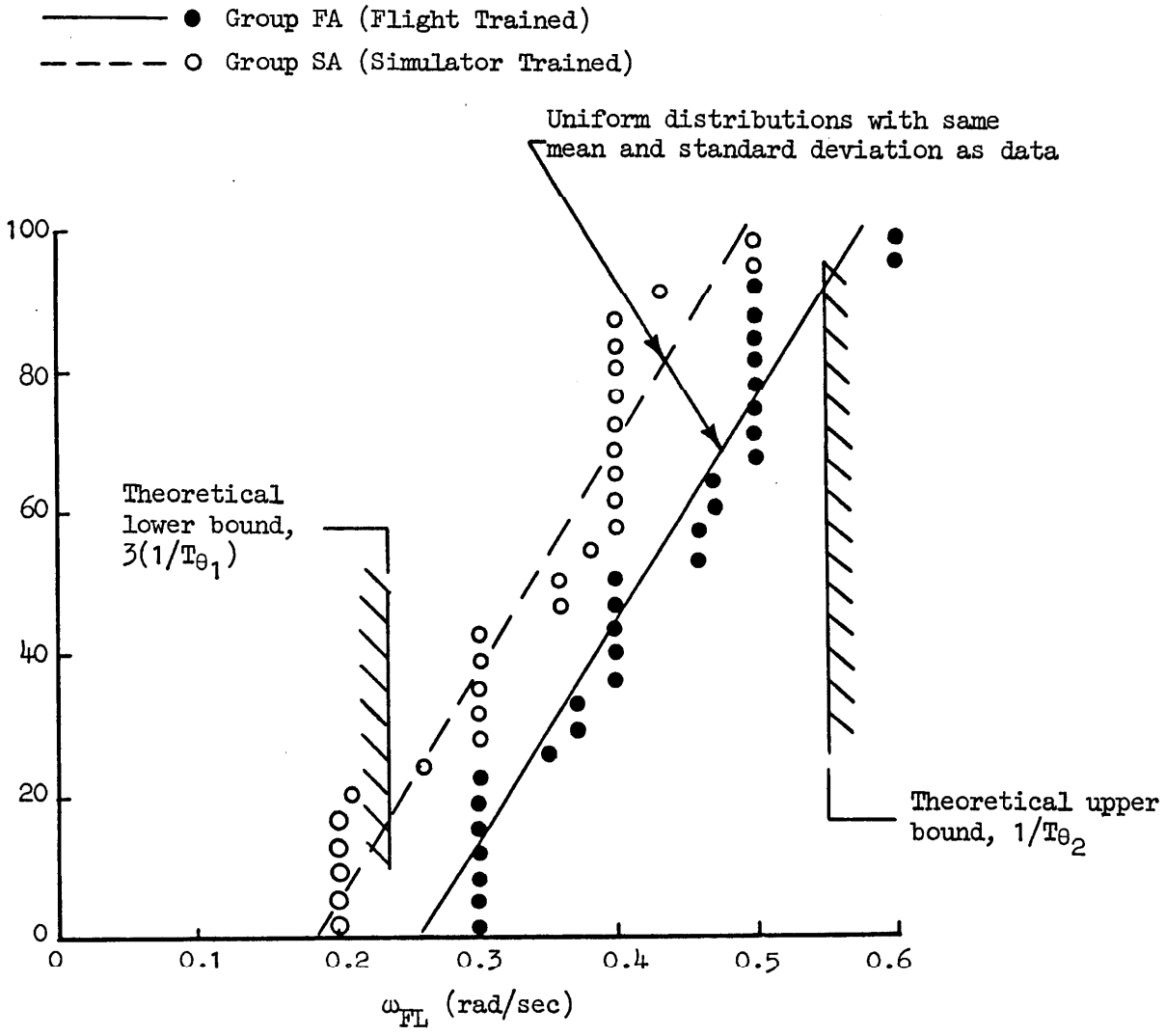

Figure 32. Cumulative Probability of ω_{FL} for Successful Flight-Trained Pilots Compared to Successful Simulator-Trained Pilots

TABLE 6

SUMMARY OF EFFECTS OF TRAINING

Group	Pilots	Landings	Touchdown Sink Rate ($\dot{h}_{TD}$) Performance (ft/sec)			Metrics of Piloting Technique		Remarks
			Median	90 Percentile	Max	Lead T_L(sec)	Lag T_I*(sec)	
Flight Trained								
FA	10	29	3	5	6	1.9	5.3	Aggressive, well compensated
FC	3	8	6	8-9	9	2.7	9	Timid, excessive lag, under compensated
Simulator Trained								
SA	9	27	4	5	6	2.0	5.3	Timid but well compensated
SB	6	18	5	10	12	2.0	8	Timid, moderate lag, and under compensated
SC	4	12	7	10-12	12	2.8	∞	Timid, large lag, and under compensated

*T_I = effective first-order lag time constant inclusive of flight path and pitch attitude response lags.

In terms of landing sink rate performance, there were mixed results in terms of direct flight versus simulator comparisons depending upon the group. As shown in Fig. 33, all of the simulator-trained pilots had comparable sink rate performance in the simulator with medians in the 6 to 7 ft/sec range. Group SC exhibited about the same level of sink rate performance in the actual aircraft, and Group SB was only slightly better. Group SA, however, showed a substantial improvement in going from simulator to flight. Clearly the use of simulator touchdown sink rate was not a reliable predictor of in-flight performance nor a means of discriminating pilot skill. On this basis alone, the simulator validity should, therefore, be considered poor.

Taking the simulator versus flight results a step further, there is a variety of differences in terms of closed-loop performance and inferred piloting technique. Table 7 summarizes mean performance in terms of $\bar{\zeta}_{FL}$, and $\bar{\omega}_{FL}$ and the ensemble lag and lead parameters which imply technique, $1/T_I$ and T_L. These results are also plotted in terms of the $2\zeta_{FL}\omega_{FL}$ versus ω^2_{FL} regression analysis solutions from Figure 34.

The chief common feature in all of the simulator data is the relatively low ζ_{FL}. As indicated earlier, this should necessarily correlate strongly with hard landings since the ratio h_{TD}/h_{max} was used to determine ζ_{FL}. In searching for a cause of the poor performance in terms of technique, two factors appear to be involved: excessive lag, T_I, and inadequate lead, T_L. In the simulator Group SA suffered from a very large effective lag although the lead was comparable to their flight value (and that of FA). Groups SB and SC exhibited both long lag and short lead in the simulator.

In transitioning from simulator to flight, each of the three groups made substantially different adjustments. SA kept T_L about the same (already about optimum) and greatly reduced T_I to the correct value. Group SB did relatively little in the simulator to flight transition except to increase T_L slightly to the correct level; T_I remained long. Group SC appeared to make an already large T_I much larger and to try and compensate by a large, but inadequate, T_L.

Thus the nature of the pilot compensation adjustments made by each group was fundamentally different except for a net upwards shift in the $2\zeta_{FL}\omega_{FL}$ versus ω^2_{FL} regression line. Only in the case of Group SA did this shift yield good sink rate performance, however.

Another feature of the simulator versus flight pilot behavior was the degree of aggressiveness shown in terms of ω_{FL} or ω^2_{FL}. Group SB exhibited a mean $\bar{\omega}^2_{FL}$ in the simulator which was comprable only to that of Group FA; however, in-flight SB regressed to the same less-aggressive ω^2_{FL} as the other groups.

A final feature of the simulator landings was an absence of any substantial "duck under" tendency such as noted earlier. This can be observed by direct inspection of the simulator phase plane trajectories.

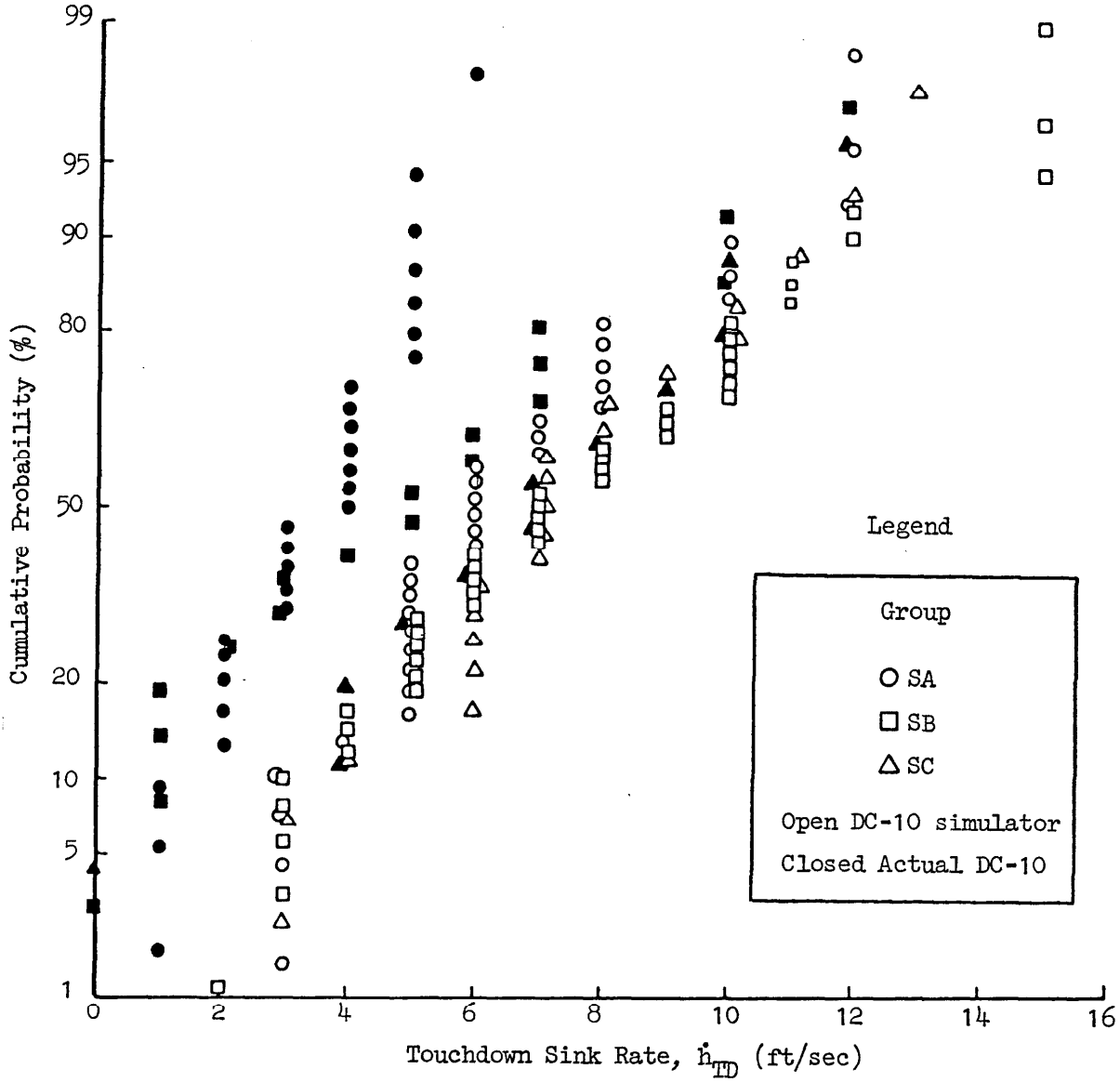

Figure 33. Cumulative Probability Distributions of Simulator-Trained Groups--Simulator Versus Actual DC-10

TABLE 7

SUMMARY OF ANALYSIS RESULTS FOR SIMULATOR VERSUS FLIGHT

	$\bar{\zeta}_{FL}$	$\bar{\omega}_{FL}$	$\overline{\omega^2_{FL}}$	$1/T_I$	T_L	Remarks
Actual DC-10						
FA	0.68	0.42	0.19	0.19	1.9	Aggressive, well compensated
SA	0.70	0.34	0.12	0.19	2.0	Less aggressive, but well compensated
SB	0.62	0.36	0.13	0.12	1.9	Long lag
SC	0.60	0.35	0.13	0	2.8	Very long lag, over compensated lead
DC-10 Simulator						
SA	0.57	0.33	0.12	0.05	2.1	Long lag
SB	0.54	0.40	0.20	0.09	1.5	Long lag, short lead
SC	0.54	0.32	0.13	0.11	1.6	Long lag, short lead

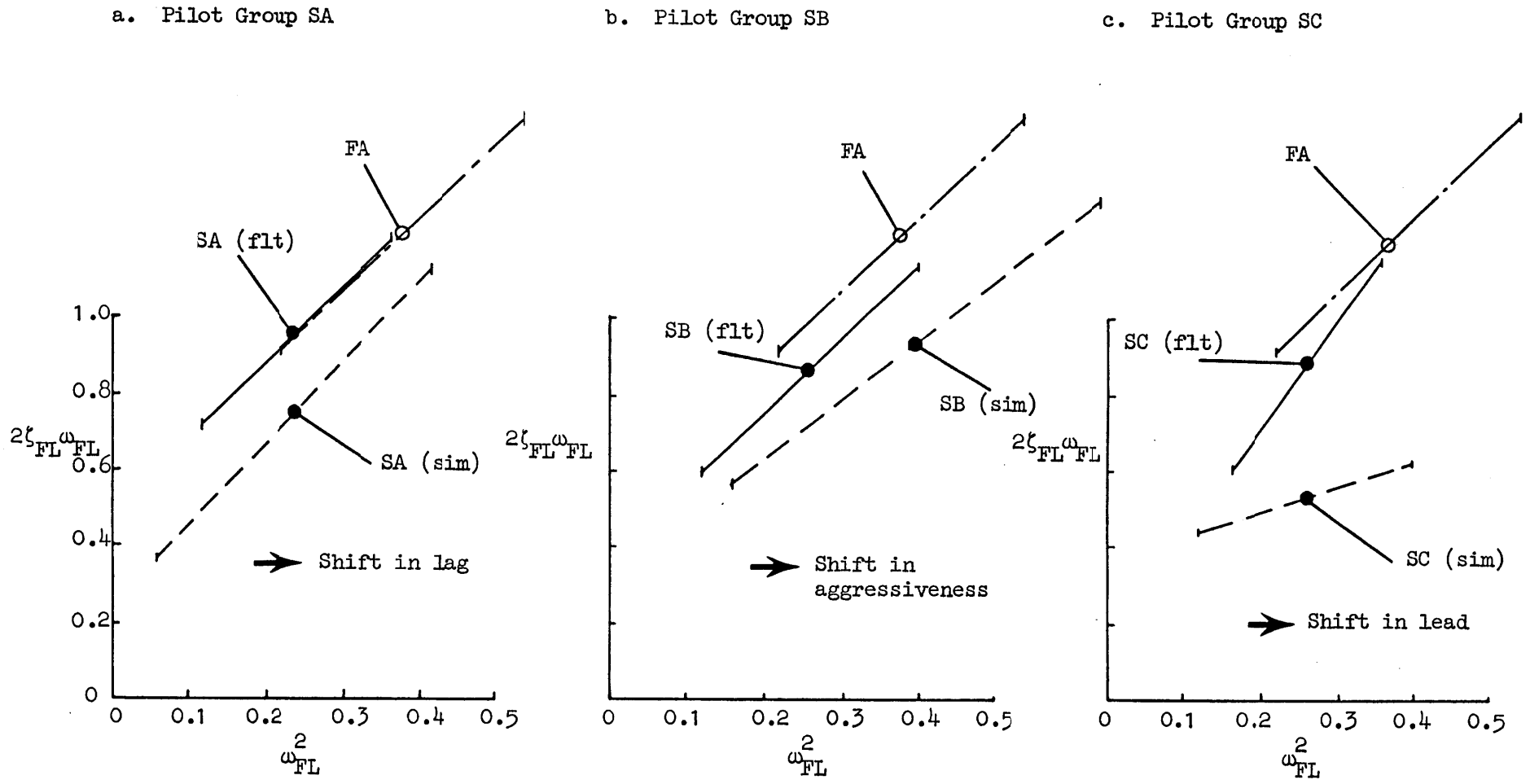

Figure 34. Piloting Technique Trends for Simulation Versus Flight and Comparison with Baseline Group FA

Based on all of the foregoing differences noted between simulator and flight, the overall assessment regarding simulator fidelity must be that it was deficient. There were no substantial indications that the general piloting technique induced in the simulator was the same as that induced in flight. Furthermore none of the various groups operated the simulator in a way comparable to that of Group FA, the assumed standard of good technique and performance.

The unsatisfactory piloting technique feature common to all simulator groups was excessive effective lag, T_I. Therefore it seems wise to examine possible explanations. Based upon an examination of the previously discussed pilot-vehicle model of the landing, there are various factors which can appear as a system lag or delay. These include:

- Slow sampling of flight path changes and subsequent adjustment of attitude
- Low closed-loop bandwidth for pitch attitude regulation and control
- Slow airframe flight path response (e.g., due to an incorrect simulator mathematical model)
- Simulator system lags or delays (e.g., in the visual display)
- Pilot neuromuscular delay (which can be affected by simulator motion distortion)
- Lack of direct vertical-velocity or flight path feedbacks
- Combinations of any or all of the above.

The relatively large amount of effective lag inferred from the simulator landings suggests serious perceptual blocks which inhibit the pilot from making rapid closed-loop adjustments during the flare. The lags computed were substantially greater than one might reasonably attribute just to simulator system lags or mathematical model discrepancies. As further evidence, the absence of a "duck under" for a terminal correction of touchdown point suggests a lack of or indifference to low altitude visual perception of height, flight path, or distance along the runway, i.e., spatial perception in general.

The simulator does appear to be supporting the generation of effective lead compensation. This may be a function of the pilot selecting a suitable "preview distance," that is, obtaining height at a distance of $T_L \cdot U$ ahead of the aircraft (nominally about 400 ft).

CONCLUDING REMARKS

The airline landing data analyzed in this report have yielded a rich variety of results with implications in several areas including quantification of piloting technique, transfer of training using simulators, and the fidelity and validity of an airline training simulator for the landing maneuver. Besides providing important quantification in these various areas, the data have also provided the basis for a revised analytical model of the flare maneuver. In fact, the model developed provides a useful bridge between the raw data collected and the ensuing interpretations of those data.

Several metrics have evolved with regard to describing the landing maneuver. The first metric is the phase plane representation to characterize the flare maneuver, not only in terms of the ultimate landing performance but also how that performance was achieved: whether the flare was the result of a last-minute abrupt pull-up leaving no room for error or misjudgment, or whether it was the result of an exceedingly gentle decay in sink rate which might be accompanied by a large loss of airspeed prior to touchdown. The phase plane also indicates directly where there are dangerously high sink rates at low altitudes or if there was a floating or ballooning tendency. Pilot misjudgment of height is also discernible from phase plane portraits. The primary value of the phase plane comes from the ability to portray two related states, i.e., sink rate and altitude, using a single curve. Use of time histories to present such information requires two separate curves. Time can be shown on a phase plane as a third dimension if so desired.

Metrics which describe the effective closed-loop response and which were easily obtainable from the phase plane plots are the effective second-order damping ratio, ζ_{FL}, and natural frequency, ω_{FL}. Closed-loop damping ratio can be obtained from the ratio of final sink rate to maximum sink rate and, hence, is significant. Natural frequency describes the abruptness of the flare maneuver and can be obtained from the curvature and steepness of the final segment of the phase plane trajectory. Transparent overlays of phase plane trajectory families serve as a useful means of identifying closed-loop parameters.

Metrics indicating the nature of the open-loop pilot-vehicle response can be inferred from ensemble analysis of individual landings made by a single pilot or group of pilots exhibiting similar performance. One of these metrics, T_L, describes the effective lead compensation which can be expressed as a mathematical equivalent of vertical-velocity or flight-path-angle feedback. The amount of lead compensation can also be related to a preview distance from which the pilot obtains height information. The value of the effective lead time interval can be directly related to the regression line slope for ensemble landing data plotted in the $2\zeta_{FL}\omega_{FL}$--ω_{FL}^2 plane.

An effective pilot-vehicle lag, T_I, can also be computed using ensemble data and represents a variety of pilot and airframe lags and delays. Two of

the main components are the airframe flight path lag, T_{θ_2}, and any effect of a flight path/pitch command sample-and-hold technique.

Another metric of interest is the degree of aggressiveness indicated by either ω_{FL} or ω_{FL}^2, the latter of which is more closely tied to the pilot's effective height gain, k_h.

Some metrics no longer hold the same degree of interest as they did prior to this study. Most notable is the idea of a single, nominal flare height. The large number of flare trajectories shown in the data suggest that there is no single preferred flare height, and the revised model demonstrates how good landing performance need not depend upon initiating the flare over a narrow range of altitude. Instead flare height is better associated with an outer loop involving the pilot's aim point along the runway. In effect, the flare control strategy is initiated higher or lower depending upon the amount of adjustment to the point of touchdown.

An important aspect of the analysis performed here is the quantification of the landing maneuver as it is performed on the actual aircraft. This provides an important baseline for examining the effects of training and simulator fidelity. Without this description of piloting technique, one would have to rely far more heavily upon terminal landing performance (i.e., scoring of the touchdown sink rate or distance along the runway) or on strictly subjective judgments.

The nominal landing technique involved nearly optimum closed-loop parameters clustered about $\zeta_{FL} \approx 0.7$ and $0.3 < \omega_{FL} < 0.6$. Using ensemble data, it was found that $T_L \approx 1.9$ sec and $1/T_I \approx 0.19$/sec. Such values of compensation tended to yield good touchdown sink rate performance over a reasonably wide range of flare maneuver aggressiveness. In order to attain this kind of closed-loop behavior with the known or suspected lag elements, however, there is an implied necessity of higher than first-order lead. This higher order lead is possible through either visual or vestibular pathways. Furthermore the same pilot control strategy evident in the flare could be associated with any pre-flare duck-under type of maneuver.

There appear to be fundamental differences in the technique of pilots trained in the landing on a flight simulator as compared to the technique of pilots trained on the actual flight vehicle itself. Those pilots trained on the simulator do not exhibit the same degree of success as those trained on the actual aircraft. Of the thirteen flight-trained pilots, all but three achieved consistently good landing performance. Only nine of nineteen simulator-trained pilots demonstrated comparable touchdown sink rate performance, but these same pilots, on the average, flared less aggressively thus inviting larger speed loss during flare.

The less successful flight- and simulator-trained pilots all shared greater amounts of effective lag, T_I. In the extremes this lag was, in part, compensated by an increased but ineffectual lead, T_L.

Training simulator fidelity and validity did not appear adequate to perform correctly the landing maneuver. The specific differences were varied, however. In general, touchdown sink rate compared well between simulator and flight only for those less successful groups of pilots. In all cases the piloting technique inferred from simulator results did not correspond to that from flight. The one feature common to all simulator groups was excessive effective lag, T_I. The source of this lag could not be isolated, however. It is believed to be connected with inadequate spatial perception near the ground. Simulator system lags or mathematical model discrepancies are less likely problems due to their relative amounts when compared to the overall T_I.

A number of recommendations seem appropriate in view of the success of the basic technical approach in illuminating so many areas; however, even though several questions have been answered, new questions arise. Ways to improve analysis techniques are also apparent.

The first recommendation is that, for future measurements of the landing maneuver, additional aircraft states, besides height and acceleration, need to be recorded. In descending order of their priority, the desired states are: altitude (radar--not barometric), normal acceleration, pitch attitude, cockpit control deflection, airspeed, range from the runway, throttle, and pitch rate. These data would offer a higher-quality definition of the outer flight path loops plus a description of the inner control loops.

Data reduction procedures should be improved in two ways. Where data are sparse and noisy, as in this study, there is the need for improved data smoothing and estimation techniques. Such techniques are now available but are generally not convenient to implement. The second improvement which should be instituted is automatic parameter identification procedures. The landing maneuver model resulting from this study makes automatic procedures more feasible. The technique described in Ref. 23 would be especially suitable owing to its ease of operation and undemanding computer requirements.

The analytical model development should be fully expanded to account for the higher-order pilot-vehicle system effects. As mentioned earlier, the landing model loop structure which has been defined is compatible with any degree of system complexity. It was simply not possible to pursue a detailed analytical development which would tie together aircraft stability and control, performance, flight control system features, atmospheric disturbance effects, and any other aspect which is dependent upon or related to the pilot landing task.

In a similar vein, the model of the landing maneuver can and should be extended to other aircraft types. Some cases more critical than a jet transport include carrier recovery of fighter/attack aircraft, short-field operation of powered-lift aircraft, non-aviation ship recovery of helicopters and VTOL aircraft, and, because of sometimes limited skill levels, landing of light aircraft. Such analysis efforts would first require accomplishment of the next recommendation, however.

It is absolutely essential that studies of manual flight tasks include actual flight measurements. Additional flight measurements should be made for the cases studied involving pilots with varying levels of skill. It is most important to acquire data for highly skilled and experienced DC-10 pilots in order to improve quantification of the baseline piloting technique parameters.

With regard to pilot training, it is recommended that pilot behavior in terms of essential loop development and operation be studied in conjunction with training procedures and techniques. In this study the analysts lacked any intimate knowledge of how flight instructors interacted with subjects and how such interaction affected piloting technique development. It is now feasible to consider on-line monitoring of pilot psychomotor and cognitive behavior along the lines demonstrated. Such monitoring could be of direct use to instructors as well as to the evaluation of instructors or evaluation of instructional techniques.

Perceptual pathways--their use and their dynamics--require far more study. While the overall pilot-vehicle response in the landing maneuver implies certain effective feedback loops or compensation, their nature is not clear. It can only be reasoned by deduction that visual pathways are more likely than vestibular ones and that pilot generation of compensation by judgment of height involves a preview distance is more likely than by a flight path angle or vertical velocity feedback.

Finally, it is recommended that simulator training for the landing maneuver not be assumed fully equivalent to flight training without careful study of essential loop development. Simulator training should not be discouraged, however. Rather, there should be strict accounting of the piloting technique developed on the simulator versus that required for flight. Where piloting technique deficiencies are noted, then remedial measures should be taken.

Ames Research Center
National Aeronautics and Space Administration
Moffett Field, California 94035
July 1981
Revised May 1982

APPENDIX

Review of Earlier Models of the Landing Maneuver

The landing flare is regarded as the critical flight phase and has been studied by a number of researchers. A number of measurements of touchdown parameters such as sink rate and touchdown point have been made without any particular regard for the specific pilot behavior involved. In a few cases, however, analytic models of the flare maneuver have been suggested and these were worth reviewing in order to revise the modeling hypothesis which was applied to the data acquired in this experiment. Some of the questions include: (a) Is the maneuver chiefly open loop or closed loop? (b) Is the maneuver segmented or continuous? and (c) Are the perceptual pathways used by the pilot mainly visual, mainly vestibular, or both?

It is tempting to treat the landing maneuver as a segmented multistage process in view of the apparently different actions which take place over the entire time frame of the landing. References 24 and 25 describe a model which is representative of this segmented maneuver point of view. In effect the landing is broken into three phases following the final approach. Phase 1 consists of the initial flare to reduce the approach flight path angle to essentially zero and terminates 5 to 10 ft above the ground. The second phase is called the float and consists of easing of the airplane down from the 5- to 10-ft height, accompanied by reduction of thrust to idle. Finally the third stage is the touchdown itself and is characterized by the impact sink rate and the structural loads thus imposed. The stated purpose of this kind of breakdown of the maneuver was to aid in identifying critical pilot actions and sources of inaccuracies in the flare. At the same time, this model implies that the pilot is, in fact, shifting from one mode of action to another for each segment. A cleaner model would involve a unified set of control laws which still produce the actions just described, yet without any particular segmentation of behavior required.

The model in Ref. 26 describes the flare in pilot-centered terms rather than the trajectory terms of the previous model. In effect the pilot is considered to close a feedback loop around sink rate which is initiated at a prescribed flare height. This kind of flare law yields an exponential decay of sink rate or, in terms of a phase plane, leads to an essentially straight-line segment for sink rate versus altitude following flare initiation. The form of this model is useful because it shows how the pilot can participate as part of a closed-loop system in what is known to be a highly critical flight phase. This particular model also consolidates at least two of the segments proposed in the previously described model, i.e., the Phase 1 flare and the Phase 2 float. There is, however, believed to be an essential element missing in the specific command loop structure suggested, that is, an outer loop feedback of height. Without height feedback, landing performance depends greatly upon both precise flare initiation height and a sink-rate-decay time constant. This leads to the third model to be discussed.

A command loop structure which provides certain beneficial results is described in Ref. 13 and involves altitude as the outer loop in a pilot-centered flare model. The implication of an altitude command loop is that there is a distinct closed-loop preference for altitude. Hence there is some degree of compensation for a miscue in flare height. This would not be the case in the model mentioned previously. Any error in flare initiation would have a direct and significant impact on touchdown sink rate or tendency to float. This is because the last chance that the pilot has for altitude to influence control commands is at the perceived flare height. The altitude command loop model described in this third case also involves use of a nominal flare height and, while touchdown conditions are more tolerant of flare height miscue than the previous model, the requirement for the pilot to cue on a nominal flare height is, nevertheless, present. There is another troublesome aspect of this third flare model in that the flare command to the closed-loop block diagram is not equal to zero altitude but rather to flare altitude. A literal interpretation of this model would say that the pilot is, in fact, attempting to close an altitude loop about the flare height and this does not seem to agree with the actual intentions of the pilot. Therefore the model described in Ref. 13 should be discarded.

Each of the above models, summarized in Fig. 35, offers some important notions about how the pilot is executing the landing maneuver but none of these really provides a satisfying description of the pilot behavior which covers all areas of concern. There are also features of the new landing data which force consideration of some additional requirements for a flare model. Most important of these is that there does not appear to be any particular preference for a nominal flare altitude even though the airline flight manual (Ref. 12) gives a suggested range for flare initiation. As shown in the data, the flare trajectory begins as low as the nominal 30 to 40 ft suggested by the flight manual but also as high as 80 or even 100 ft above the ground. The question which is posed is, How does one formulate a model of the flare maneuver which could yield consistently reasonable touchdown sink rates regardless of the height of flare initiation?

To summarize, the features which should be consolidated into a revised model of the flare maneuver are:

- Evidence of the three distinct phases of the landing maneuver including flare, float, and touchdown
- A pilot-centered description which relates the resulting trajectory to the pilot-vehicle dynamics
- A capacity to manage or regulate sink rate
- A preference for height relative to the decrease in sink rate
- A tolerance for a wide range of flare initiation heights.

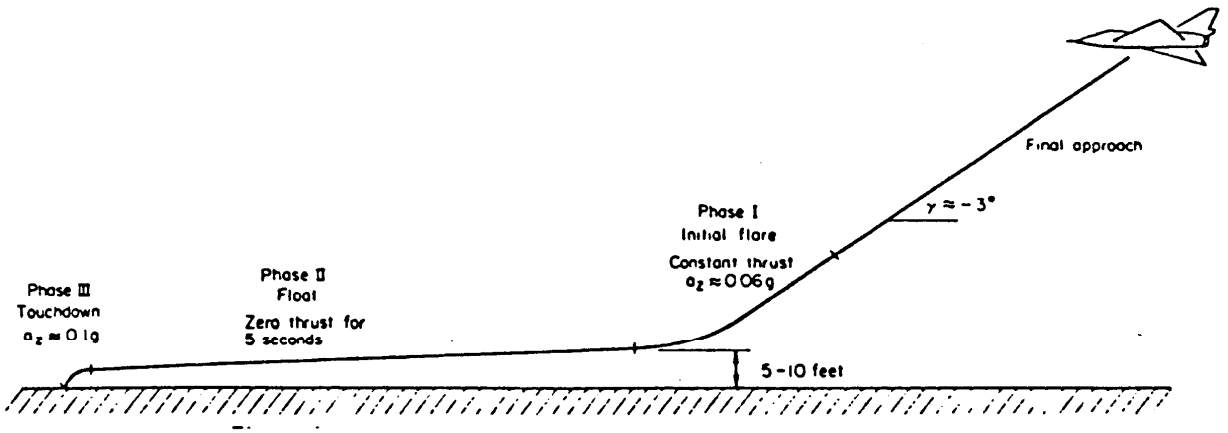

a. Model From Refs. 24, 25

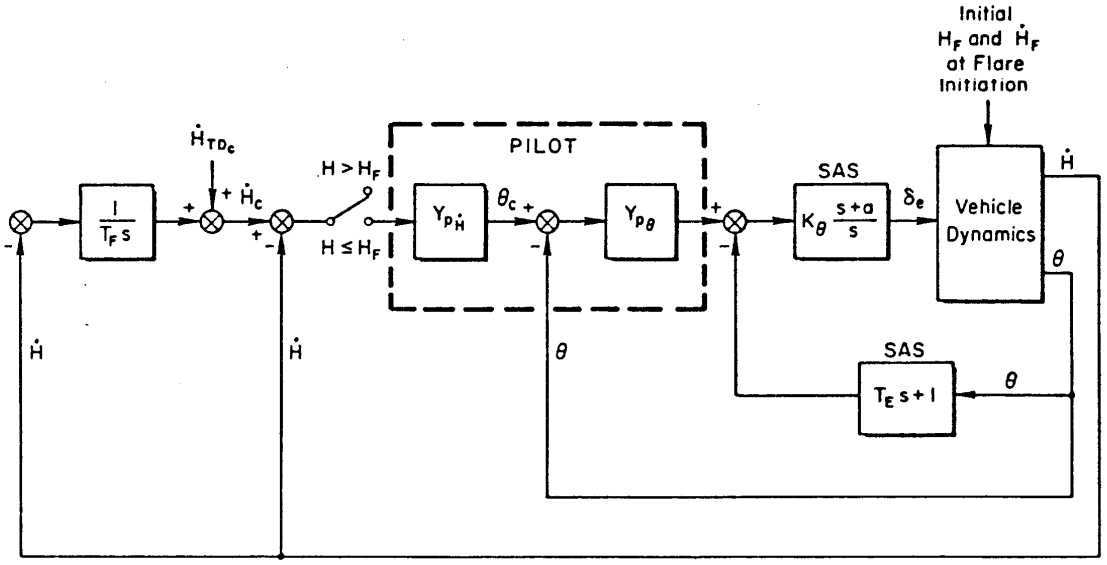

b. Model From Ref. 26

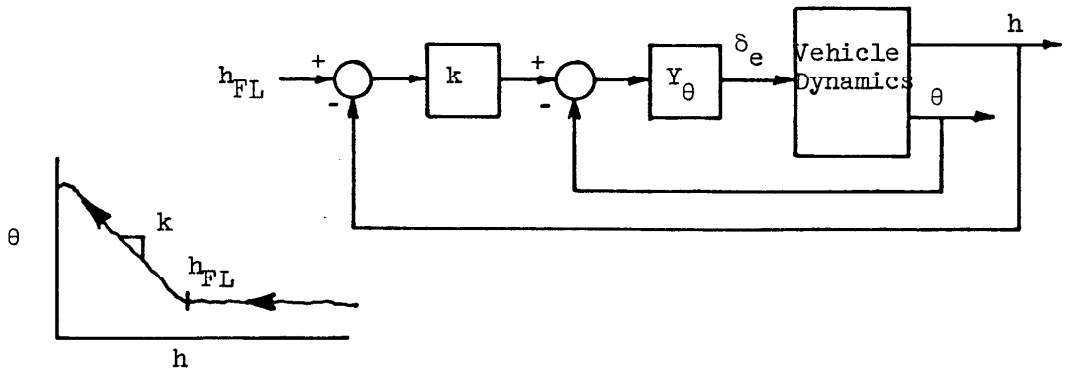

c. Model From Ref. 13

Figure 35. Review of Earlier Landing Models

In addition there should also be accommodation of pilot actions associated with landing at a desired point on the runway although this aspect is somewhat beyond the scope of the experimental data obtained.

Now consider a number of flare control strategies taken in a generic sense which can be studied in terms of the implied pilot control laws and the resulting dynamic response especially in terms of a phase plane trajectory. This survey is restricted only to the vertical translational degree of freedom and neglects the airspeed response aspects which are known to be higher-order effects unless the flare is not sufficiently abrupt (i.e., it is reasonable to assume that a partitioning of response is in the z-axis and x-axis of the aircraft). The analytic approach could, of course, be extended to additional degrees of freedom if they were believed to be important.

Table 8 describes several generic control strategies which would yield differing kinds of flare maneuvers. Each of these flare types is, strictly speaking, closed loop in some respect. For example, the angle-of-attack-command flare (α-command) assumes that the pilot is commanding a desired angle of attack which could consist of either a step or ramp command beginning at a particular altitude. The α-command would also be representative of a control column command where the short period response of the aircraft is sufficiently fast compared to the heave response (this would usually be the case in the landing).

The pitch attitude command flare (θ-command) also assumes that the pilot would be commanding either a step or a ramp attitude change at a predetermined altitude. Note that in this case there is an exponential response mode not present in the α-command trajectory. Further this response mode corresponds to the heave damping of the aircraft which is a strong function of wing loading and wing aspect ratio.

The normal acceleration command flare ($\ddot{h}$-command) assumes that the pilot applies an instantaneous step command in normal acceleration at a given flare height. It should be noted that this is really dynamically the same as the alpha-command flare type.

The sink rate command flare ($\dot{h}$-command) type is equivalent to that suggested in Ref. 26 and assumes that, at a given flare height, the pilot commands a predetermined touchdown sink rate. The value for the exponential decay factor, k, would be dependent upon a combination of aircraft heave damping and the pilot loop gain on sink rate.

The final flare type is the so-call altitude command which involves a preference for both altitude and sink rate. Normally h_c would be equal to zero (the ground) and $\dot{h}_c$, for most aircraft, would be nearly zero.

TABLE 8

GENERIC CONTROL STRATEGIES FOR THE LANDING MANEUVER

Flare Type	Equation of Motion	Laplace Transform	Time Domain Solution
α-command (or δ_e)	$\ddot{h} = \frac{U}{T_{\theta_2}}(\alpha_c + \dot{\alpha}_c t)$ $(\alpha = \alpha_c)$	$\dot{h}(s) = \frac{\dot{h}_o}{s} + \frac{U}{T_{\theta_2}}\frac{\alpha_c}{s^2}$ $+ \frac{U}{T_{\theta_2}}\frac{\dot{\alpha}_c}{s^3}$	$\dot{h}(t) = \dot{h}_o + \frac{U}{T_{\theta_2}}(\alpha_c t + \dot{\alpha}_c \frac{t^2}{2})$
θ-command	$\ddot{h} = -\frac{1}{T_{\theta_2}}\dot{h} + \frac{U}{T_{\theta_2}}(\theta_c + \dot{\theta}_c t)$ $(\theta = \theta_c)$	$\dot{h}(s) = \frac{\dot{h}_o}{s + \frac{1}{T_{\theta_2}}} + \frac{U\theta_o}{T_{\theta_2}}\frac{1}{s\left(s + \frac{1}{T_{\theta_2}}\right)}$ $+ \frac{U\dot{\theta}_c}{T_{\theta_2}}\frac{1}{s^2\left(s + \frac{1}{T_{\theta_2}}\right)}$	$\dot{h}(t) = \dot{h}_o e^{-t/T_{\theta_2}} + U\theta_c(1 - e^{-t/T_{\theta_2}})$ $+ U\dot{\theta}_c(t - T_{\theta_2} + T_{\theta_2}e^{-t/T_{\theta_2}})$
$\ddot{h}$-command	$\ddot{h} = \ddot{h}_c$	$\dot{h}(s) = \frac{\dot{h}_o}{s} + \frac{\ddot{h}_o}{s^2}$	$\dot{h}(t) = \dot{h}_o + \ddot{h}_c t$
$\dot{h}$-command	$\ddot{h} = k(\dot{h}_c - \dot{h})$	$\dot{h}(s) = \frac{\dot{h}_o}{s+k} + \frac{k\dot{h}_c}{s(s+k)}$	$\dot{h}(t) = \dot{h}_o e^{-kt} + \dot{h}_o(1 - e^{-kt})$
h-command	$\ddot{h} = k_1(h_c - h)$ $+ k_2(\dot{h}_c - \dot{h})$	$\dot{h}(s) = \frac{s\dot{h}_o + k_1 h_c + k_2\dot{h}_c}{s^2 + k_2 s + k_1}$	$\dot{h}(t) = \dot{h}_o e^{-at}(\cos bt - \frac{a}{b}\sin bt)$ $+ (k_1 h_c + k_2\dot{h}_c)\frac{e^{-at}}{b}\sin bt$ $a = k_2/2 \quad b = \sqrt{k_1 - \frac{k_2^2}{4}}$

REFERENCES

1. Construction of the Man-Vehicle Systems Research Facility, FY1981, Preliminary Engineering Report, Ames Research Center, July 1980.

2. Clement, Warren F., Allen, R. Wade, Heffley, Robert K., et al., Functional Requirements for the Man-Vehicle Systems Research Facility, Systems Technology, Inc., Technical Report No. 1156-3, October 1980.

3. "NASA To Build Man-Vehicle Systems Research Facility," Air Force Magazine, Vol. 64, No. 3, March 1981.

4. McRuer, Duane T., Clement, Warren F., and Allen, R. Wade, A Theory of Human Error, Systems Technology, Inc., Technical Report No. 1156-1, May 1980.

5. Clement, Warren F., Heffley, Robert K., Jewell, Wayne F., and McRuer, Duane T., Technical Approaches for Measurement of Human Error, Systems Technology, Inc., Technical Report No. 1156-2, July 1980.

6. Randle, Robert J., Jr., Tanner, Trieve A., Hamerman, Joy A., and Showalter, Thomas H., The Use of Total Simulator Training in Transitioning Air-Carrier Pilots: A Field Evaluation, NASA TM 81250, January 1981.

7. McRuer, D. T., and Krendel, E. S., Mathematical Models of Human Pilot Behavior, AGARD-AG-188, January 1974.

8. Heffley, Robert K., Clement, Warren F., Ringland, Robert F., et al., Determination of Motion and Visual System Characteristics for Flight Simulation, Systems Technology, Inc., Technical Report No. 1162-1, April 1981.

9. Key, David L., (Ed.), Fidelity of Simulation for Pilot Training, AGARD Advisory Report No. 159, October 1980.

10. Heffley, Robert K., Clement, Warren F., and Craig, Samuel J., "Training Aircraft Design Considerations Based on the Successive Organization of Perception in Manual Control," Sixteenth Annual Conference on Manual Control, Massachusetts Institute of Technology, Cambridge, MA, May 1980, pp. 119-127.

11. Anon., DC-10 Flight Crew Operating Manual, McDonnell-Douglas, November 1, 1974.

12. United Airlines, DC-10 Flight Manual, Training and Reference, United Airlines Flight Training Center, Stapleton International Airport, Denver, Colorado, October 17, 1977.

13. Heffley, Robert K., Closed-Loop Analysis of Manual Flare and Landing, AIAA Paper 74-834, August 1974.

14. Smith, Jon M., Mathematical Modeling and Digital Simulation for Engineers and Scientists, John Wiley and Sons, New York, 1977, pp. 195-199.

15. Truxal, Prof. John G., Automatic Feedback Control System Synthesis, McGraw-Hill Book Company, Inc., New York, 1955.

16. Flügge-Lotz, Irmgard, Discontinuous Automatic Control, Princeton University Press, Princeton, New Jersey, 1953.

17. McRuer, Duane, Ashkenas, Irving, and Graham, Dunstan, Aircraft Dynamics and Automatic Control, Princeton University Press, Princeton, New Jersey, 1973.

18. Grunwald, Arthur J., and S. J. Merhav, "Vehicular Control by Visual Field Cues--Analytical Model and Experimental Validation," IEEE Transactions on Systems, Man, and Cybernetics, Vol. SMC-6, No. 12, December 1976.

19. Cooper, George E., unpublished communications, March 5 and May 13, 1982.

20. Taylor, John W. R. (Ed.), Jane's All The World's Aircraft, 1973-74, McGraw-Hill Book Company, New York, 1973.

21. Litchford, George B., The Duck-Under Maneuver, Presented at the Thirteenth ALPA Air Safety Forum, October 4-5, 1966.

22. Litchford, George B., "The 100-ft Barrier, Reducing the Minimum Height for Pilot's Visual Reference in Low-Visibility Landing Should be a Step Taken Circumspectly," Astronautics and Aeronautics, July 1964, pp. 58-65.

23. Jewell, Wayne F., and Schulman, Ted M., A Pilot Control Strategy Identification Technique for Use in Multiloop Control Tasks, Systems Technology, Inc., Technical Report No. 1153-2, August 1980.

24. White, Maurice D., Proposed Analytical Model for the Final Stages of Landing a Transport Airplane, NASA TN D-4438, April 1968.

25. Seager, D. B., The Landing of Advanced Flight Vehicles, AGARD Report 427, January 1963.

26. Hoh, Roger H., Craig, Samuel J., and Ashkenas, Irving L., Identification of Minimum Acceptable Characteristics for Manual STOL Flight Path Control. Volume III: Detailed Analyses and Tested Vehicle Characteristics, FAA-RD-75-123, III, June 1976.

1. Report No.	2. Government Accession No.	3. Recipient's Catalog No.

4. Title and Subtitle	5. Report Date
An Analysis of Airline Landing Flare Data Based on Flight and Training Simulator Measurements	Revised May 1982
	6. Performing Organization Code
7. Author(s) Robert K. Heffley, Ted M. Schulman, Robert J. Randle, Jr., and Warren F. Clement	8. Performing Organization Report No. STI-TR-1172-1R
	10. Work Unit No.
9. Performing Organization Name and Address Systems Technology, Inc. 2672 Bayshore Frontage Road, Suite 505 Mountain View, California 94043	11. Contract or Grant No. NAS2-10817
	13. Type of Report and Period Covered Final Report
12. Sponsoring Agency Name and Address National Aeronautics and Space Administration Ames Research Center Moffett Field, California 94035	14. Sponsoring Agency Code

15. Supplementary Notes

16. Abstract

Landings by experienced airline pilots transitioning to the DC-10, performed in flight and on a simulator, were analyzed and compared using a pilot-in-the-loop model of the landing maneuver. By solving for the effective feedback gains and pilot compensation which described landing technique, it was possible to discern fundamental differences in pilot behavior between the actual aircraft and the simulator. These differences were then used to infer simulator fidelity in terms of specific deficiencies and to quantify the effectiveness of training on the simulator as compared to training in flight. While training on the simulator, pilots exhibited larger effective lag in commanding the flare. The inability to compensate adequately for this lag was associated with hard or inconsistent landings. To some degree this deficiency was carried into flight, thus resulting in a slightly different and inferior landing technique than exhibited by pilots trained exclusively on the actual aircraft.

17. Key Words (Suggested by Author(s))		18. Distribution Statement
Aircraft Landing	Manual Control	UNCLASSIFIED - UNLIMITED STAR Category - 08
DC-10 Aircraft	Training Simulators	
Flight Tests	Pilot Performance	
Flight Simulation	Pilot Model Parameter Identification	
Pilot Training		

19. Security Classif. (of this report)	20. Security Classif. (of this page)	21. No. of Pages	22. Price*
Unclassified	Unclassified	117	

*For sale by the National Technical Information Service, Springfield, Virginia 22161